PRESS AND DRYER ROLL SURFACES AND WEB TRANSFER SYSTEMS FOR ULTRA HIGH PAPER MACHINE SPEEDS

Final Report
On
Project DE-FC36-99GO10384

T. F. Patterson
March 15, 2004

PROJECT OVERVIEW

This is the final report for Project DE-FC36-99GO10384. This section provides a summary of the projective objective, motivation, problems encountered, original project tasks and final status of those tasks, publications that resulted from the project or related work, and personnel that contributed to the projected.

In follow-on sections, separate reports are provided for Tasks 1, 2, 3, 4, and 6 of the project. These sections are self contained. Tasks 3 and 4 are covered in a single section. There is no section for Task 5.

Project Objective: The objective of the project was to provide fundamental knowledge and diagnostic tools needed to design new technologies that will allow ultra high speed web transfer from press rolls and dryer cylinders.

Fundamental Questions: From a fundamental standpoint, it was assumed that roll surface performance depends on the composition of contaminants that deposit on those surfaces during use, as well as the materials and finishing techniques used in manufacturing these surfaces. There was a need to understand: the contamination process, the influence of contamination on work of adhesion, the roles of surface topology, film splitting, and process conditions on web transfer.

BACKGROUND AND SUMMARY

This project was originally proposed and funded with Dr. David Orloff of IPST as the Principal Investigator and a scheduled duration extending from October 1999 to October 2002. Beloit Corporation was a partner in the proposal and was to provide the cost share for the project.

During the course of the project Beloit Corporation declared bankruptcy. After the bankruptcy IPST provided the portion of the cost share that was to be provided by Beloit. In 2000, David Orloff's job function at IPST changed and he was no longer able to continue as Principal Investigator. Timothy Patterson was named Principal Investigator.

Given the demise of Beloit Corporation there were some schedule interruptions and schedule changes. As a result, a one year no cost extension was requested and granted. While the official interactions with the Department of Energy have concluded, work in this area continues under the sponsorship of the IPST Member Companies.

One of the primary results of the Beloit bankruptcy was that the Beloit pilot equipment was no longer available for use by this project. Therefore, Task 5, which was envisioned to use that equipment, was adversely affected. There was an attempt to utilize equipment at IPST, but the equipment was inadequate for the required work.

Task 6 was modified to make use of equipment provided by AstenJohnson. This equipment had greater capability and provided a more realistic testing environment then the IPST equipment that was originally planned to be used.

In addition to the Project Management difficulties that resulted from the Beloit bankruptcy, the technical complexity of the project was considerably greater than originally envisioned. Consequently, the project concentrated on web transfer in the dryer section as opposed to both the dryer and press sections of the papermachine.

There were four significant results from the project

1. Development of the Web Adhesion and Drying Simulator (WADS). This device is unique in that it allows the measurement of the work of web separation under a wide variety of both drying and pressing conditions. It continues to be used for the study of web separation. It has also been used for the study of cockle development due to dryer can contamination.

2. Development of a web separation mathematical model. The geometry of web separation from the WADS more closely resembles actually paper machine web separation than has previously been simulated or modeled. The web follows a catenary curve as it leaves the roll surface, this web path is difficult to treat analytically. A model which does accurately treat this geometry was developed and verified.

3. Development of a lumped parameter dryer section model. This model allows the estimation of productivity losses due to dryer can contamination.

4. Preliminary development of a polymer roll wipe for contamination control. A solid polymer roll wipe, not a doctor blade, was successfully tested using pilot scale equipment. This work was initiated after the no cost extension period of the project. Plans are in place to test the system on a production paper machine.

PROJECT TASKS & FINAL STATUS

Task 1.
Identify composition of contamination and topology of press and dryer roll surfaces at commercial mills

Final Status: Completed

Task 2.
Develop the facilities to simulate the contaminant deposition process under controlled experimental conditions (Contamination Test Stand – CTS)

Final Status: Equipment and test stand were built, however it proved inadequate for studying contamination initiation and buildup.

Task 3.
Develop facilities to simulate web transfer from contaminant surfaces and measure work of adhesion (Web Adhesion and Drying Simulator – WADS).

Final Status: Completed

Task 4.
Develop models of contamination, adhesion, and picking.

a. Define model contamination systems.
b. Simulate contamination process using the CTS and compare to mill data.
c. Simulate web transfer during pressing and drying and measure both work of adhesion and picking
d. Explore variables and develop correlations

Final Status: Sub-Task a. – completed
Sub-Task b. – not completed, apparatus did not produce required data
Sub-Task c. – drying simulation completed, pressing simulation not completed
Sub-Task d. – correlations completed

Task 5.
Develop and verify models to predict various aspects of web transfer at ultra high paper machine speeds.

a. Incorporate correlations into a web transfer model.
b. Evaluate web transfer models on a pilot paper machine.
c. Verify at mills.

Final Status: Sub-Task a. – not completed due to Beloit Corporation bankruptcy
Sub-Task b. – not completed due to Beloit Corporation bankruptcy
Sub-Task c. – not completed due to Beloit Corporation bankruptcy

Task 6.
Develop and demonstrate new roll surface conditioning technologies, including PTFE roll wiping technology for use on dryer cylinder rolls.

a. Develop contamination control options on CTS.
b. Develop options for controlling roll surface topology on CTS.
c. Evaluate desirable options on pilot machine.

Final Status: Sub-Task a. – Various polymer roll wipe materials were tested using pilot machine equipment provided by AstenJohnson. (work was initiated and completed after the no cost extension had ended. This work was funded by the IPST Member Companies)

Sub-Task b. – not completed, apparatus did not produce required data

Sub-Task c. – A Fluro-Polymer roll wipe was tested and its viability verified using pilot machine equipment provided by AstenJohnson. (work was initiated and completed after the no cost extension had ended. This work was funded by the IPST Member Companies)

RELATED PUBLICATIONS

1. Ahrens, F., Patterson, T., Mueller, S., Hojjiate, B. "*Investigation of Paper Dryer Picking, Web Transfer and Quality Issues Using a New Web Adhesion and Drying Simulator*", to be presented at 2004 International Drying Symposium, Sao Paulo, Brazil, August 2004.
2. Ahrens, Mueller, S., Patterson, T., Bloom, F., *"Mathematical Modeling of Web Separation and Dynamics on a Web Adhesion and Drying Simulator"*. International Journal of Applied Mechanics and Engineering v. 9, n. 3. 2004.
3. Mueller, S., Patterson, T., Ahrens, F., *"Peel Testing on Web Adhesion and Drying Simulator"*, Pressure Sensitive Tape Council Conference, Atlanta, GA. April 2002. (Presented by S. Mueller).
4. Patterson, T., *Fluro-polymer Roll Wipe*, Patent application submitted February 2003.
5. Ahrens, F., Rudman, I., "*The Impact of Dryer Surface Deposits and Temperature Graduation on Drying Productivity*", Proceedings Tappi 2003 Spring Technical Conference

CONTRIBUTING PERSONNEL

Marcos Abazeri, IPST
Frederick Ahrens, IPST
Medea Alexander, IPST
Melissa Austin, IPST
Sam Baker, AstenJohnson
Frederick Bloom, N. Illinois U.
Jere Crouse, Beloit Corporation
Yulin Deng, IPST
Daniela Edelkind, IPST
Edward Lindahl, IPST
James Loughran, IPST
Shana Mueller, IPST
Hiroki Nanko, IPST
David Orloff, IPST
Timothy Patterson, IPST
Paul Phelan, IPST
Isaak Rudman, IPST

Task 1

Identify composition of contamination and topology of press and dryer roll surfaces at commercial mills

Final Status

Completed

DRYER SURFACE CONTAMINATION EVALUATION: PROCEDURES, EXAMPLE RESULTS AND APPLICATION OF RESULTS

Fred Ahrens

Timothy Patterson

Paul Phelan

David Orloff

Isaak Rudman

PROJECT OVERVIEW 1
INTRODUCTION 7
BACKGROUND 7
OBJECTIVES 8
COLLECTION OF MACHINE DATA 9
MACHINE AND OPERATING DATA 10
SELECTED DRYER CANS 11
COLLECTION OF CONTAMINANT DEPOSITS 11
DRYER CAN SELECTION CRITERIA 12
PHOTOGRAPHS 12
CONTAMINANT THICKNESS MEASUREMENT 13
CONTAMINANT COLLECTION 15
SURFACE REPLICAS OF BARE METAL 16
ANALYSIS OF THE SAMPLES 17
AMOUNT OF CONTAMINANT AND CONTAMINANT THICKNESS 18
ORGANIC CHEMICAL COMPOSITION 18
IDENTIFICATION OF INORGANIC COMPONENTS AND SPATIAL DISTRIBUTION 18
CONTACT ANGLE WITH WATER 19
SURFACE TOPOLOGY MEASUREMENTS 19
EXAMPLE RESULTS 19
CONTAMINANT LOADING 20
CHEMICAL ANALYSIS 21
SCANNING ELECTRON MICROSCOPY (SEM) ANALYSIS 23
CONTACT ANGLE WITH WATER 24
SURFACE TOPOLOGY 24
DISCUSSION 27
EFFECT OF DEPOSITS ON DRYING RATE AND DRYING ECONOMICS 27
EFFECT OF DEPOSITS ON PICKING/STICKING 28
CONCLUSIONS 29
LITERATURE CITED 30

DRYER SURFACE CONTAMINATION EVALUATION: PROCEDURES, EXAMPLE RESULTS AND APPLICATION OF RESULTS

INTRODUCTION

This work is an integral part of a joint IPST and Department of Energy (Agenda 2020) project investigating dryer can contamination and its impact on sheet sticking, dryer can heating performance, and the resultant decrease in machine productivity and product quality. The ultimate goal of the project is to better understand the contamination and sheet sticking process and use that understanding to develop ways to reduce or eliminate dryer can contamination and sheet sticking. The result would be increased machine speeds and increased sheet quality. The objective is to collect samples from a large number of machines in an attempt to characterize contamination by the most appropriate common denominator.

In this report, a set of procedures for systematically collecting dryer can contamination samples is described. The procedures describe methods for:

1. Photographing the contaminants
2. Documenting the location of contaminants
3. Determining the thickness of the contamination
4. Collecting contaminant samples
5. Characterizing the bare metal dryer can topology

Also included in the report, are examples of work done with previously collected samples and methods for analyzing the collected contaminant samples. The analysis includes both chemical/physical sample evaluation and calculations to estimate the effect of the contamination on dryer section productivity. Appendix A provides data sheets for collection of mill samples. Appendix B provides methods for calculating the detrimental heat transfer and economic impacts of dryer can contamination.

BACKGROUND

The work described in this report is part of a project that is motivated by the fact that, for most paper grades, the first several dryer cans (usually up to ten) are operated at very low steam pressure (surface temperature). This is done to avoid/reduce various runnability and paper quality problems that were found to occur at higher temperature. Problems identified as being significant include picking/sticking, surface deposits, cockle, sheet floating, sheet sealing and blistering/delamination.

A consequence of the first dryer section low temperature operating strategy is a loss of productivity due to one or more of the following.

1. Fiber sticking/picking and increased probability of web breaks. It is generally known that foreign material adhering to the cylinder surface,

especially in the first several dryer cans, can increase sticking of the wet web to the dryer can. It may aggravate fiber picking resulting in higher required peeling tension and more web breaks.

2. Necessitated reduction of the temperature of the first few dryer cans and decrease of average drying rate. In order to inhibit/reduce fiber sticking/picking, papermakers usually reduce the temperatures in the first few dryer cans. However, reducing temperatures has an adverse effect on the dryer productivity and is not a desirable option.

3. Reduction in overall heat transfer coefficient and decrease of the drying rate. Contaminant buildup, which may be scale, corrosion, paper fibers and other organic and inorganic deposits, reduces the overall heat transfer from the steam to the paper web. This results in a decrease of the drying rate and machine speed, decreasing productivity. Nuttal (1967) estimated that contaminants on the outer cylinder surface and the air film between this surface and the wet web may account for up to 80% or more of the total heat transfer resistance.

4. Non-uniformity of drying and increased probability of cockle, over-drying, wet spots, sheet breaks. Because the distribution of contaminants on the dryer can surface is not usually even, non-uniformity of heat transfer and drying rate may also be a consequence. Non-uniformity of drying may be manifested in wet or over-dried streaks, which makes the web more prone to breaks and increased variability in its mechanical properties. Additionally, non-uniformity of drying may be the reason for sheet cockling.

5. Runnability and sheet quality problems caused by chunks of contaminant deposited on the web .

6. Increased downtime for cleanup of dryer surfaces.

OBJECTIVES

The project goal is:

Increase paper machine productivity via reducing / eliminating impediments to the use of higher surface temperatures in the first dryer section.

In order to gain a better understanding of the above problems and evaluate potential solutions for eliminating or minimizing deposit buildup on dryer cans, the following project objectives were set. This report covers progress in meeting the first two objectives.

1. To develop and implement the procedures for the collection and analysis of the contaminants formed on the surface of the first several dryer cans. The results of contaminant analysis would be used for simulating contamination of the coupons on the Contamination Test Stand (CTS) and studying web sticking to the contaminated coupons on the Web Adhesion and Drying Simulator (WADS).

2. To evaluate the detrimental effect of the dryer can contaminants on the heat transfer, drying rate, and economics of the drying process.

3. To identify potential variables affecting the contamination process.

4. To elucidate the possible correlation between dryer can contamination, furnish, and operational variables of a paper machine.

5. To develop practical recommendations for reducing dryer can contamination.

COLLECTION OF MACHINE DATA

Contamination of the dryer can surface is a complex dynamic process. The potential variables characterizing and affecting formation of the deposits can be categorized into two groups. The first group of variables comprises general machine and operating conditions that may be potential contributing factors to dryer can contamination. This group can be roughly categorized into the factors associated with

1. Machine Characteristics
2. Stock and Sheet Characteristics.

The second group of variables characterizes the contamination deposits. It consists of

1. Deposit amount and thickness
2. Deposit distribution
3. Deposit chemical composition
4. Deposit porosity
5. Substrate surface characteristics.
6. Rate of deposit rate accumulation

Thorough documentation and measurement of these factors is of great importance for establishing possible correlations and an in-depth understanding of the contamination process, and, ultimately, its elimination or reduction. Listed below is a general overview of the machine operating conditions information desired. In the next section, types of

samples needed to characterize dryer can contaminants and detailed procedures for sample collection are given.

Machine and Operating Data

As there is not yet a complete understanding of dryer can contamination process, the list of desired operating condition information is extensive. Information, which is important for a certain paper machine, may be redundant for another machine. It is believed, however, that the suggested list of data and samples to be collected captures the majority of potential variables. Further investigation will help to define in more detail the data to be collected. The data desired is listed below.

Machine Configuration

- Type of forming section
- Number of presses
- Type of presses
- Single or double felting
- Dryer can and dryer section configuration
- Number of dryer cans
- Location of dryers with doctor blades

Operating Conditions

- Machine speed
- Press loadings
- Solids at press section exit
- Sheet temperature at press section exit
- Dryer can steam pressures
- Dryer can surface temperatures

Stock and Sheet Characteristics

- Product
- Basis weight
- Fiber type(s)
- Freeness
- Ash content
- Filler content and type
- Additives used
- Water hardness and Ph

Selected Dryer Cans

Only selected dryer cans need be examined in detail. The primary idea is to select cans that either show significant contamination or changes in the amount or type of contamination. For the selected dryer cans the following information is desirable.

- Can surface temperature
- Number of spoiler bars
- Doctor blade location on the can
- Wrap angle
- Length of draw
- Fabric tension
- Pocket ventilation – flow rate, temperature
- Can surface material
- Can Diameter
- Can shell thickness
- Surface treatments
- Schedule and method for can cleaning

Appendix A provides forms for documenting the general machine operating conditions, sheet characteristics, dryer section configurations and the details of the dryer cans selected for contaminant sampling.

In addition to the information on the forms, documentation of any observed changes in paper machine operation over the period during which the deposits were accumulated would be helpful. Communication with mill personnel and the records of their observations as to changes in the drying rates, sticking, and other technical documentation would be useful. Comparison of the performance of a given mill with similar or other mills may also provide valuable information as to the sources of can dryer contamination and preventive measures.

COLLECTION OF CONTAMINANT DEPOSITS

Past experience has shown that the dryer cans with the greatest amount of surface contamination tend to be at the beginning of the dryer section and after sizing or coating operations. The amount of contamination decreases as the sheet moves down the machine. In addition, contamination tends to increase when the side of the sheet that contacts the dryer can is reversed. How much contamination builds up appears to depend on sheet surface solids on the side contacting the dryer can, can surface temperature, the chemical/physical properties of the sheet, and the can surface properties. These factors also influence how far down the machine the contamination continues. On some machines, the build up appears to be non-uniform or appears in rings around the dryer can. It is suspected that some of the non-uniformity is due to moisture streaks, basis weight non-uniformity, can surface non-uniformities or can heating non-uniformities.

The objective of the sampling process is to characterize as completely as possible the contamination and how it develops on the machine.

The data and sample collection process is summarized below.

1. Document general machine operation data (as outlined in previous section).
2. Select specific dryer cans for sampling and document can characteristics
3. Photograph contaminated dryer cans
4. Contaminant thickness measurement (optional, based on time and can temperature)
5. Contaminant collection
6. Can surface replication (optional, based on time and can temperature).

Dryer Can Selection Criteria

The objective in selecting the dryer cans for contaminant sampling is to select cans that illustrate the progression of the contamination build-up as one moves down the machine. Ideally, four dryer cans should be selected. The procedure is as follows.

1. Identify the can with the greatest amount of contamination.
2. Move down the machine and identify the first can that has almost no contamination.
3. Identify the can 1/3 of the way between the can selected in (1) and the can selected in (2).
4. Identify the can 2/3 of the way between the can selected in (1) and the can selected in (2).

Given that time is always at a premium, the priority is to collect samples from the locations that shows the greatest contamination. This will usually be at the beginning of the dryer section. If time or conditions do not allow taking 4 samples, pick as many cans as possible between the two extremes. Record all of the dryer can information on the forms in Appendix A.

The pattern of high contamination at an early can, with the contamination diminishing farther down the machine may be repeated after a sizing press or when the side of the sheet contacting the dryer can is changed. If possible, it is desirable to take samples when the pattern is repeated. The same dryer can selection procedures should be used.

Photographs

Photographs provide qualitative description of the contaminant deposits. They supplement visual description and provide information regarding the uniformity of contaminant distribution and spatial features of the contaminant layer such as streaks, patches, bands, rings, etc. While pictures in any form are useful, digital pictures are the easiest to process and send to IPST. All photographs should have some form of label

attached that indicates the can number, some machine identification information, and the date.

The photographs should be supplemented by visual examination of the selected dryer cans. General observations regarding the nature, color, morphology, and relative amount of each type of distinct material that appears to be present including fibers, solid particulates or grains, sticky agglomerations, foreign objects, etc., should be documented.

Contaminant Thickness Measurement

Measurement of the contaminant thickness is useful for two purposes, determination of the accumulation rate and determination of an approximate heat conduction coefficient. Given a known dryer-can cleaning schedule, the thickness can be used to calculate the rate of contaminant accumulation. Given a known mass per unit area and chemical composition of the contaminant, the thickness can be used to calculate the contaminant porosity. The porosity, in combination with the chemical composition, can then be used to determine an approximate heat conduction coefficient for the contaminant layer. Usually, the most significant factor affecting the magnitude of the heat conduction coefficient is the porosity. While chemical composition does have an effect, it is generally does not result in the same variability. The method for calculating the heat conduction coefficient is given in Appendix B.

If the procedure can be performed on only one can, it should be done on the can with the greatest amount of contaminant. Care should be taken during the sampling process to avoid injury from residual heat in the dryer can. If necessary use gloves and arm protection. The area selected for measurement should have a uniform layer of contaminant and be at least 15" from the edge of the cylinder. If there is no area of uniform contamination, select an area that appears to have the thickest contamination.

The contaminant thickness can be measured in one of two ways. The first requires the most effort. In this method, a small strip of the contamination is removed, using a single edged razor blade, exposing the bare metal of the dryer. The scraped area should resemble a narrow “trench” in the contaminant, measuring approximately 1/8" wide (MD Direction) and about 2" long (CD Direction) (see Figure 1). A polymer casting is made of the “trench” allowing its depth to be determined using microscopy techniques.

The procedure is as follows

1. Select a uniformly contaminated area that is no less than 15 in. (38 mm) from the edge of the dryer can.
2. Using a single edged razor blade scrape a “trench” in the contaminant as shown in *Figure 1*.
3. Mix the polymer casting material as described in Appendix C.

4. Using a cotton ball, coat the trench and surrounding area with the release agent, specified in Appendix C.
5. Apply the polymer casting material to the "trench" and surrounding area, being careful not to spread the polymer beyond the release agent coated area. See *Figure 1*.
6. The material will polymerize in a few minutes. When it becomes rubbery the process is complete and it can be peeled from the surface.
7. Wrap the replicas in tissue paper and put them in a plastic bag. The bag should be labeled with the can number, machine ID information, date, and contact information for the individual collecting the sample.
8. This test should be repeated on the same dryer cylinder in three different places.

The casting is brought back to the laboratory and examined under a scanning laser microscope. The thickness of the contaminant is determined by measuring the height of the "trench" impression.

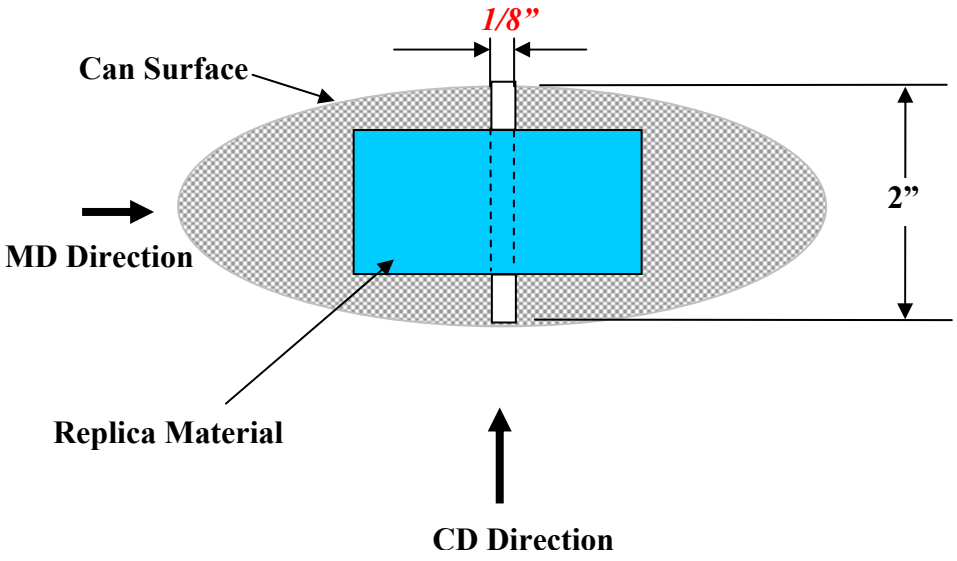

Figure 1 Thickness Measurement Replica

At dryer can surface temperatures above 100 °F, the organic components in the replica material will vaporize and cause bubbles to form. The result will be a poor quality replica. If the dryer can surface temperature is above 100 °F, this procedure is not recommended. This will probably be the case if the machine has been shut down for less than 6-8 hours.

An alternative to the casting method is to use an instrument such as Coating Measurements Instruments' coating thickness instrument CGX-C2. This instrument makes use of eddy currents and the ferromagnetic nature of the dryer can material. The instrument must be calibrated and the correct probe must be used, but it produces the thickness measurement directly. Typical instruments are capable of measuring material thicknesses up to 120 mils (3.05 mm). It displays the distance between the probe face and the nearest ferromagnetic material. The device must be calibrated and the correct probe must be used, but it produces the thickness measurement directly. If such an instrument is used the same selection procedures should be used.

The procedure for use is:

1. Ensure device is calibrated.
2. Place device probe against the dryer can.
3. Record contaminant thickness.
4. Repeat thickness measurement in total of five locations.

The thickness measurement should be recorded on the form in Appendix A.

Contaminant Collection

The simplest and potentially most useful portion of the sample taking process is scraping the contaminant from surfaces of selected dryer cans and collecting all of the scraped material. This is the most important part of the sampling process. It provides data on the total amount of contamination and its chemical composition. If only one of the sampling tasks can be completed, this is the task that should be done. As with the previous sample procedure, care should be taken during the sampling process to avoid injury from residual heat in the dryer can. If necessary use gloves and arm protection.

An important part of the collection process is to collect the contaminant from a known area. To simplify matters, this area should always be 12 in. x 12 in.

Selected area should adequately represent distribution of contaminant in terms of amount, spatial distribution and specific features. If significantly different patterns of the deposit distribution on the dryer can surface are observed, the samples from several areas are to be collected. The location of the areas should be specified relative to some reference point of the dryer can. It could be also practical to separate the contaminant scraped from the sub-areas of selected area.

To ensure accuracy, it is best to measure and mark the area using an ink marker. The procedure for collecting contaminant samples is as follows:

1. Measure and mark a 12 in x 12 in area using an ink marker

2. If the contamination appears in well defined rings, the sample area may be modified to include just the contamination ring. Any alterations in the sample area should be specifically noted.
3. Using a single edged razor blade, scrape all of the contamination in the marked area and collect the contamination in a lint free cloth or plastic sheet.
4. The cloth should then be sealed in a plastic bag.
5. The bag should be labeled with the can number, machine ID information, date, and contact information for the individual collecting the sample.

In the laboratory, the deposit is recovered from the lint-free cloth using a powder collection system with a Whatman's glass microfiber filter 934-AH, with pore size of 1.5 μm. The filter is weighed before collecting the deposit material and the net weight determines the "basis weight" of the contamination. Chemical analysis is performed primarily using FTIR and Scanning Electron Microscopy techniques. Other chemical analysis techniques will be used when appropriate. The information

obtained from this collection process will be used for a number of purposes.

1. Producing a database on dryer can contamination.
2. Formulating contamination "recipes" for use on IPST's Contamination Test Stand (CTS). This apparatus consists of a heated roll and a continuous "felt" that has the contamination recipe applied to it. The intent is to simulate the contamination process and develop empirical models of the contamination process and to evaluate means for inhibiting the contamination process.
3. Calculating the effect of the contamination on the heat transfer, drying rate and the economics of drying.

Surface Replicas of Bare Metal

It is believed that the dryer can surface roughness has an influence on both the type of contaminants that build up and in the rate of build up. The roughness of the roll surface can be characterized using either 1-dimensional (surface profile along a line) or 2-dimensional (surface profile over an area) topology measurements. Current research indicates that the 2-dimensional topology measurements are the most useful as these measurements provide a more complete description of the surface. There are 16 different 2-dimensional surface characterization parameters. The question that needs to be answered is, which one of these characterizations correlates best with contaminant build up. Since these parameters cannot be measured in the field, a casting or replica of the roll surface that preserves the three-dimensional characteristics of the surface is made.

These replicas will be returned to IPST for analysis of the can surface topology. As with the coating thickness castings, dryer can surface temperatures in excess of 100 °F result in poor replicas. In those cases, this sampling process can be skipped. Again, care should be taken during the sampling process to avoid injury from residual heat in the dryer can, i.e., gloves and arm protection may be appropriate.

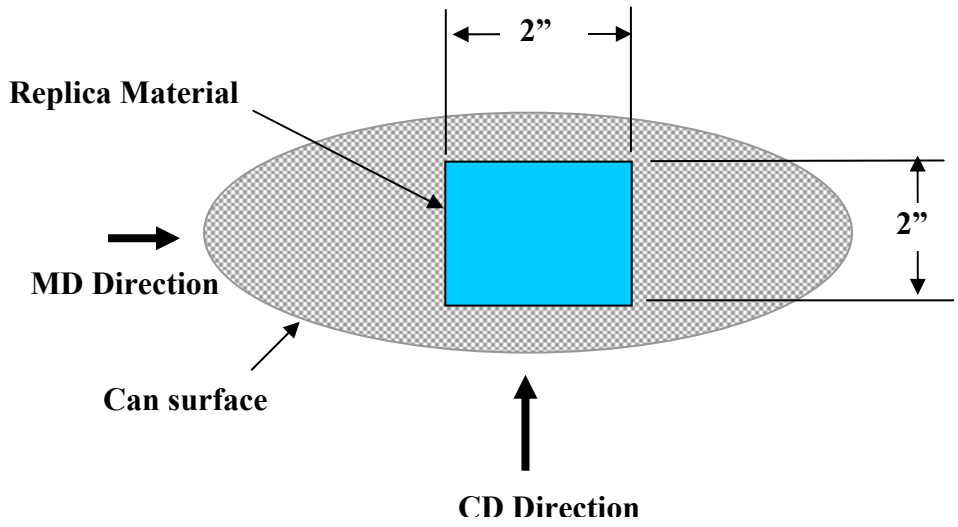

Figure 2. *Bare Metal Replica*

The area that was scraped clean for contaminant collection procedure can be used for taking bare metal surface replicas. The procedure is as follows

1. Within the cleaned area, mark two areas measuring approximately 2 in x 2 in, see Figure 2.
2. Mix the polymer casting material as described in Appendix C.
3. Using a cotton ball, coat an area slightly larger than the marked areas with the release agent.
4. Apply the polymer casting material to the two marked areas.
5. The material will polymerize in a few minutes. When it becomes rubbery the process is complete and it can be peeled from the surface.
6. Wrap the replicas in tissue paper and put them in a plastic bag. The bag should be labeled with the can number, machine ID information, date, and contact information for the individual collecting the sample.

ANALYSIS OF THE SAMPLES

The objective of the sample analysis is to characterize what was found, how much of it was found, the topology of the surface on which it was found. Ideally, the analysis should provide a breakdown of the contaminants in terms of their components and concentrations, adhesive properties, and spatial distribution. The following types of evaluations are to be performed.

- Amount of Contaminant and Contaminant Thickness
- Evaluation of Chemical Composition

- Identification of Inorganic Components and Spatial Distribution
- Contact Angle with Water
- Surface Topology Measurements

Amount of Contaminant and Contaminant Thickness

The total amount and the thickness of the contaminant are useful for a number of reasons. If the roll cleaning schedule is known, the total amount of contaminant can be used for calculating a rough accumulation rate number. The thickness of the contaminant layer, the total amount of contaminant, and the contaminant composition can be used to calculate the contaminant porosity. Porosity is an important parameter in determining the heat transfer properties of the contaminant.

The amount of contaminant is found by simply weighing the collected sample that was scraped from the 12in. x 12 in. area on the roll. After weighing, the sample is saved for later chemical analysis. The thickness of the contaminant is determined by examining the thickness replica under either the scanning electron microscope or the scanning laser microscope.

Organic Chemical Composition

The primary means employed for analyzing the organic chemical composition of the samples is Fourier Transform Infrared (FTIR) Spectroscopy analysis. A portion of sample collected by scraping the 12 in. x 12 in. area is used for the FTIR analysis.

The results made it possible to identify the major organic compounds in the deposits. If necessary, additional chemical tests can be performed to aid in the component identification.

Identification of Inorganic Components and Spatial Distribution

The total amount of inorganic material in the sample is found by measuring total ash content. A portion of the contamination sample is weighed, then heated to and held at 525°C for an extended time period. The material that remains is composed of only inorganic components. The percent inorganic content is found by comparing the before and after weights.

Two different SEM techniques can be used to identify the elemental composition of the sample. The first technique makes use of the back-scattered electrons produced by the electron beam impinging on the sample. The primary use is to identify the presence and spatial distribution of those components with higher atomic weights, generally greater than that of carbon. In the resultant image, the portions of the sample with high atomic weight appear lighter than those with low atomic weights. The second method is energy dispersing spectroscopy (SEM/EDS). It produces more quantitative information. This method makes it possible to determine the specific elemental composition with relative ease. Determining the concentration of particular elements is more complex and requires the use of software based analysis techniques.

Contact Angle with Water

The contact angle of the deposits with water is thought to affect the adhesive properties of the deposits. It is hypothesized that there may be a possible correlation between contact angle and sticking/picking of a wet web to the dryer surface.

It is not possible to measure contact angle of the deposit while it is on the roll. In removing the deposit from the roll the geometry of the deposit structure is altered (the scraping generally results in the deposit taking the form of flakes or small "chunks"). Measurement of contact angle requires a flat surface. Therefore, the procedure for measuring contact angle requires that the collected deposits first be compacted into flat pellets. The contact angle with water is then measured using standard laboratory techniques and the surface energy of the contaminant calculated.

Surface Topology Measurements

It is believed that the roll surface topology plays a roll in both whether a contaminant will adhere to the surface and the rate at which it builds up. A number of methods have been developed over the years for measuring surface topology, both contact and non-contact methods. All of the methods required complex equipment that is not easily transported to a mill or used on a roll surface. An alternative is to bring the equipment to the surface to be evaluated is to bring a replica of the surface to the measuring equipment. For accurate measurement of the surface characteristics the material used for the casting must reproduce the surface at a microscopic scale (<1 μm). Given the small scale of analysis required, non-contact methods are the most applicable.

Two types of surface topology measurement are possible, 1-dimensional (the topology along a line) and 2-dimensional (the topology over a surface). The 2-dimensional measurements provide the most complete characterization of the surface. Only one laboratory was found that had the equipment to perform a 2-dimensional topology measurement using non-contact methods – CyberMetrics of Alpharetta, Ga. This laboratory has a scanning laser device for measuring both 1-dimensional and 2-dimensional topology. The high-resolution measurement system is used for mapping the roughness of paper and printed surfaces. With a spot size less than a micron in diameter and a vertical resolution of only three nanometers, the resolution is more than adequate.

EXAMPLE RESULTS

In the spring of 1999, IPST personnel collected samples from two coated paper machines. In November of 1999, IPST personnel collected surface deposits from dryer cans on two different board machines, one producing 42# liner and the other producing 26# medium. In this section, the analysis results for selected samples are presented. The collected scrapings were analyzed according to the procedures described in Section 6.

Contaminant Loading

Deposit samples were taken from three cylinders on the linerboard machine and from three cylinders on the medium machine (Figure 3). It was not possible to measure the contaminant loading on the first of the three cylinders examined on the medium machine, cylinder #16. The region of the greatest contamination on cylinder 16 was not close enough to the catwalk and could not be accessed safely. The cylinder was heavily contaminated, the thickness of the deposit was approximately a sixteenth of an inch.

In addition to the contaminant data, surface temperature measurements were also made. These measurements are presented in Figure 4 (linerboard machine) and Figure 5 (medium machine).

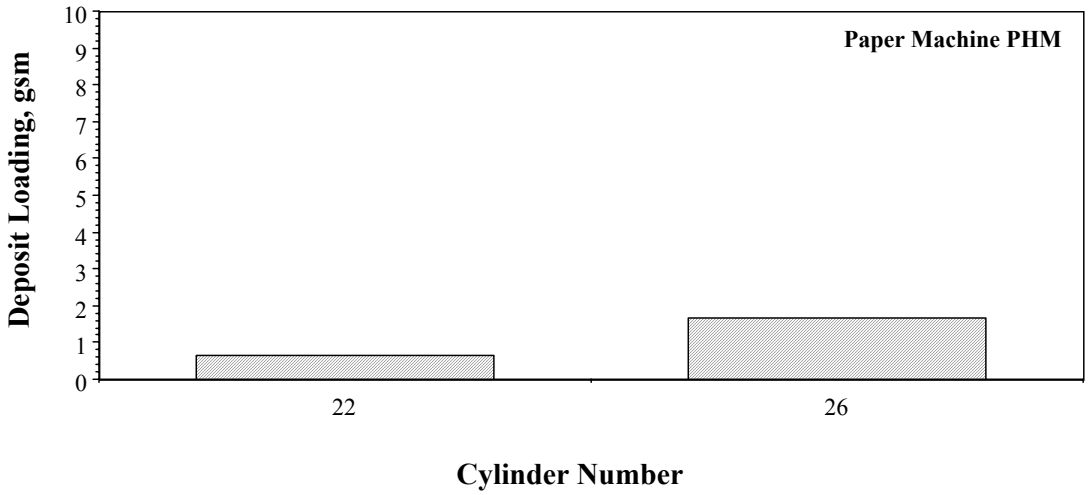

Figure 3. Deposit Loading for Dryer Cylinders on the Commercial Paper Machine Producing Medium

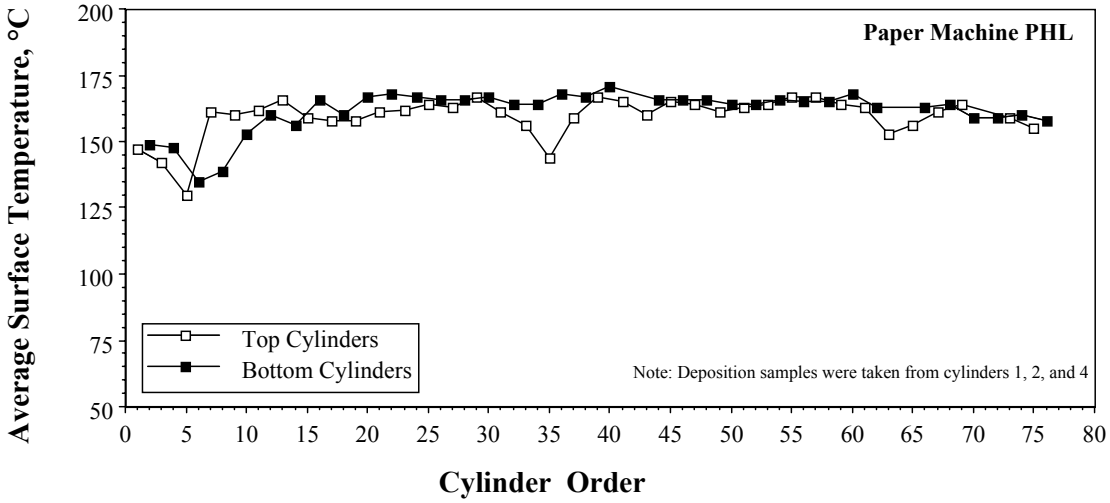

Figure 4. Average Dryer Cylinder Surface Temperature – Linerboard Machine

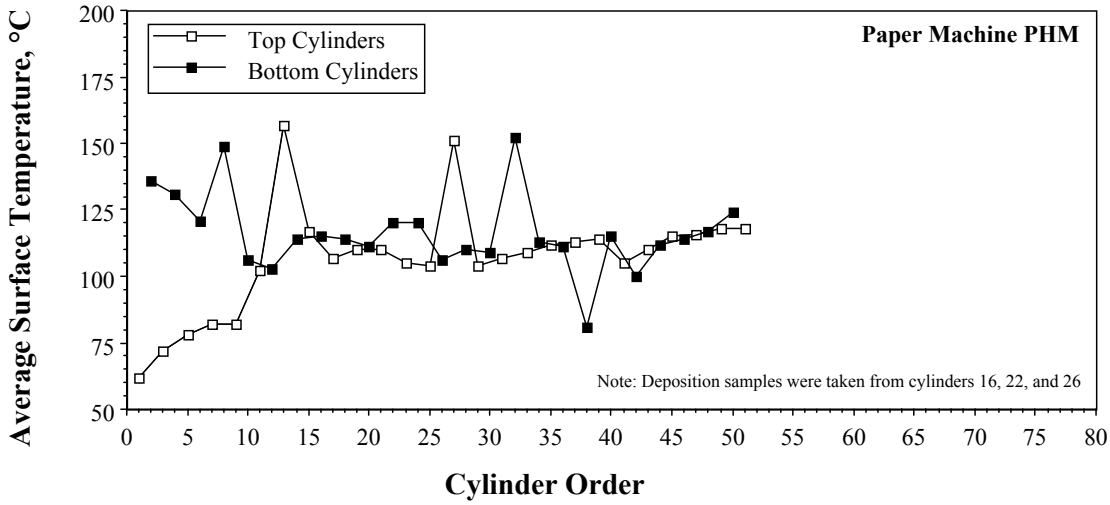

Figure 5. Average Dryer Cylinder Surface Temperature – Medium Machine

Chemical Analysis

The results of chemical analysis for the six dryer cans inspected are tabulated in Table 1 (Ahrens and Patterson, 2000).

Table 1. Contaminant Composition and Loading – Linerboard and Medium

Components	**LinerBoard**			**Medium**		
	Dryer #1	**Dryer #2**	**Dryer #4**	**Dryer #16**	**Dryer #22**	**Dryer #26**
Wood fiber	**36.52**	**10.32**	**6.64**	**21.05**	**43.92**	**52.83**
Tacky Polymer (mostly PVAc)	50.22					
Miscellaneous (Starch, Felt Fiber, Plastics)	4.57					<0.587
Polystyrene		<0.129				
Styrene-butadiene Polymer Residue				58.94		
Wood Extractives (Resin & Fatty Acids)				4.21		
Solvent Extractable HC (Defoamer Residue)		2.58	1.66			5.87
Solvent Extractable Residue					4.88	
Plastics (Polymethacrylate)					<0.488	
Total Organic (ExcludingWood Fiber)	**54.78**	**2.58**	**1.66**	**63.15**	**4.88**	**5.87**
Calcium Carbonate	3.92	26.13	64.19	3.16	2.56	2.07
Silicates Including Clay	3.92	60.97	27.51	12.64	48.64	39.24
Rust	0.87	<4.355	<4.585			
Total Inorganic	**8.70**	**87.10**	**91.70**	**15.80**	**51.20**	**41.30**
Contaminant Loading, gsm	**1.30**	**6.50**	**3.20**		**0.60**	**1.70**

Depending on the influence of the deposits on the heat transfer and sheet sticking/picking, other differentiation of the components may be more relevant. By comparing the results of chemical analysis with chemical analysis of the pulp, water, fillers, additives, felts used, etc., some conclusions may be drawn as to the origin of the contaminants. If web peeling is the subject of investigation, then the components may be differentiated according to the adhesive properties and the causes of increased web sticking may be identified.

Scanning Electron Microscopy (SEM) Analysis

An illustration of backscattered and SEM/EDS images are shown below in Figure 6 for the deposits collected from the dryer of a coated paper machine. The samples were collected of the spring of 1999.

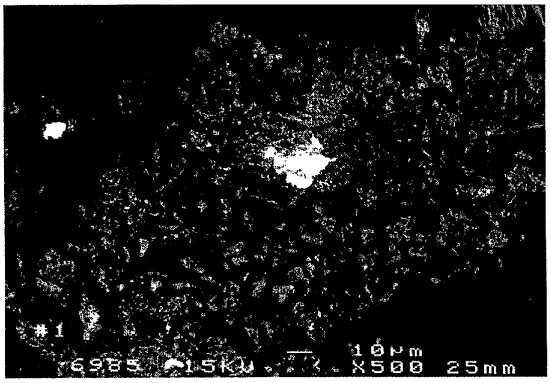

Backscatterd Electron Image

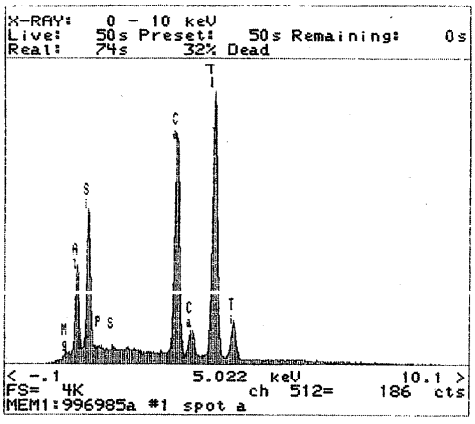

EDS Analysis

Figure 6. Backscattered Electron Imaging and EDS Analysis

The first chart in Figure 6, is a backscattered image. The white spots represent the areas where higher atomic weight elements are located such as Ti, Si, Ca, etc. The second

chart is the output from and EDS analysis. The abscissa of the graph identifies the elements in the sample. Each element has a characteristic energy level (keV) associated with it. The ordinate shows X-ray intensity in counts per second, which is roughly proportional to the concentration of a given element.

In this sample, the thickness was not measured. Because of the unknown thickness and surface geometry of the sample, corrections associated with the atomic weight of the elements, absorption coefficient and fluorescence were not made and it was not possible to determine the exact concentrations of the elements.

Contact Angle with Water

The deposits collected from each of the coated paper machine dryer cans were compacted into flat pellets. The contact angle for water was measured. As organic solvent penetrated into the bulk of the pellet, the surface energy of the contaminant was not calculated. The contact angles for samples from the two machines (machine A and machine B) are tabulated in Table 2.

Table 2 Contact angle for Deposits and Cast Iron

PM-Cylinder #	Contact Angle, ^{o}
B-3	79
B-5	75
B-7	78
C-1	101
C-8	115
C-10	98
Clean Cast Iron	77

Surface Topology

Both one and two-dimensional topology measurements were made on surface replicas from the linerboard (PHL) and medium (PHM) machines. In addition, four other replicas were evaluated, two from fine paper machines (B and C) and two from cast iron coupons (CI Smooth and CI Scratched) that were of the same material and finish as new dryer cans. The “CI scratched” coupon had a number of inadvertently made scratches on it.

Figure 7. shows some calculated values made from the one-dimensional topology measurements. Note that the topology of the IPST smooth cast-iron coupon is similar to

that of the linerboard machine (PHL). The plot of the scratched cast-iron coupon is similar to that of the medium machine (PHM).

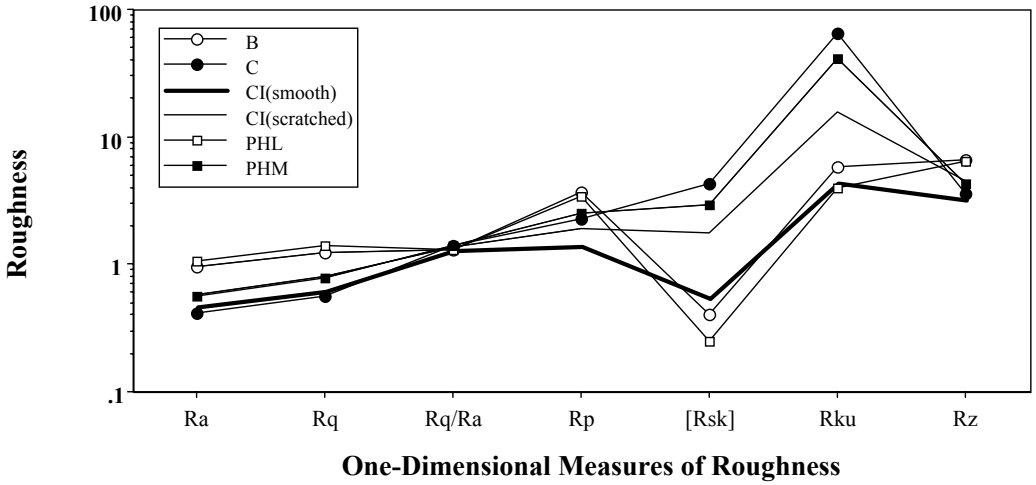

Figure 7. One Dimensional Measurements of Roughness

Each of the calculated one-dimensional roughness parameters is defined below.

R_a = Average roughness, arithmetic mean deviation of the profile from the mean surface height.

R_q = Root-mean-square roughness, root mean square deviation of the profile from the mean surface height.

R_p = Maximum peak height within a sampling length, also referred to as depth of surface smoothness.

R_{sk} = Skewness of the profile – a measure of the sharpness and shape of the peaks, indicates unsymmetrical frequency of distribution having the mode at a different value from the mean ($R_{sk} = 0$ for rounded symmetrical peaks).

R_{ku} = Kurtosis of the assessed profile - indicates the peakedness ($R_{ku} > 3$) or flatness ($R_{ku} < 3$) with respect to the concentration of the values near the mean as compared with the normal distribution

R_z = Average peak-to-valley height (taken over 5 adjoining sample lengths)

Figure 8shows the two-dimensional measurements for the cast iron coupons and the linerboard and medium machines. Both coupons and the commercial surfaces have similar topologies.

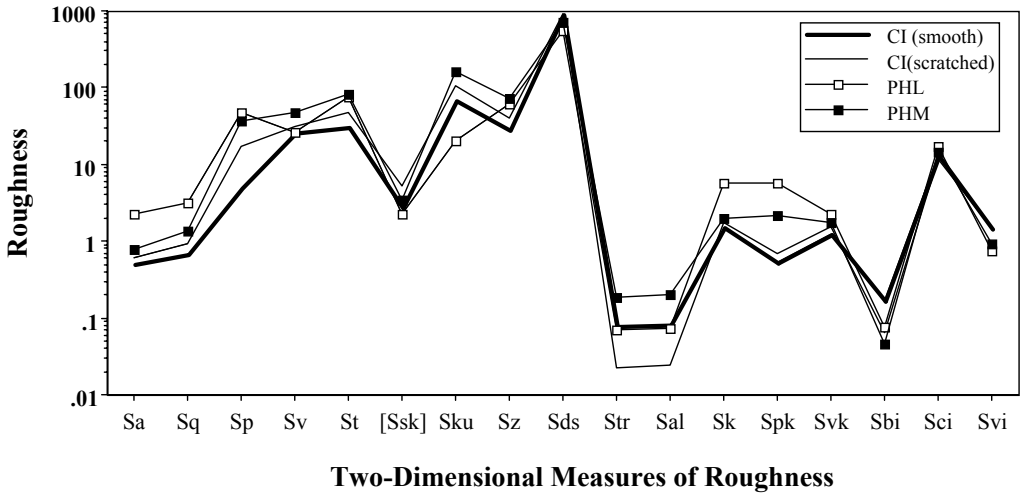

Figure 8. Two Dimensional Measurements of Roughness

Each of the two-dimensional parameters is defined below.

Amplitude

S_a = Average roughness, arithmetic mean of the deviations from the mean surface height.

S_q = Root-mean-square roughness, quadratic mean of the deviations from the mean surface height.

S_p = Maximum height of peaks, relative to the mean surface.

S_v = Maximum depth of valleys relative to the mean surface.

S_t = Total height of the surface, distance between the highest peak and deepest hole.

S_{sk} = Skewness of the peaks, a surface with one plateau and deep fine valleys, $S_{sk} < 1$; a surface with many peaks on a plane, $S_{sk} > 1$.

S_{ku} = Kurtosis of the peaks.

S_z = Ten point height of the surface, mean difference between the 5 highest peaks and 5 deepest valleys.

Spatial Parameters

S_{ds} = Density of peaks.

S_{tr} = Texture aspect ratio of the surface, has the same characteristics in all directions, $S_{tr} \approx 1$; has an oriented or periodic structure, $S_{tr} \approx 0$.

S_{al} = Fastest decay autocorrelation length

S_k = Core roughness depth

S_{pk} = Reduced summit height

S_{vk} = Reduced valley depth

Functional Parameters

S_{bi} = Surface bearing index ($0.3 < S_{bi} < 2$), larger values indicate a greater number of wear shelves.

S_{ci} = Index of core retention, a measure of fluid retention.

S_{vi} = Index of valleys retention.

DISCUSSION

Effect of Deposits on Drying Rate and Drying Economics

In addition to providing data about the contamination process, the dryer can samples can also be used to estimate the resultant reduction in dryer can heat transfer coefficients. A reduction in the overall dryer can heat transfer coefficient (steam to paper), reduces the energy transferred to the sheet and in turn results in decreased machine productivity. Once the reduction in heat transfer coefficient is calculated, the drying rate and possible cost implications due to the decrease of drying rate can also be calculated.

Calculations for the deposits collected are shown in Appendix B. Based on the analysis of deposits collected, the overall reduction of heat transfer coefficient may be up to 40%. A summary of the results describing the effect of deposits on the drying rate, decrease of water removal, outgoing solids and outgoing sheet temperature is given in Table 3.

Table 3. Effect of Heat Transfer Reduction on Drying.

Heat Transfer Coefficient Reduction (%)	**Heat Transfer Coefficient** (W / (m^2 K))	**Average Drying Rate** (kg/(m^2 hr))	**Water Removal** (g/m^2)	**Water Removal Reduction** (%)	**Outgoing Solids** (%)	**Outgoing Sheet Temperature** (^oC)
0	491	21.8	24.22	0	45.66	71.9
20	393	19.6	21.76	10.2	45.26	68.5
40	295	17.5	19.43	19.8	44.88	64.6

As it is seen from Table 2, decrease of heat transfer coefficient by 40% resulted in decrease of drying rate by about 20 %. At higher heat transfer coefficient, negative effect of contaminant is more pronounced. For the case, when heat transfer coefficient was 628 $W/(m^2 K)$, the reduction of heat transfer coefficient by 40%, led to the decrease of drying rate by 21.2%.

In addition, a lower outgoing sheet temperature due to contamination of the first dryer cans entails the reduction of the drying rate in subsequent groups of cylinders.

Hence, in reality, an adverse effect of the contamination on the first dryer cans on the performance of the whole dryer section could be worse than that calculated above.

For a dryer-limited linerboard paper machine producing 235000 tpy, a reduction of average drying rate of 1% results in decreased production of $1,000,000 due to decreased machine speed. If additional dryer cans are installed to prevent the reduction of speed and paper output, annual capital costs and energy consumption increase by about $1/ton (See Appendix B for details of the calculations).

Effect of Deposits on Picking/Sticking

Establishing a correlation between the dryer deposits and web picking/sticking may make it possible to reduce or eliminate the deposits. An increase in sticking can be identified by an increase of the wrap angle and the draw. An increase of the web draw leads to higher web tension and probability of web breaks, resulting in increased down time and a reduction of paper output.

Web picking rate ($g/(m^2 s)$) can be determined by collecting fibers doctored off of the dryer can surface over a given period of time. If the dryer can does not have a doctoring mechanism, the concentration of fibers in deposits is an indicator of web picking. Web picking rate is calculated by dividing the weight of doctored off fibers by the product of the web contact area and run time:

Peeling rate =

Weight of Doctored Fibers / [(Web Contact Area on the Can)(Run Time)]

This value should be related to adhesion (sticking/picking) force and internal bond strength (Z-direction tensile) of the wet web. Adhesion force can be calculated from the tension force based on the Mardon equations. Unfortunately, no standard method exists for measuring internal bond strength for wet samples. TAPPI Test T541 om-89 for dry paper would not work for a wet sheet.

Picked fiber loading may be determined as the product of the picking rate and the contact time of the web on the dryer can. The ratio of the picked fiber loading to the web basis weight indicates the fiber loss due to picking.

CONCLUSIONS

Guidelines and procedures for sampling and analysis of contamination deposits on the dryer can surface were developed and implemented. Scrapings were used for identification of chemical composition of the deposits and deposit loading. Back-scattered scanning electron microscopy with energy dispersing spectroscopy analysis (SEM/EDS) was used to identify the presence and spatial distribution of inorganic components in the deposits. Fourier Transform Infrared (FTIR) Spectroscopy coupled with ash content test identified most of the major components present in a deposit. These data were used as input variables for determining the adverse effect of the dryer can deposits on drying rate and productivity of a paper machine.

Replicas of the dryer can surface were used for measuring deposit thickness and surface topology of the contaminated dryer can and bare metal substrate. Application of non-contact high-resolution laser-based measurements provided a map of the surface roughness for the contaminant layer and substrate.

A method for calculating the effect of the contaminant layer on the heat transfer coefficient and drying rate was developed. The contaminant layer was considered as an additional heat transfer resistance. Drying rate was calculated from transient heat balance equation using the analogy between heat and mass transfer.

At a contaminant loading of not more than 10 gsm, the calculated reduction of heat transfer is about 20-40% for highly porous contaminated layer. No reliable results for the porosity of the contaminated layer on the inspected dryer cans were obtained. A decrease of heat transfer coefficient by 40% results in a decrease of drying rate by about 20%. At higher heat transfer coefficient, negative effect of contaminant is more pronounced.

The potential decrease of sales due to the necessitated reduction of dryer speed may be about $1,000,000 per each percent of decrease of average drying rate in the whole drying section. If additional dryer cans are installed to prevent the reduction of speed and paper output, annual capital costs and energy consumption increase by about $1/ton. The above numbers are conservative estimates, because they do not account for reduction in the productivity in subsequent sections of the dryer induced by lower sheet temperature after contaminated dryer cans.

LITERATURE CITED

Ahrens, F., Orloff, D. Drying Productivity. Project F021. Status Reports to the Papermaking Project Advisory Committee, Volume II, March 24-25, 1999.

Ahrens, F., Patterson, T. Drying Productivity. Project F021. Status Reports to the Papermaking Project Advisory Committee, March 8-9, 2000.

Appel, D. W.; Hong, S. H. OPTIMIZING HEAT TRANSFER USING BARS IN DRYERS. Paper Technol. 16, no. 4: 264-269 [T171-176] (Aug. 1975).

Burgess, B.W., Seto W., Koller E. and Pye, I.T. The Pappridryer Process. Part II – Mill Trials. Pulp and Paper Mag. of Canada, Vol.73, #11, November 1972, 73-81.

Chance, J.L. State of technology on drying of paper. Svensk Papperst., #14, 1983, 18-25.

Containerboard. Pulp & Paper, January 2000: 55,62.

Fusco, S.P. Guidelines for the Safe Operation of Steam Heated Paper Machine Dryers, 1995

Gavelin, G. (Edited by) Drying of Paper and Paperboard. 1972

Han, T.S. and Ulmanen, T. Heat Transfer in Hot Surface Drying of Paper. Tappi, Vol.41, #4, 185 – 189, April 1958.

Janson, L. and Nordgren, B. Drying of paper on the felt-covered drying cylinder. Svensk Papperstid., 61 (19): 834 - 843 (1958).

Karlsson, M (Edited by) Papermaking Part 2, Drying. 2000

Nuttal, G.H. Theory and Operation of Fourdrinier Paper Machine. 1967.

Pulkowski, J.H. and Wedel, G.L. The effect of Spoiler bars on dryer heat transfer. Pulp & Paper Canada 89:8 (1988), T258-T263.

Ratto, P. and Rigdahl, M. Temperature distributions in a paper sheet subjected to a short pressure pulse from a heated plate. Nordic Pulp and Paper Res. J, Vol.13, #2, 101-106, 1998.

Reese, J. Private Communications, November 2000

Reese, R. Revised TAPPI drying-rate curves. Tappi J., December 1988, 231-233.

Rohsenow & Hartnett, Handbook of Heat Transfer, 1973

Task 2

Develop the facilities to simulate the contaminant deposition process under controlled experimental conditions (Contamination Test Stand – CTS)

Final Status

Equipment and test stand were built, however it provided inadequate for studying contamination initiation and buildup.

CONTAMINATION TEST STAND (CTS)

Timothy Patterson

Daniela Edelkind

EQUIPMENT AND TEST PLAN OVERVIEW

The CTS (see figure and pictures on following page) was intended to simulate conditions in the dryer section of a paper machine. It has an upper roll, which can be heated to dryer can temperatures by means of an induction heater. A press felt was run against the lower surface of the hot roll and around rollers in a closed loop. Arced pieces of metal (coupons - steel, cast iron or steel with chrome surface) are attached to steel rings which in turn are attached to the upper roll. The intent was to test the tendency of each surface type to promote sticking from a wet sheet similar to what would be present at the entrance of the dryer section. The felt was run though a bath of pulp and contaminants, the intent being to have the felt simulate a wet sheet. Slurry is added to the bath at a steady rate so that a constant supply of fresh ingredients is always being applied to the felt. After exiting the bath, the felt was vacuumed to remove excess slurry. The bath and supply tank for the bath are kept continuously agitated. The slurry forms a film on the surface of the felt. This film is then brought into contact with the heated roll as the felt contacts the lower surface of the roll. Fiber, resins, and or polymers in the slurry which have a tendency to adhere to the heated roll surfaces should then build up on the test surfaces. It was assumed that different surfaces would have different tendencies to adhere. The speed of the machine is adjusted to give specific contact times (dwell times) between the contaminant-containing felt and the hot roll.

Test variables were:

- Roll Temperature (determined by induction heater power output)
- Roll speed – dwell time
- Slurry concentration
- Bath pH
- Contaminants (polymers from model contaminant identified in Task 1)

Measurements of all of these factors were be checked hourly and adjusted as necessary. It was planned to analyze buildup on the roll by examining the size and constituents of deposits on the coupons. Build up rates were to be measured by removing coupons from the roll at 1/3 and 2/3 of the way through a particular test. The contaminated coupons were to be removed, inspected visually for signs of picking (fibers from paper stuck to the coupon) and stickies. The coupons could then be used to obtain work of adhesion via the WADS apparatus.

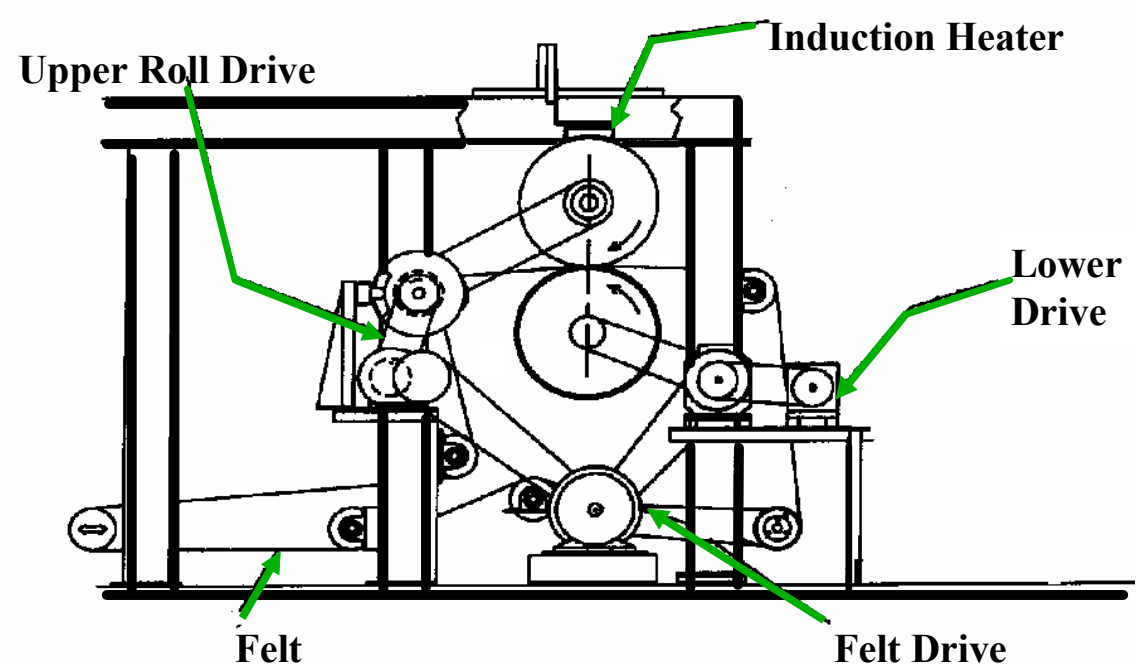

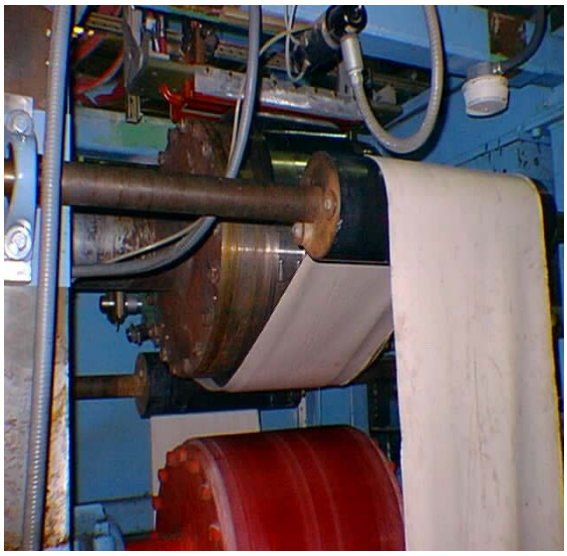

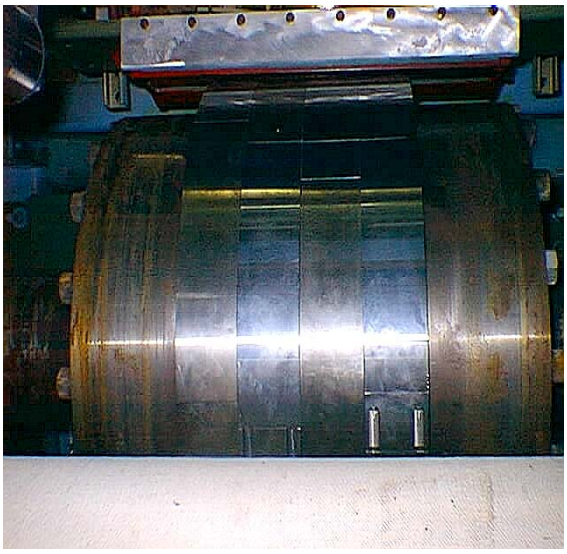

Contamination Test Stand

CONTAMINATION TEST STAND MODIFICATIONS

1. The Roll Test Stand was pressure washed and a general clean up of the surrounding area was performed.
2. Non working sensors (roll speed and felt break sensors) were replaced.
3. Broken airline filter was replaced.
4. Wiring for non existent instrumentation was removed from the control panel cabinet and wire trays. This will enhance signal quality from existing sensors.
5. Felt tracking mechanism was repaired.
6. Doctor blade system was pressurized and correct operation was confirmed.
7. Correct operation of Roll Test Stand control system was confirmed. A maximum speed of 2600 rpm was attained.
8. The induction heater was turned on, arcing between the heater and the roll was observed. The heater was returned to the manufacturer (IndcuctoHeat) for repair/rebuild.
9. Induction heater cooling system was flushed and filled with fresh deionized water. The conductivity of the water was tested to confirm it was within specified limits.
10. The machine felt run was altered to ensure the slurry wetted flet would run up against the lower surface of the heated roll.
11. Runnability of the wet felt over the anticipated speed range was confirmed.
12. A slurry preparation and application system, consisting of a 250 gallon mixing tank, piping and an application bath were constructed.
13. A catch pan was fabricated. The current plan is to recycle the fluid used to contaminant the felt and coupons. Previous experience has shown that the felt will shed liquid over the entire length of the felt run. All of this liquid needs to be recovered, both for recycling purposes and to insure proper disposal at the conclusion of testing.
14. A data acquisition system was setup to monitor machine conditions.

PLANNED CTS COUPON USAGE

Coupon Types	Number Available
CIR – Cast Iron, non-polished surface	9
CIS – Cast Iron, polished surface	3
Ch – Chrome	12
ST – Steel	6

Bold Font – Coupon installed at the beginning of the test.
Regular font – Coupon installed during the test.

START to 1/3 Time

	Ring 1		Ring 2		Ring 3		Ring 4	
	Type	ID	Type	ID	Type	ID	Type	ID
Half A								
Position 1	**CIS**		**Ch**		**Ch**		**ST**	
Position 2	**CIR**		**CIS**		**CIS**		**ST**	
Position 3	**CIR**		CIR		CIR		**CIR**	
Half B								
Position 1	**Ch**		**CIR**		**CIR**		**CIR**	
Position 2	**Ch**		**Ch**		**CIR**		**Ch**	
Position 3	**ST**		**Ch**		**Ch**		**Ch**	

Added: CIR (9), CIS (3), Ch (9), ST (3)

1/3 Time to 2/3 Time

	Ring 1 - removed		Ring 2		Ring 3		Ring 4	
	Type	ID	Type	ID	Type	ID	Type	ID
Half A								
Position 1	--	--	**Ch**		**Ch**		**ST**	
Position 2	--	--	**CIS**		**CIS**		**ST**	
Position 3	--	--	CIR		CIR		**CIR**	
Half B								
Position 1	--	--	**CIR**		**CIR**		**CIR**	
Position 2	--	--	**Ch**		**CIR**		**Ch**	
Position 3	--	--	**Ch**		**Ch**		**Ch**	

Removed: CIR (2), CIS (1), Ch (2), ST (1)
Added: none

2/3 Time to Finish

	Ring 1 - removed		Ring 2		Ring 3		Ring 4	
	Type	ID	Type	ID	Type	ID	Type	ID
Half A								
Position 1	--	--	ST		Ch		Ch	
Position 2	--	--	ST		**CIS**		ST	
Position 3	--	--	**ST**		CIR		Ch	
Half B								
Position 1	--	--	**CIR**		**CIR**		**CIR**	
Position 2	--	--	**Ch**		**CIR**		**Ch**	
Position 3	--	--	**Ch**		**Ch**		**Ch**	

Removed: CIR (2), CIS (1), Ch (2), ST (1)
Added: ST (3), Ch (3)

TEST RESULTS

The methodology employed for simulating roll contamination did not produce the anticipated results. There were two inherent problems

1. Application of the slurry to the felt
2. Use of the slurry wetted felt to simulate a wet sheet

The application of the slurry to the felt using the bath was extremely difficult to control. The pulp in the bath tended to form flocs making for non uniform fiber application. Slurry pH also tended to vary excessively during any given test. An attempt was made to use spray nozzles instead of the bath for slurry application. The nozzles clogged continuously.

Despite running a number of test conditions (fiber concentration, contaminant concentration, slurry pH, slurry application rate, roll temperature, dwell time), contamination was never observed to build up on the test surfaces.

Rather than continue to invest time in this task it was abandoned.

Task 3

Develop facilities to simulate web transfer from contaminant surfaces and measure work of adhesion (Web Adhesion and Drying Simulator – WADS).

Task 4

Develop models to of contamination, adhesion, and picking.

a. **Define model contamination systems.**
b. **Simulate contamination process using the CTS and compare to mill data.**
c. **Simulate web transfer during pressing and drying and measure both work of adhesion and picking**
d. **Explore variables and develop correlations**

Final Status

Task 3 – Completed
Task 4

Sub-Task a. – completed
Sub-Task b. – not completed
Sub-Task c. – drying simulation completed, pressing simulation not completed
Sub-Task d. – correlations for completed

Laboratory Studies of Picking & Sticking Using the Web Adhesion and Drying Simulator

Fred Ahrens
Medea Alexander,
Melissa Austin
Fred Bloom
Daniela Edelkind
Edward Lindahl
Shana Mueller
Timothy Patterson
David Orloff

Table of Contents

I. Objective: Page 3

II. Background: Pages 3-5

III. Experimental Conditions/Procedures: Pages 5-10

IV. Results & Discussion: Pages 10-32

V. Conclusions: Pages 32-33

VI. Future Work: page 33

VII. References: Page 34

VIII. Appendices

Objective

This work addresses the problems of sticking and picking during web separation from dryer can surfaces. Web interaction with, and the build up of, surface contamination were the primary focus. The objectives of the work were to:

1. Characterize and quantify the factors controlling adhesion of the web to the dryer can surface during the web separation process.
2. Characterize and quantify the factors controlling web picking during the web separation process
3. Develop Methods for minimizing the work required to achieve web separation and for minimizing web picking and dryer can contamination.

Background

Dryer can contamination can create significant operating problems for the papermaker. The contamination generally has "sticky" components that result in picking and sticking of the paper web. In addition to the detrimental effect on paper quality, the machine productivity is affected by increased web breaks and downtime for cleaning the dryer cylinders. Typically, the first dryer section is also run at lower than maximum temperatures in an effort to decrease the rate of contaminant buildup, further reducing machine productivity. As the contaminants accumulate on the dryer surface, the heat transfer rate from the can to the sheet is decreased as well.

The interaction between two competing factors; web adhesion to the cylinder surface and web cohesion, results in varying degrees of picking and sticking. The working hypothesis was that as adhesive forces exceed the cohesive strength of the web, picking and sticking will increase and the energy required to separate the web from the cylinder surface will also change. By recognizing what causes and fosters this phenomena, ways of preventing and reducing picking and sticking, as well as optimum dryer operating strategies (if any) can be determined. The primary tool used was the Web Adhesion and Drying Simulator, a laboratory device that incorporates the ability to measure peel force under simulated dryer conditions.

Literature Review

While appeasing environmental concerns, the use of recycled materials has some drawbacks for the paper manufacturer. The introduction of tacky adhesives into the pulp mixture results in deposition onto dryer cylinder surfaces and the consequent picking and sticking problems. There have been a few related investigations of picking and more commonly sticking of the paper web to dryer cylinder rolls. The majority of the literature concerns the identity and properties of the contaminants or "stickies" themselves. These articles focus primarily on controlling the problem through chemical modifications and additives.

Meinecke, et al [1988] conducted a study relating picking to ingoing solids, surface temperature and machine speed (contact time). This was however not a quantitative

study and the corresponding work of adhesion was not measured. The investigation did yield the following surface map (**Figure 1**) of the data

In his paper, Meinecke points out that in order to resolve a picking problem from a given condition, a large increase or decrease in temperature is necessary. He postulates that this primary dependence on temperature is due to the change in softening point of lignin and hemicelluloses with water content. Picking occurs when the temperature of the sheet meets or exceeds the softening point, which can be lowered by the presence of water.

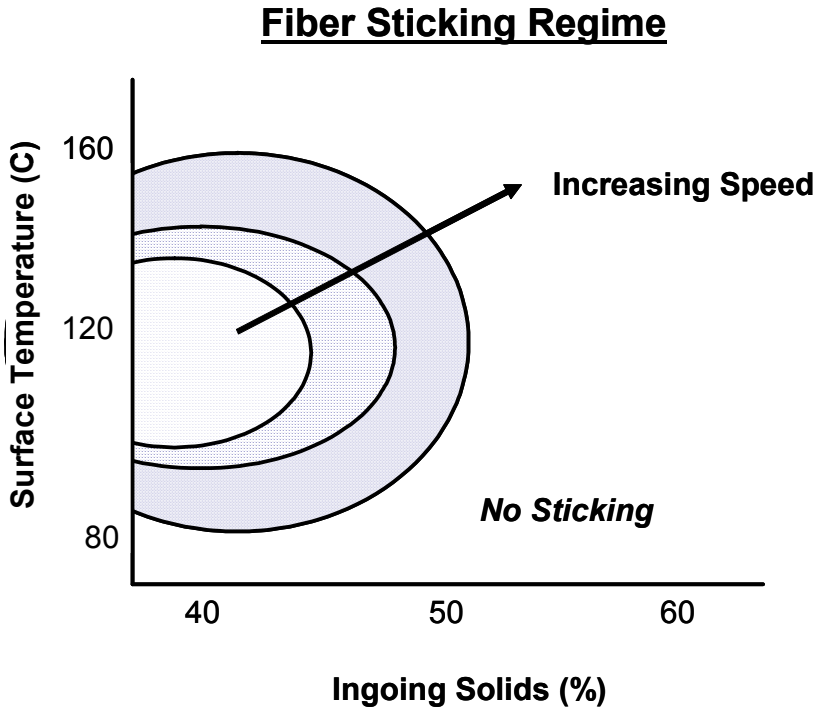

Figure 1: "Meinecke" Suface Map

Much of the pioneering work to quantify the sticking phenomena was done by J. Mardon [Mardon et al, 1976, 1967]. He built a low speed laboratory peel tester to measure the peel force (tension) and relate it to peel angle and speed. As a result of his work, he developed an equation correlating the peel force to the Work of Adhesion:

$$T' = \frac{W''}{1-\cos\phi} + mV_1^2$$

T' = Tension
W" =Work of Adhesion
m = Mass per unit area
V_1= Velocity
ϕ = Peel Angle

Work of Adhesion or Separation is a fundamental parameter that depends on a number of factors including surface topology, surface materials, surface energy, contaminants, fiber characteristics, application pressure, surface and sheet temperature and moisture content. Picking/sticking occurs when the adhesion between the web and the dryer roll surface is of the same order of magnitude as the internal cohesion of the web. The interaction between cohesion and adhesion is a dynamic one that changes as the web passes through the dryer section. Picking/sticking is most significant in the first dryer section where it appears that adhesive forces are high and cohesive forces low.

Mardon's sheet stripper apparatus could not employ heated surfaces so it could not simulate realistic dryer conditions. The Web Adhesion Drying Simulator (WADS) was thus developed as a tool to aid in understanding the mechanisms behind picking and sticking under simulated dryer conditions.

Experimental Conditions/Procedures

Chemical Analysis

As a first step in eliminating/reducing dryer can contamination, it was necessary to identify the components of contamination. In addition to a thorough literature review, actual dryer can contamination samples were collected from several different paper machines. Scrapings of dryer rolls, as well as paper samples were collected from various positions of the paper mill. The material collected was analyzed using standard chemical analysis techniques including reactivity/solubility tests, FTIR (Fourier Transform Infrared) Spectroscopy, GC/MS (Gas Chromatography/Mass Spectrometry), ICP (Inductively Coupled Argon Plasma Emission Spectroscopy) and CIE (Capillary Ion Electrophoresis).

For the majority of the cases, the analysis revealed polyvinyl acetate (PVAC), polyacrylates and wood fibers to be the primary components on dryer cans closest to the press section (first dryer section). At one mill, the first dryer showed significant styrene-butadiene polymer residue while other rolls were contaminated with silicates (with clay), calcium carbonate and unbleached fibers and fines. Also present, though to a much lesser extent, were "solvent extractable hydrocarbons" thought to be defoamers, surfactants and wood resins/soaps. Mills producing coated paper can have especially significant dryer can deposits. In mills visited by IPST personnel, this was the result of returning broke to the production stream. The dryer can deposits in these mills contained high levels of the latex-based materials used to coat the paper.

A literature review supplemented the findings from the mill samples [Douek et al, 1997]. Fine paper mills using a high percentage of de-inked office waste in their pulp have sticking problems and spots in their finished product. The high levels of contaminants in the recycled pulp render usual screening and cleaning techniques insufficient to remove most of the polymeric material. Rejects from one particular fine paper mill were found to contain synthetic polymers (including PVA, EVA, polyacrylates, SBR-styrene-butadiene rubber), wood resin, clay and calcium carbonate.

In newsprint mills, studies show both organic and inorganic material deposits in the press/dryer section. The contaminants commonly found include polyethyl acrylate (from Pressure Sensitive Adhesives – PSA's), wood resins and their derivatives, and synthetic polymers such as ethylene vinyl acetate, polyvinyl acetate and polyacrylates.

Board mills often use old corrugated containers (OCC) for the recycled portion of their furnish. Many of the contaminants hail from the hot melt adhesives used for labels and packaging. These adhesives often are not tacky at room temperature but become so at higher temperatures. Consequently, they deposit in the dryer section, the hottest part of the papermaking process. Most complaints from board mills reference deposits on dryer fabrics. Analysis of dryer fabrics shows that these deposits can consist of a mixture of wood resins, other hydrocarbons, PVAC, EVA, SBR, wood fibers and inorganics. In one mill, a dryer fabric deposit was discovered to be all PVAC, while specks on the king roll of the wet calendar and on the finished product proved to be mostly starch.

With the results of the mill scrapings and literature search, a series of contaminants to be tested in conjunction with the WADS were identified. The tacky components of stickies were determined to be polymers from binders, coatings, and pressure and heat-sensitive adhesives as well as fatty acids (metal soaps) and resins found in wood fibers. Three polymer materials: a PVAC based adhesive (Vinac 884 from Air Products), a polyacrylate based adhesive (Carbotac 16171 from BF Goodrich) and a SBR latex compound were selected to represent the typical polymer contaminants. These compounds are not in their pure forms but rather in water-soluble emulsions chosen for ease of use in the lab setting.

The metal soaps, most commonly calcium and aluminum oleates, present a more difficult problem. These metal soaps form when dissolved soap anions (long hydrocarbon chains like fatty acids) combine with metal cations such as calcium and aluminum. While a sample of aluminum oleate soap powder was obtained from a rare-chemical supplier, it did not dissolve in water or several different alcohols, thus making coating on a coupon impractical. Currently an adequate solution for testing a metal soap on the WADS has not been identified.

WADS Equipment Description

The WADS system, shown below in **Figure 2**, consists of a belt driven flywheel to which a removable "coupon" is attached. Coupons (3inx 12.325in), which represent the dryer cylinder surface, are made of various materials including cast-iron, steel and chrome-plated steel and can be pre-coated with various model surface contaminants before installation on the WADS system for peel testing. Because the coupon is removable, the WADS can easily be used to investigate the effect of various surface materials and surface treatments on the peel force and work of adhesion.

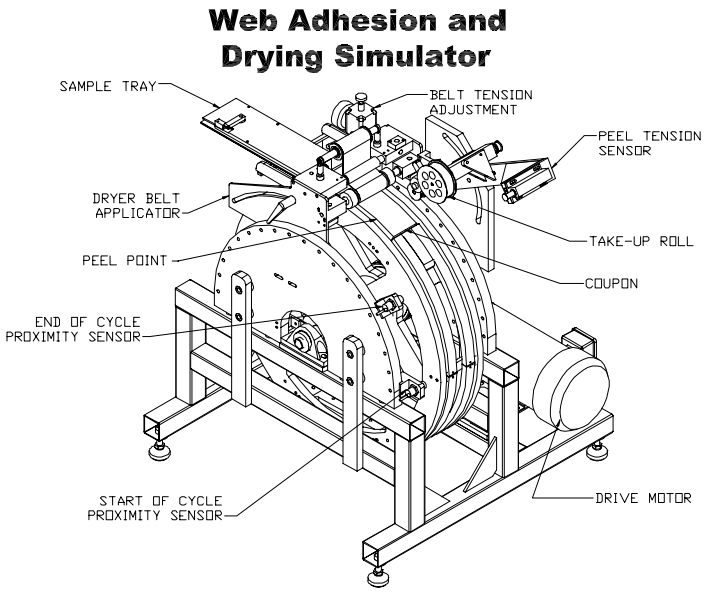

Figure 2: WADS Unit Schematic

The WADS has the ability to control and vary several parameters important in simulating realistic dryer roll conditions. The coupon surface temperature, one of the key testing parameters, can be varied from ambient to 350ºF. Peel angles can be adjusted from 0 to 90 degrees and a range of peel velocities, from 20 ft/min to approximately 400 ft/min is available. Dwell time (contact time between the paper and coupon) is adjustable using a combination of the fly wheel rotational speed and dryer belt wrap length and can be varied from 0.05sec to approximately 5sec. Web application pressure is controlled by belt tension and can be increased to several psi. In place of the dryer belt, a press roll attachment is also available and can be used to achieve application pressures of several hundred psi. The sample inlet (web) temperature, which plays a role in the degree of sticking, can also be adjusted in a range of 70ºF to 200ºF.

During an experiment (see **Figure 3**), the coupon makes one revolution from its start position at a set peel speed. The dryer belt (or optional press roll) acts to laminate the web (pulled in from the sample tray) onto the coupon as it makes its way around the wheel. The speed of the wheel and paper contact length of this dryer belt, both user specified parameters, determine the dwell time. After passing through the applicator section, the paper is pulled from the coupon at the specified peel angle and peel point with a length of inelastic fiberglass tape that is tracked over the tension sensor. The sensor records the peel force (tension) required to separate the paper web from the coupon. Note that the measured peel force includes not only the force required to overcome adhesion at the peel point, but also forces resulting from changes in web potential and kinetic energy that occur between the peel point and tension sensor.

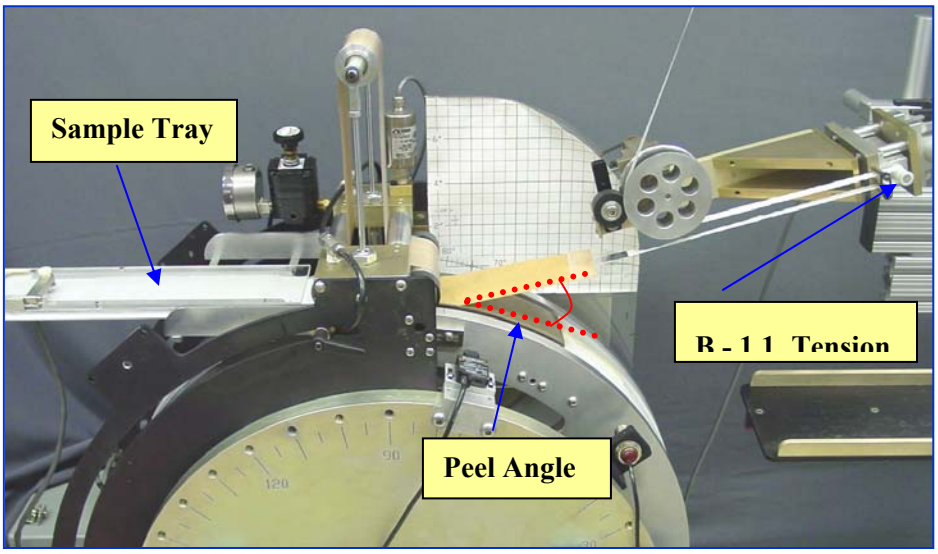

Figure 3: WADS Unit During a Peel Event

Upon completion of the peel event, a proximity sensor triggers the brake. The data acquisition program (Labview) collects the peel speed, tension, belt application pressure, and coupon surface temperature throughout the course of an experiment as shown in **Figure 4**:

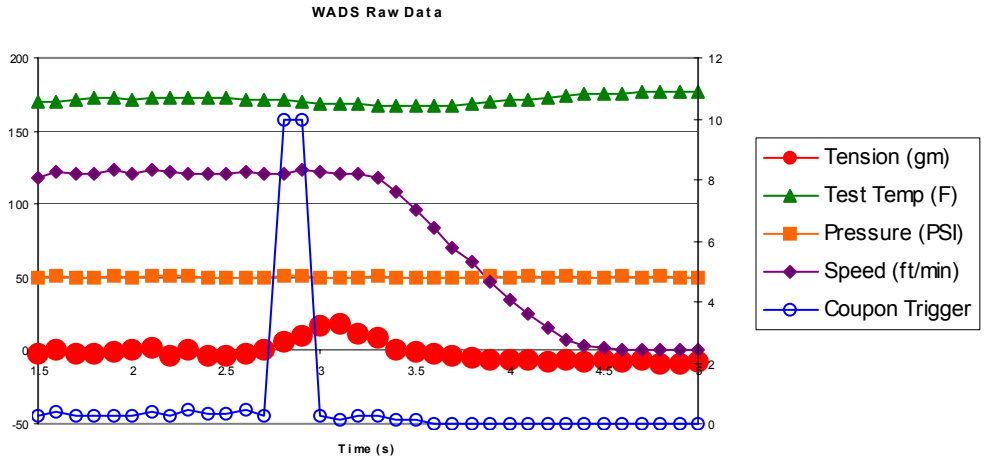

Figure 4: WADS Raw Data

A proximity sensor provides a voltage spike (coupon trigger curve shown in the graph) which functions as a time stamp at a specific point in the peel event. This allows the onset and end of the peel to be identified and the data to be synchronized with the high-speed video.

Video images taken during the equipment debugging stage showed that the actual peel angle varied significantly from the set point for some conditions. If the paper does peel at the correct peel point (radial point read from the grid) of 75 degrees it does not peel at the proper peel angle. **Figure 5** is an example of this – though the machine is set for a 15° peel angle, the actual angle is approximately 9°. This is primarily due to the fact that the paper does not peel from the coupon surface at a sharp angle. Rather, there is some curvature due to lack of adhesion and inherent stiffness of the paper creating this discrepancy. Since the peel angle is required in the Mardon Equation to solve for work of adhesion, an accurate angle measurement is critical. Similar results were observed by Mardon who found that at set points of 90°, the actual angle was about 45° [Mardon, 1976]. He used a Fastex camera to account for the actual angle in the calculations. A high speed digital camera (Olympus PCI-2000S) was thus incorporated into the WADS setup in order to accurately measure peel angles. A frame-by-frame image analysis using Optimas (see Appendix B for a more detailed description), an image analysis software program, was employed to measure peel angles correlating with tension measurements. The Mardon equation was then be applied locally for each discrete point.

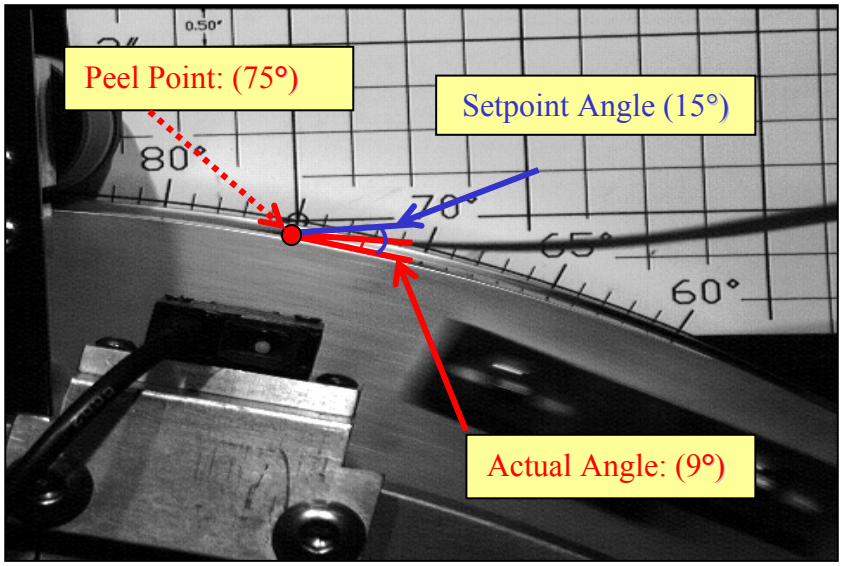

Figure 5: Peel Angle Variation

Initial experiments on the WADS unit showed a significant level of noise with the tension sensor. Viscoelastic vibration damper material was used to mechanically isolate the frame which supports the sensor. In addition, a low pass filter was installed into the

system to electronically reduce noise. Static calibration of the sensor demonstrated that readings are accurate within +/- 0.1g. Dynamic tests show a consistent 1g frictional drag of the tape over the sensor apparatus which increases the tension output. This factor is incorporated into the data analysis when determining the real peel force.

WADS Sample Preparation

For all WADS experiments, paper samples were formed using a Formette Dynamique. Unless otherwise specified, Virgin Kraft Liner Board (VKLB) at 100 g/m^2 and 500-550 CSF was used. The formette sheets were initially pressed to approximately 35% solids with a standard roll press apparatus. The sheets (35in x 10in) were then cut into 2 ½in x 11in sections and joined with the pull tape and Mylar joint to create a WADS paper sample as illustrated in **Figure 6**. Immediately prior to testing, the sample was dried to the correct moisture content with restrained drying under blotter paper (often weighted).

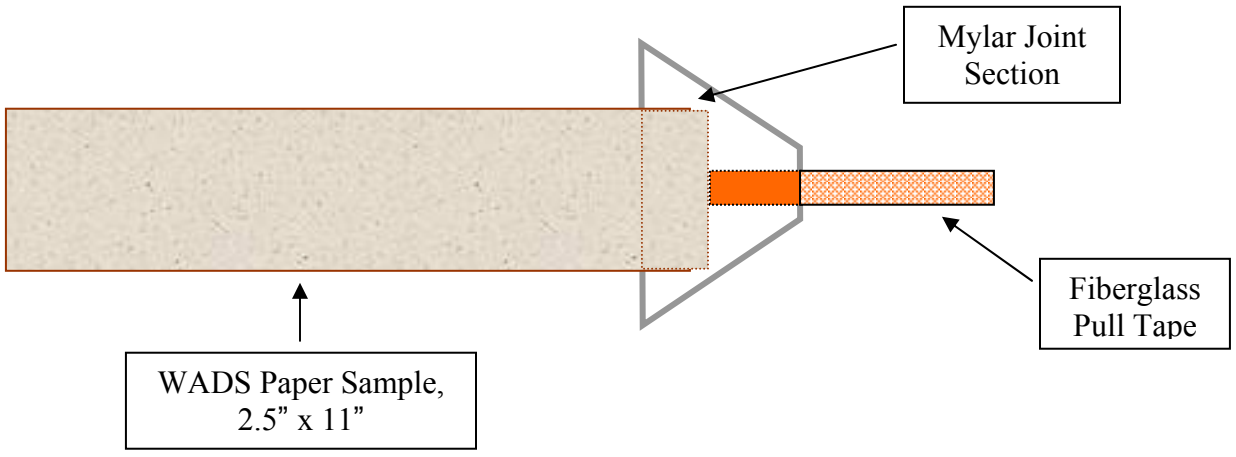

Figure 6: WADS Paper Sample

Contaminated coupons were prepared by coating the appropriate compound (either Carbotac or Vinac as mentioned earlier) with a gauged metering rod (RDS, Inc) to ensure uniform thickness. For most of the data presented in this paper, two coats with the 18µm metering rod were applied before curing. After curing, thickness across the surface was measured and recorded using a CMI (Coating Measurement Instruments) thickness probe. The thickness tolerance was 25µm +/- 5µm. The coupon was then attached to the WADS unit and preheated to the test temperature.

Results/Discussion

Clean Coupon/Roughness Tests

Initial tests were performed with clean, uncontaminated cast-iron (unpolished Class 40 Cast-Iron) coupons. The conditions evaluated are summarized in the **Table 1.**

% Solids (Initial)	Coupon Temperature (ºF/ºC)	Dwell Time (s)
40	194/90	0.194
50	248/120	0.426
60	302/150	

Table 1: Clean Coupon Experimental Conditions

A total of 18 separate experiments, with 5 repeats of each test, were conducted. As expected, the clean coupons showed negligible sticking and picking. No measurable quantities of picking were observed. Achieving the desired set point peel point, 75º, proved to be extremely difficult as there was very little sticking to create an adequate peel event. For many cases, the paper appeared to simply slide across the surface rather than peeling at a sharp angle.

An analysis of the data revealed work of adhesion values that were extremely low, in the range of 0.03 –0.09 g/cm. The general trends showed work of adhesion decreasing with increasing temperature and increasing solids. The results were inconclusive for dwell time; some conditions generated increasing work while others demonstrated the opposite trend. Another important observation was made with the peel angles – during these runs, it was found that the peel angle appeared to increase during the course of the peel event. This corresponded with the peel point decreasing during the peel event. This phenomenon appeared to occur because of the low adhesion to the roll.

Next, a study of surface roughness effects was initiated. Three types of clean coupons were used – a normal (unpolished Class 40 Cast-Iron), a smooth (polished) and rough (sandblasted). Only 3 conditions, based on the results from the clean coupons tests, were tested. A “sticky” case (40 % Solids, 194 F, 0.426 s), a “non-sticky case” (50% Solids, 248 F, 0.426s) and a longer dwell time case (40 % Solids, 194 F, 0.542 s). Five repeats of each condition were performed. The results for two tests are shown in the figure below (**Figure 7**). There was insufficient data for the long dwell test because the tension exceeded the maximum output of the tension sensor for many of the runs.

As expected, there was higher work of adhesion for the sticky cases than for the non-sticky, although both are in the extremely low range. Both conditions showed higher work with the normal surface than with the other two surface conditions. The rough and

smooth coupons demonstrated very similar results. A possible explanation for this result is that the rough coupon has less surface area for the adhesion to occur causing lower work of adhesion to be measured. For the smooth coupon, the opposite is true – there is much more surface area available which results in much better drying and consequently lower adhesion. These tests will have to be repeated with contaminated coupons or contaminated fabrics to establish whether surface condition affects deposition of stickies.

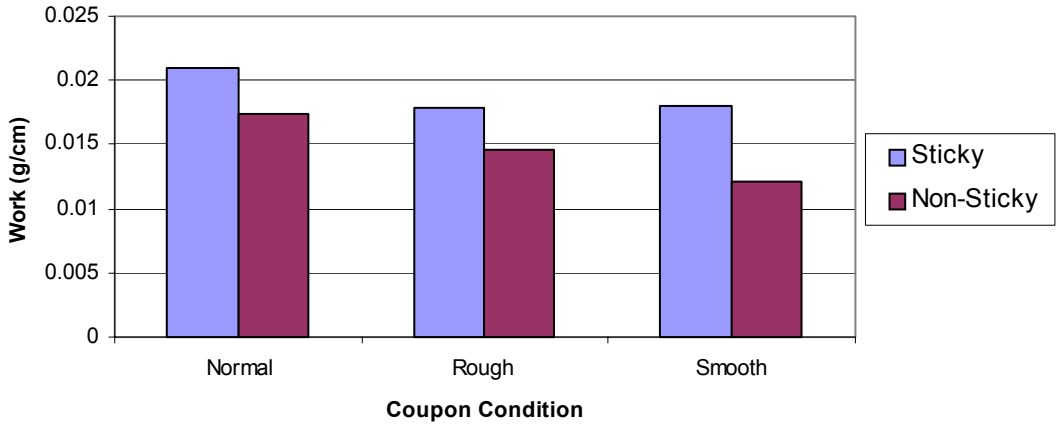

Figure 7 : Roughness Summary: Work of Adhesion as a Function of Surface Condition

Initial Carbotac Contamination Tests

Following the surface roughness tests, experiments were performed with contaminated coupons. Ten repeats of each test condition were run on a single coupon. Coupons were coated with Carbotac 26171 (BF Goodrich) according to the procedure outlined previously. For these initial tests, the following conditions were examined:

B Parameter	B Setting
Coupon Surface Temperature	194° F, 248° F, 302° F (90°C, 120° C, 150° C)
Dwell Time	0.194s, 0.426 s
Initial Sheet Temperature	100° F (38 °C)
Initial Sheet Solids	40%, 60%
Peel Speed	150 ft/min (0.50 m/s)
Set Point Peel Angle	15 degrees
Paper Type	Liner Board
Contaminant	Carbotac 26171 (B.F. Goodrich)

Table 2: Initial WADS Contaminant Testing Conditions

Work of adhesion values were 100 times greater than with clean coupons, so sticking was very significant. The work of adhesion data for run 1 for the different conditions is displayed in **Figure 8**.

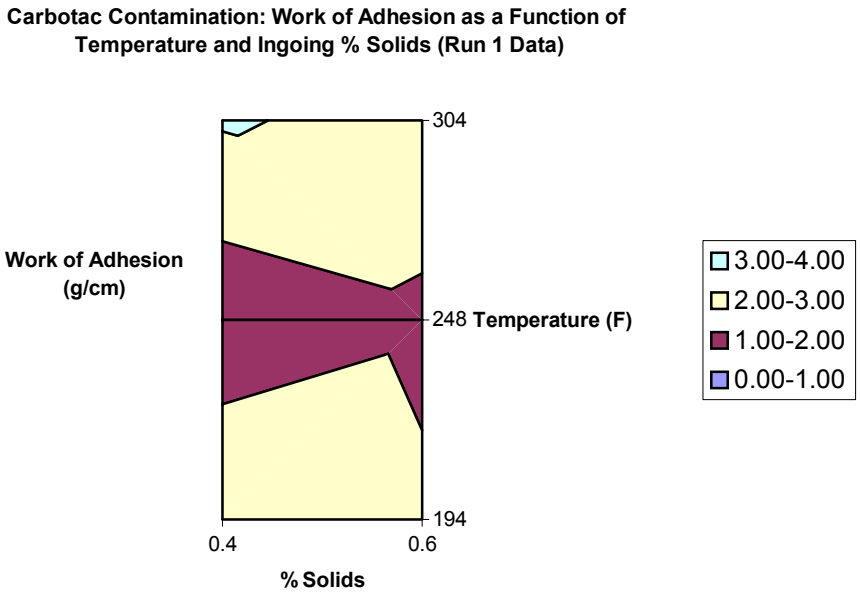

Figure 8: Work of Adhesion vs. Conditions

The results indicate that there is an area of lower work around the midpoint temperature at 248ºF with higher work of adhesion at lower and higher temperatures. Several industry representatives had stated that due to heavy picking at temperatures near 200ºF, they had lowered their dryer cylinder surface temperatures to the 150ºF range. So the intermediate temperature was replaced with a lower temperature condition at 149ºF (65ºC). The experiment was rerun, again with ten repeats on a single contaminated coupon. For the longer dwell time tests, the tension was beyond the range of the tension sensor and therefore not recorded although picking data were still collected. The data, shown in **Figure 9**, have revealed that these are not in fact repeats since picked fibers remaining on the surface result in changing surface conditions. Runs 1 and 2 show high levels of sticking and consequently work of adhesion. With each subsequent run, more fibers deposit on the surface, reducing the sticky surface area and giving intermediate work results. By run 10, the work of adhesion values plateau to a low level in which no additional picking was observed. In the real dryer section, the deposition of contamination on the dryer cylinder surface is a continuous one, so the sticking levels may not diminish as multiple layers of contaminant/fiber are formed.

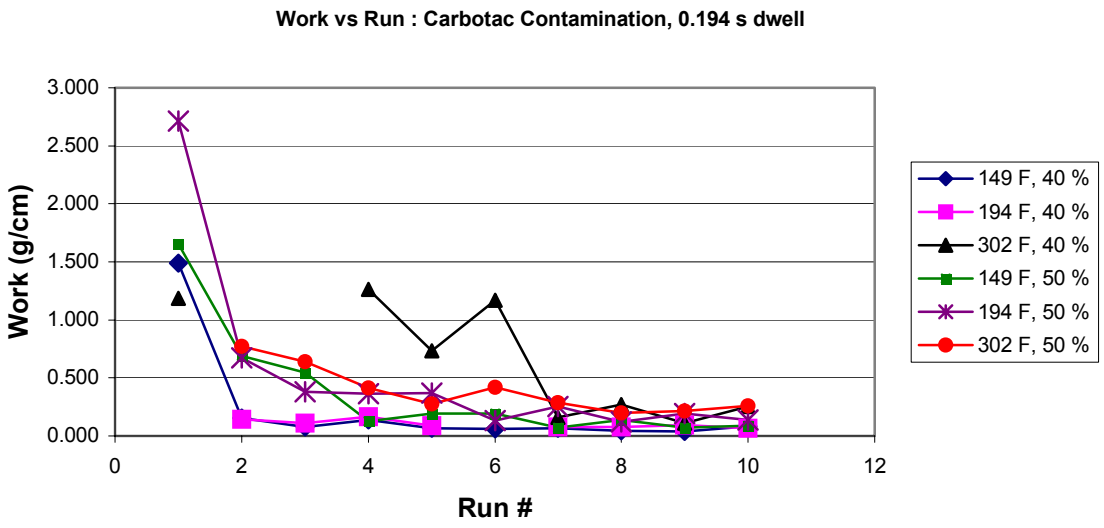

Figure 9: Work of Adhesion vs. Run #

These initial results indicated that the work of adhesion for the first run of each condition shows a primary dependence on temperature. Because these were not true repeats, a complete analysis of the relationships among work, solids and temperature could not be performed.

In addition to the work analysis, a quantitative description of picking/sticking was also determined for the conditions listed in the table above. A high-resolution digital photo of a set area of the coupon surface was taken following each run. **Figures 10 and 11** show the images taken after the first run for each test condition (first set of tests). The figures show qualitatively that the 40% solids samples had more picking than the 60% samples. There also appears to be less picking at higher temperatures, particularly at higher solids.

40 % Solids, 194 F | 40 % Solids, 248 F | 40 % Solids, 302 F

Figure 10: Picking 40% Solids Samples

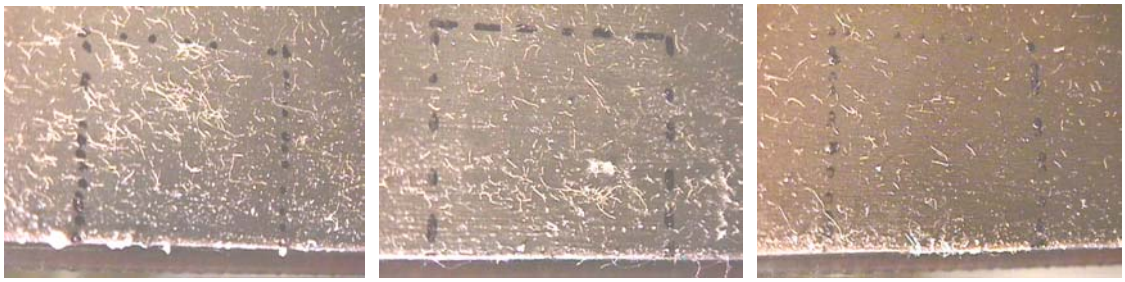

60 % Solids, 194 F 60 % Solids, 248 F 60 % Solids, 302 F

Figure 11: Picking 60% Solids Samples

A quantitative measure of the picking was determined using image analysis of the high-resolution photos to obtain a percent fiber area. Run 1 picking data for the different conditions are shown in a surface graph in **Figure 12**. This data follows the original results of Meinecke showing the same trends in picking with changing surface temperature and ingoing solids. As expected, more picking is observed at the lower ingoing solids due to poorer sheet consolidation and bonding within the web.

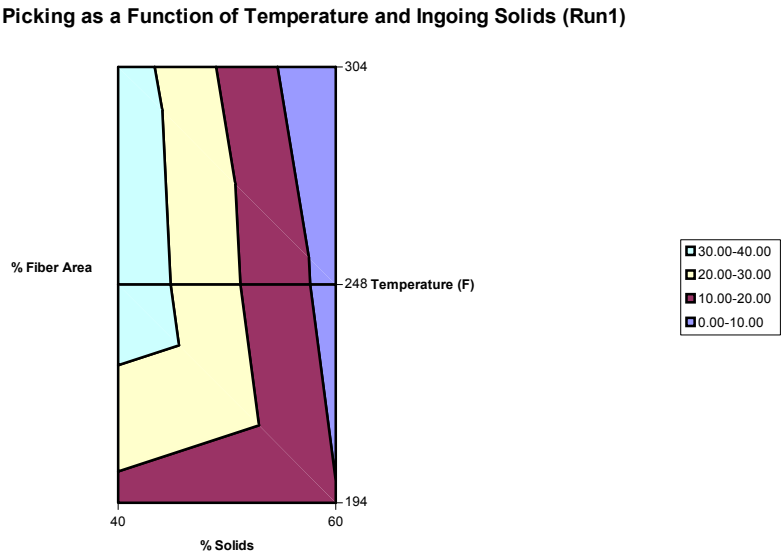

Figure 12: Run 1 Picking Data

An interesting phenomenon occurred with the 40% solids samples at 248ºF and 302ºF. During the peel, some sheets split in the in-plane direction, indicating that the adhesion to the surface overcame the cohesive forces of the web. The splitting became more severe at the higher of the two temperatures. When the sheet split, the part that remained on the coupon was easily removed in one continuous piece after the run. Not a true picking situation, it appeared that the thin layer of the sheet closest to the coupon was rapidly heated and dried by the coupon. This increased the cohesive nature of only that layer of the web. The remainder of the web retained a lower cohesive strength. The process of

heating and drying, at least momentarily, also increased the adhesion, with the result that the web split at the interface between the dry and wet regions.

The primary conclusion of this work is that both the adhesive forces between the roll and the web and the internal cohesive force of the web itself must be considered when the goal is to limit picking and sheet damage. For the contaminant studied, the adhesion decreases with increasing temperature. The sheet cohesive strength increases with web solids. The best case for reduced picking is high solids and high temperature. The worst case for picking is low solids and low temperature, however there is a complicating factor at low solids. A condition can be created, with high surface temperatures, which produces a discontinuity in the sheet cohesive strength and results in sheet delamination. This condition would probably be difficult to produce on a paper machine. Because there was no repeat data for the conditions tested, the next study planned involved multiple tests of each condition.

Carbotac & Vinac Contamination Tests

In order to perform true repeats of the test conditions, it was necessary to prepare a new contaminated coupon for each run. While this introduced some possibility for variation, coupons were carefully coated following a set procedure and monitored for thickness differences. Coupons whose coating thicknesses varied greatly from the average (more than +/- 5μm) were cleaned and recoated.

Testing became very time consuming as coupons had to be continuously coated and cleaned after only a single run. Consequently, the number of experimental conditions studied was reduced. The 60% ingoing sheet solids was eliminated since the results usually indicated only minor differences from the 50% solids runs. Furthermore, the higher dwell time test was also removed since the tension was often too high for the WADS tension sensor to record. This was due to increased work of adhesion with increased drying. As mentioned before, based on recommendations from the Papermaking Committee, the testing conditions were also modified to include a lower temperature case. Finally, the speed (but not the dwell time) was reduced to 120ft/min.

Tests had shown that the tension signal appeared smoother and more consistent at lower speeds. It was believed that this was due to some transient effect that was more prevalent at higher speeds. By expanding the belt assembly it was possible to reduce the speed while keeping the dwell time the same as in the prior tests.

The conditions were thus modified to:

B Parameter	B Setting
Coupon Surface Temperature	149° F, 194° F, 302° F (65°C, 90° C, 150° C)
Dwell Time	0.194s
Initial Sheet Temperature	100° F (38 °C)
Initial Sheet Solids	40%, 60%
Peel Speed	120 ft/min (0.40 m/s)
Set Point Peel Angle	15 degrees
Paper Type	Liner Board
Contaminants	Carbotac 26171 (B.F. Goodrich) Vinac XX-311 (Air Products)

Table 3: WADS Contaminant Testing Conditions

Experiments were performed with two contaminants – Carbotac and Vinac. The results from these tests are summarized in the chart below (**Figure 13**).

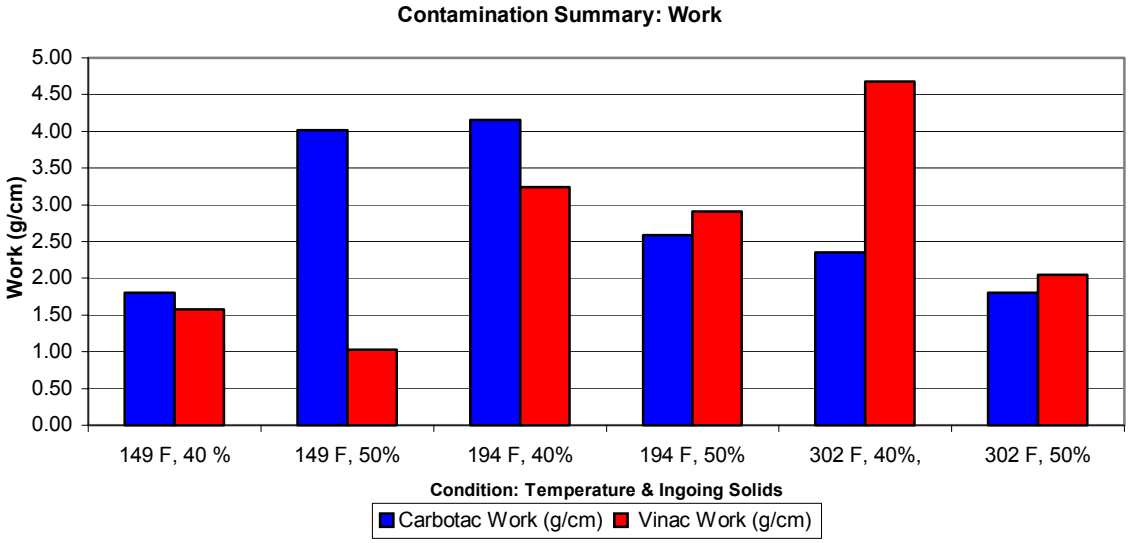

Figure 13: Contamination Summary

The chart shows similar trends for the two contaminants. In general, the work of adhesion decreases with increasing solids and temperature. This follows the relationship between tack and temperature that will be discussed in a following section. However, there is an exception at the low temperature, low solids condition (149ºF, 40 % Solids). This point does not fit the trend and the tack would normally indicate a higher work of adhesion here. It is believed that the water in the sheet at this condition actually reduces

the effective tack of the surface. This would result in less sticking and consequently lower work of adhesion. For Vinac, the tack actually shows a slight increase from 149 F to 194 F which is consistent with the results. As in prior tests, some sheet split was observed at the highest temperature at 40% ingoing solids. However, the phenomena occurred sporadically.

These results are particularly encouraging because they follow the observations of some of the PAC members. They had reported that they had moved to lower temperatures (150 F range) due to the heavy picking that was detected at the intermediate temperatures.

The picking data for both Carbotac & Vinac contaminated coupons are shown in **Figure 14.** Picking is always reduced by moving to higher solids, regardless of temperature. As the sheet dries, there is stronger sheet cohesion and consequently less adhesion to the surface of the coupon. Peak picking values occurred at the intermediate temperature, which is consistent with the trends for the work of adhesion. Sheet cohesion and the tack phenomena make important contributions .

At the highest temperature there is high sheet cohesion and a large degree of fiber to fiber chemical bonding as the sheet dries. The cohesion of the sheet dominates over the adhesion to the roll. At the low temperature, the sheet tends to remain extremely wet so it is surface tension, or physical cohesion holding the sheet together. It would be reasonable to assume that the adhesion to the roll may dominate but the tack of the contaminants presents a complication. Because the sheet is at its "wettest" (high solids and low surface temperature), the effective tack is greatly reduced as the water on the surface of the sheet comes into contact with the hydrophobic coupon surface. The water may actually act to repel the sheet away from the surface resulting in low work of adhesion. At the intermediate condition, a combination of the two phenomena occur – weak physical bonds, easily overcome by the adhesion to the roll, are present; but there is also strong local chemical bonding among fibers as the sheet dries on the hot surface. The fibers then come off in clumps with some fibers adhering to the surface and pulling off others that they are already bonded to each other. Thus the intermediate temperature condition would exhibit higher picking values than the other two. This concept is clearly visible in the photos shown in **Figure 15.**

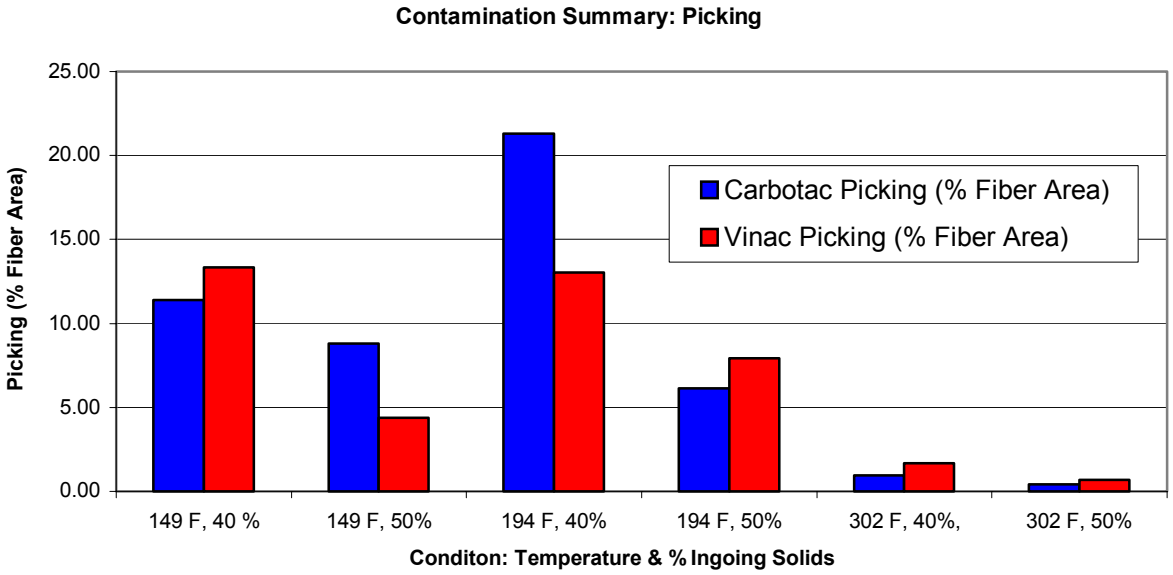

Figure 14: Contamination Summary

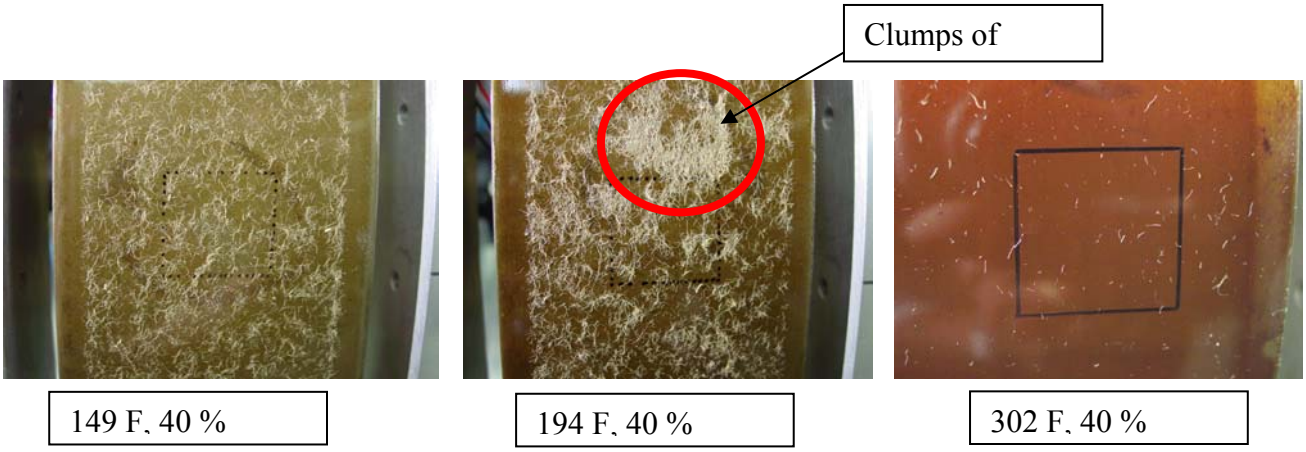

Figure 15: Picking for Contaminated Coupons

It is important to note that while the trends are similar, the work and picking data do not appear to have a direct relationship as expected. For example, the picking is significantly lower at the highest temperature than at the lowest while the work of adhesion values for the two temperatures are similar. The work results are also closely tied with the trends in tack but again not directly. Clearly, the relationship among adhesion, cohesion, picking and tack is very complicated. Picking, in particular, is a function of adhesion and cohesion. A better understanding of cohesion of the sheet at these different conditions would help significantly and is one of the major goals for the continuation of this work.

As far as the implications for operating strategies, higher ingoing solids (through better pressing) is obviously a solution. Higher temperatures need to be further examined to understand and eliminate the occurrence of sheet split. This may be remedied by better pressing as well.

Consolidation Testing

The picking and sticking phenomena are dependent on both the web adhesion to the roll as well as the cohesion (both chemical and physical) of the web. Experiments to understand web cohesion are still being developed since there is currently no reliable test to measure wet web cohesion. Previous WADS picking data have demonstrated the relationships between picking and temperature/solids which is highly dependent on web cohesion. The implication from all of this is that optimum operating strategies to reduce or eliminate sticking and picking will depend on both press and dryer operation.

A consolidation study using the WADS was initiated to evaluate the effect of pressing levels on the work of adhesion and the picking. Tests were performed with Carbotac contaminated coupons at one experimental condition – 194 F, 40 % Solids, and 0.194 s dwell time. Virgin Kraft Liner Board (VKLB) formette sheet samples of initial ingoing solids (pre-pressing) of 22.6% were used. Sheets were pressed to different calipers using a standard roll press apparatus and dried under restraint to achieve the initial 40 % solids condition. Three pressing levels, detailed in **Table 4**, were investigated:

Pressing Level	Apparent Density (g/cm^3)	Caliper
1 (High)	0.264	Low
2 (Medium)	0.217	Medium
3 (Low)	0.209	High

Table 4: Pressing Levels for Consolidation Study

The results indicate that pressing does have an impact on both work of separation and picking. **Figures 16 and 17** show the work of separation and picking as functions of pressing level. As expected, a significantly lower picking level is observed when the sheet is pressed to a smaller caliper (Pressing Level 1). At this condition, the fibers are better consolidated and the cohesive forces between them are greater than the adhesion to the roll. At Pressing Level 3 (larger caliper), the adhesion to the roll surpasses the cohesion of the web allowing more fibers to pick onto the coupon surface. The work of separation results are not as straightforward to analyze. The data suggest that the work of separation is lower for the sheet pressed to a smaller caliper and higher for the less consolidated sheet. It is important to note that the work data may be partially masked by the strain – in a less consolidated sheet, the paper may stretch more, increasing the work

that contributes to strain. The surface topology of the sheet can also influence the work of separation – pressing can change the effective surface area and topology of the sheet. A further understanding of the relationships among cohesion, adhesion and sheet properties is necessary to analyze the work of separation data. The difference in apparent density between levels 2 and 3 is not significant and another condition needs to be tested to fill out the data set.

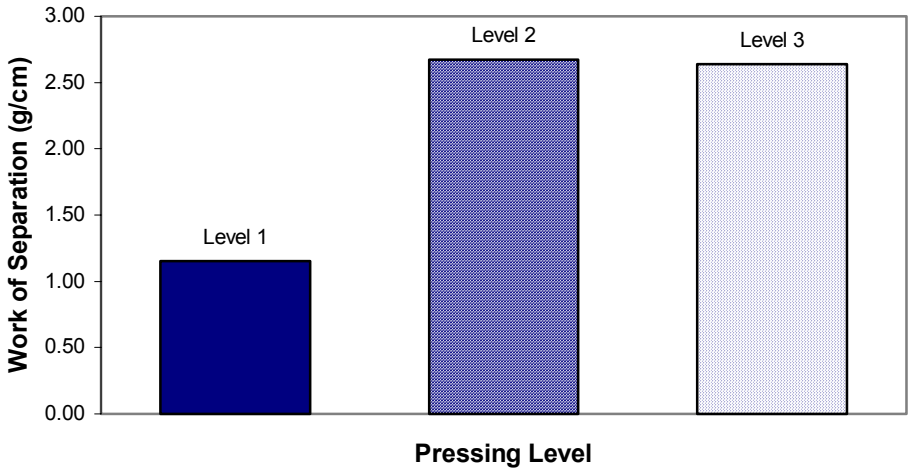

Figure 16: Work of Separation vs. Pressing Level

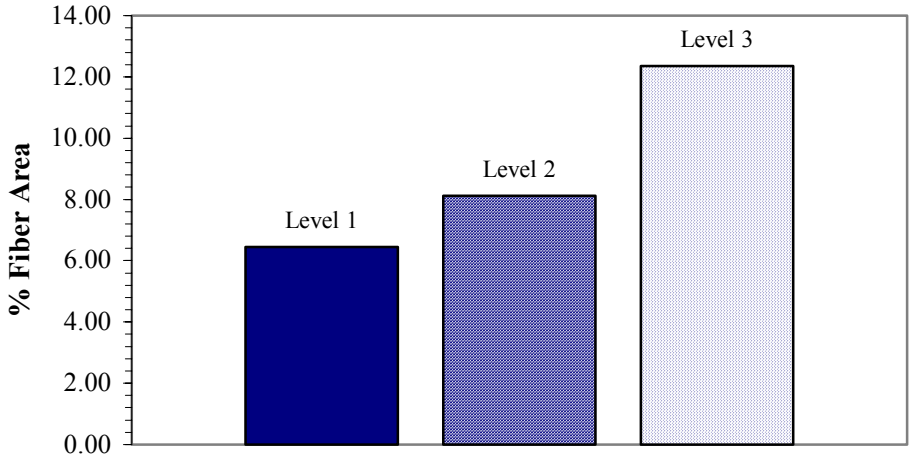

Figure 17: Picking vs. Pressing Level

Web Separation Modeling for Data Reduction

As mentioned before, the Mardon equation (with web strain neglected) has been used in this study to correlate the peel force measured from the WADS to the work of adhesion. In its simplified form, the equation is as follows:

$$T' = \frac{W''}{1-\cos\phi} + mV^2 + (strain) \qquad \textbf{(1)}$$

T' = Tension per unit width

W" = Work of Adhesion per unit area

m = Mass per unit area

V = Velocity

ϕ = Peel Angle

In the equation above, the second term (mV^2) represents the kinetic energy of the web, which increases with machine speed. The "strain" term is a potential energy term – a wet paper web can have viscoelastic properties and act as a spring-damper. To simplify the analysis, this term has been neglected thus far.

With the clean coupon tests, the equation was used as in the form above, but with several correction factors applied to the raw tension measurements. The raw tension data collected on the WADS was corrected for zero position (the sensor reads a non-zero value because of its tilted orientation) and frictional drag. During an experiment, the pull tape weight decreases as it is retracted. Conversely, the paper sample weight is being added to the total tension measured as the paper sample is pulled off the coupon. Given the unit weights of the tape and paper sample and the constant speed of the wheel, a simple linear function describes the change in weight of the paper (and tape) sample. The resulting weight is subtracted from the raw tension value to give the peel tension.

As previously mentioned, high-speed digital video images were used to measure the actual peel angle, which can vary significantly from the set-point angle. The deviation in the peel angle is due to several factors including the level of adhesion to the roll, inherent stiffness of the sheet and the curvature of the sheet as it bends under its own weight. The peel angle measured from the video images was used in conjunction with the corrected tension data to calculate the work of adhesion.

In order to account for the geometry of the WADS, and the effect of the weight of the paper and tape, a more sophisticated equation was derived and used to calculate tension:

Tension Calculation:
$$T = T' - \rho v g t \left\{ \frac{\cos\tilde{\phi} - \cos\theta}{\sin(\theta - \tilde{\phi})} \right\} \qquad \textbf{(2)}$$

where $\rho vgt = \rho_p vgt + \rho_T vg(\frac{\Gamma}{v} - t)$ (takes into account tape + paper weight)

T' = Raw tension collected from WADS
T = Tension adjusted for paper/tape weight
γ = angle between the radial line from the roll center to the peel point and vertical
θ = Set-point angle
$\tilde{\phi}$ = Local peel angle (relative to horizontal) = ϕ - γ
ρ = Mass per Unit Area (p for paper and t for tape)
Γ = Length of pull tape
v = speed

This "corrected" tension was then used in the Mardon equation to calculate work for the initial Carbotac runs.

A uniformly sticky surface, such as the one used in the WADS experiments, should result in a constant work of adhesion for the duration of the peel event. Since the web properties are constant along its length and since the coupon properties are constant along its length, the work of adhesion must also be a constant. WADS run data analyzed with the equations above always showed increasing tension and work of adhesion with time. Obtaining a non-constant work of adhesion suggests that the equation did not accurately describe the physical event. Analysis of the video images revealed significant curvature in the sheet for some cases. While the equations developed corrected for the discrepancies due to angle and weight, they did not adequately account for the curvature of the sheet. If the sheet has curvature, the tension measured at the tension sensor will be different than the tension at the peel point. The two tensions are only equal when the sheet/tape define a straight line between the peel point and the tension sensor (see Member Report 2 for a detailed explanation). Thus a modified version of the Mardon equation was developed:

$$T' = \frac{W_s}{1-\cos\phi} + \rho v^2 + \left(\frac{R_t}{\Gamma}\right) W_g(t) + \text{(strain term)} \qquad \textbf{(3)}$$

T' = Tension per unit width
W_s = Work of separation
ϕ = Peel Angle
R_t = Local radius of curvature (equation not shown here)
Γ = Length of curve followed by paper
W_g = Weight term
v = Velocity

Applying this modified Mardon equation (neglecting strain) to the Carbotac and Vinac data as well as some of the older data yielded some important results. Three categories of sticking phenomena were observed. Group 1, shown in **Figure 18,** represents the low

sticky/adhesion situation in which the paper is either barely sticking or not sticking at all to the roll but rather sliding across the surface. Picking was negligible and work values for these cases were generally below 0.02 g/cm. This condition occurred with clean coupons or with contaminated coupons that had undergone numerous runs with paper samples, thus completely covering the sticky surface with fibers. The work of adhesion calculated using the modified equation indicates a relatively constant, but low value, as is expected. The large shift from the original work curve to the modified curve demonstrates the importance of the sheet curvature effect.

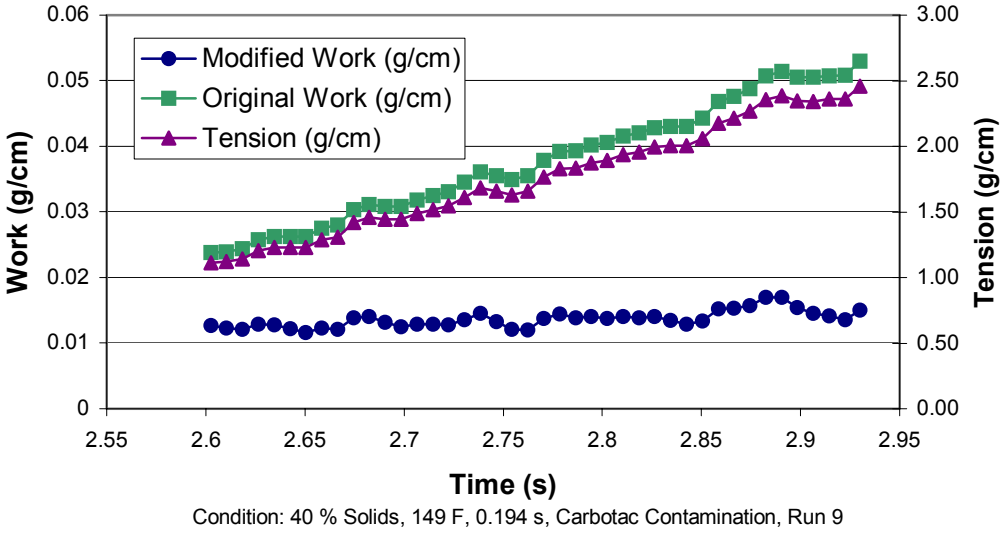

Figure 18: Group I Data, Work of Adhesion Comparison

For intermediate sticky cases, as in Group II, the curvature of the sheet plays an important role and the use of the modified Mardon equation has a significant impact on the data, correcting for the error due to curvature. As expected, for most of the peel event, the modified work curve is rather flat. The work of adhesion, as shown in **Figure 19**, is in an intermediate range, greater than 0.02 g/cm, but usually less than 0.2 g/cm. This condition occurred when some fibers were already present on the surface but enough sticky surface was still exposed to the web to allow adhesion.

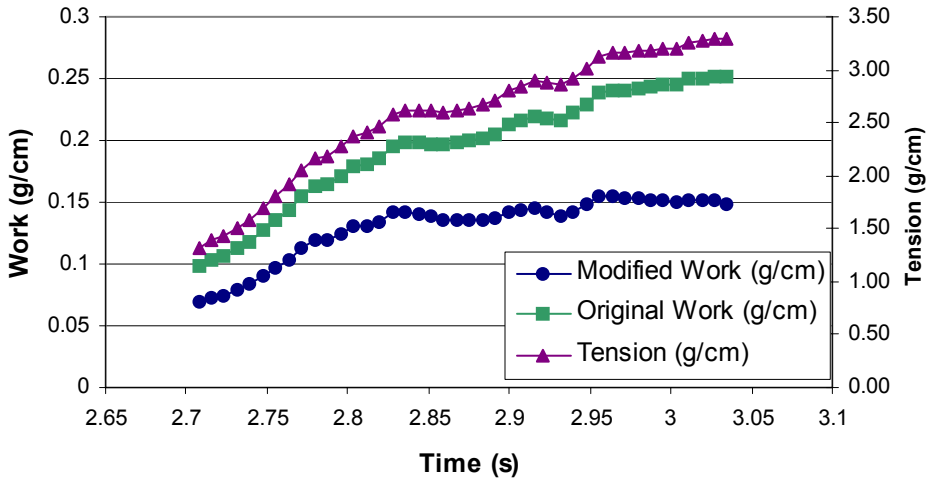

Figure 19: Group II Data, Work of Adhesion Comparison

Group III runs, as shown in **Figure 20**, demonstrate negligible curvature since the paper adheres strongly to the surface and peels off at a sharp (and mostly constant) angle. In these runs, the modified Mardon version has little impact on the data, which shows work to be increasing during the peel event. The work values are considerably greater than 0.2 g/cm and high adhesion is observed. This situation was observed for the initial few runs on a contaminated surface when a large amount of sticky surface area is exposed to the web.

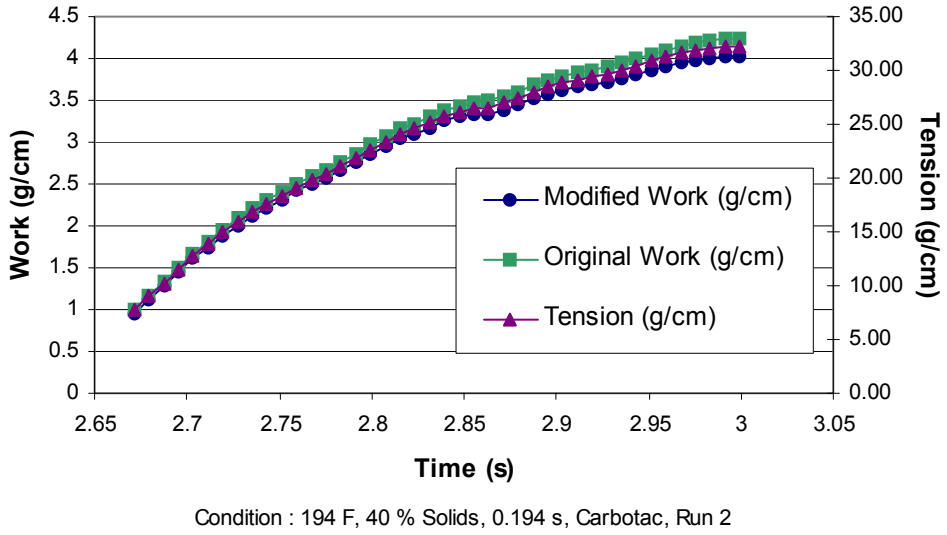

Figure 20: Group III Data, Work of Adhesion Comparison

For this high adhesion type run, it is believed that strain has a significant impact, causing the paper to stretch and the tension to increase in time. The work of adhesion is augmented by the work that goes into stretching the paper. As more paper is peeled from the coupon, a longer "spring" is created, and the strain increases incrementally. The increasing length of the web requires an incremental increase in work and therefore in tension as well. Thus the web strain must be accounted for in order to determine the true work of adhesion for high adhesion situations. Currently, it is believed that the true work of adhesion is equivalent to the work shown at the left end of the graph, before the curve rises dramatically.

To study the effect of strain and to test this theory, some dry paper tests were performed using sticky coupons. Coupons were coated with double-sided or scotch tape and WADS runs were performed with dry copy paper samples, which was expected to exhibit negligible stretching.

The results, shown in **Figure 21,** support the idea that strain is a significant factor for high adhesion runs. In the dry paper test, adhesion is in the high range (similar to Group III data) as can be seen in the work and tension values. However, the work and tension remain relatively constant for the dry paper tests, in sharp contrast to the wet paper runs. The contributing factor is the strain of the wet web, which stretches and causes the work of adhesion to appear to be increasing during the peel.

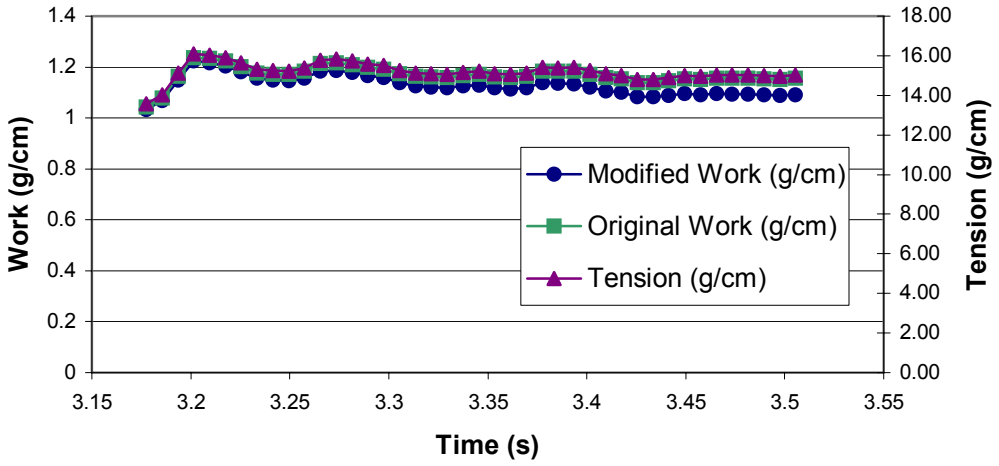

Figure 21: Dry Paper Tests, Work of Adhesion Comparison

Experiments are currently being planned to aid in determining the strain term so that the actual work of adhesion for these runs can be ascertained. There is currently little published information on the viscoelastic behavior of wet paper. What data do exist are only for low speed testing typical of a standard stress-strain test. This data indicates that wet webs below 50 % solids have definite viscoelastic properties. As the solids level decreases, the viscoelastic properties decrease as well. The authors know of only one test device capable of high-speed stress-strain testing of wet paper. The data from this

apparatus indicate that the viscoelastic properties of wet paper increase with speed. The device is owned by VTT in Jyvaskyla, Finland.

Tack Testing

A modified loop tack test was developed in order to compare and pre-screen contaminants to be used on the WADS. Work of adhesion on a dryer cylinder depends on a number of different variables including tack of the contaminated surface. The American Society of Testing and Materials (ASTM) defines tack as "the property of a material which enables it to form a bond of measurable strength immediately upon contact with another surface (ASTM D1878-61T)." There are several forms of tack; the concern of this study is adhesive tack, the separation of two dissimilar materials at the original interface (Aubrey, 1992). Once tack values are established for various contaminants, the relationship between tack and work of adhesion can be ascertained. Since the tack test is fairly quick, it can also be used to help select appropriate contaminants for WADS experiments.

The tack test has gone through three phases of development. Phases 1 and 2 involved the development of a modified loop tack test. Phase 3 included development of a new tack tester and procedure. In all three phases, an Instron Tester was used for data collection and contaminated metal plates were used to simulate the contaminated dryer rolls.

Phase 1 is the dry tack method. The test is based on ASTM D 6195 in which adhesive is coated onto a flexible tape and put in contact with a clean metal surface. The force required to remove the tape from the surface is recorded as tack. In the modified test, the adhesive/contaminant is coated onto a flat metal surface (identical to the coupons used on the WADS) and a loop of Mylar, chosen for its low surface energy, is brought into contact with the sticky surface. Using the Instron, the force required to remove the tape from the surface is measured and recorded. The test was set up so that 1 inch of the loop touched the plate when flattened. This method showed repeatability and, in general, a strong correlation between tack and work of adhesion.

Tack measurements using this method were performed on the two contaminants tested on the WADS. **Figure 22** shows the relationship between tack and temperature for polyacrylate (Carbotac) and PVAC (Vinac) based emulsions coated onto a cast-iron surface.

The WADS testing involves evaluating a number of different dryer cylinder temperatures to determine optimum conditions at which sticking and picking are minimized. The data above show that tack is not only a function of temperature but also of the contaminant type. Thus, investigating tack of a mixture of components similar to what appears on a contaminated dryer cylinder is important since the individual contaminants may behave differently.

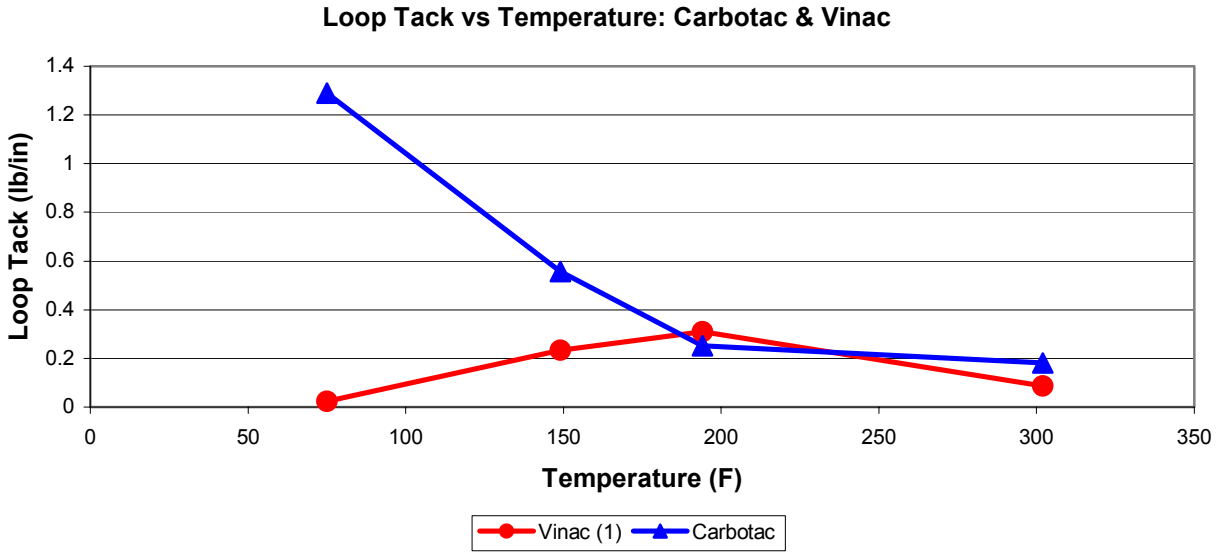

Figure 22: Loop Tack Results

The data above also demonstrate that tack generally decreases with temperature for both contaminants tested. While a direct relationship between tack and work of adhesion might be expected, this tack test does not take into account the sheet condition, i.e. the wetness of the sheet, which is an important factor in sticking/picking. A preliminary study showed that the dampness significantly diminishes the tackiness of a given contaminant on the coupon surface.
Thus, in Phase 2 wet paper was used in the tack test. The same method was used as in Phase 1 except that a strip of paper was wrapped around the Mylar loop. However, when the tests were run, good repeatability could not be achieved. Sliding of the loop on the plate caused non-uniform contact. Also, as the loop was flattened on the plate, the dwell time at the center of the loop was considerably longer than the dwell time at the ends of the 1 inch section.

In order to remedy the problems seen in Phase 2, a new tack testing device for use on the Instron was designed and built in Phase 3. As seen in **Figure 23**, the device has a 1 inch flat surface to provide uniform contact of the appropriate area, clips to hold the paper, and rounded edges to prevent tearing. The springs between the top and bottom plates of the device are to allow for pressure to be applied at the interface of the paper and the contaminated surface without damaging the load cell on the Instron. To ensure that the pressure applied is equal each time the test is run, the contaminated plate and the bottom plate of the tack testing device are initially positioned 1 inch apart, and the maximum extension on the Instron is set at the same level, 1.05 inch, for every test. The results obtained in Phase 3 proved to be repeatable.

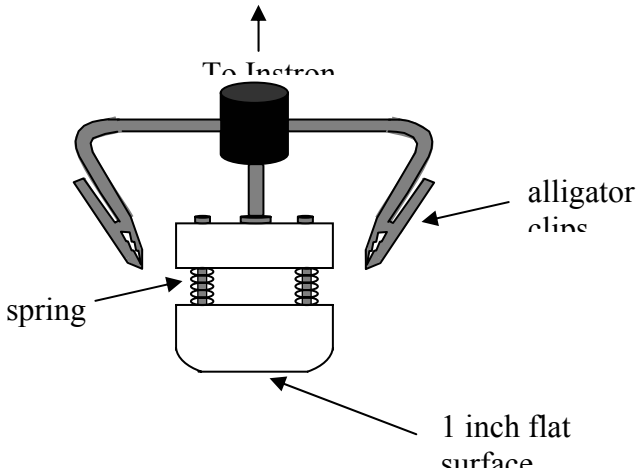

Figure 23: Loop Tack Tester

The conditions tested are summarized in **Table 4**. For each condition 16 samples were tested. The dwell time was determined using high speed photography.

Contaminant	Plate Temperature, °F	Initial Sheet Solids	Dwell Time	Paper Type
Carbotac 26171 polyacrylate (BF Goodrich)	149°F, 194°F, 302°F (65°C, 90°C, 150°C)	40%, 50%	0.651 s	Liner Board
Vinac PVAc (Air Products)	149°F, 194°F, 302°F (65°C, 90°C, 150°C)	40%, 50%	0.651 s	Liner Board

Table 4: Tack Test Conditions

It should be noted that Vinac at 302°F is not a reliable test. The Vinac appears very dark and mottled after heating to this temperature. Even after cleaning, the plate still holds the pattern. The results shown here include Vinac at 302°F only to round out the data set.

Figure 24 and **Table 5** show the results of the Tack Tests. The standard deviations were small for each condition, so the average of the 16 samples was used. For Carbotac, the sheet condition seems to have a substantial effect on the tack value, especially in its relationship to temperature. Vinac, however, appears to follow the same trend at both 40% and 50% solids with an insignificant change in tack value with temperature.

Condition	149°F	194°F	302°F
Carbotac, 40% solids	2.693 ± 0.204 lb/in	3.020 ± 0.281 lb/in	3.010 ± 0.254 lb/in
Carbotac, 50% solids	2.818 ± 0.284 lb/in	2.496 ± 0.261 lb/in	2.658 ± 0.098 lb/in
Vinac, 40% solids	2.674 ± 0.232 lb/in	2.612 ± 0.266 lb/in	2.670 ± 0.142 lb/in
Vinac, 50% solids	2.768 ± 0.238 lb/in	2.673 ± 0.197 lb/in	2.738 ± 0.184 lb/in

Table 5: Average Tack Results

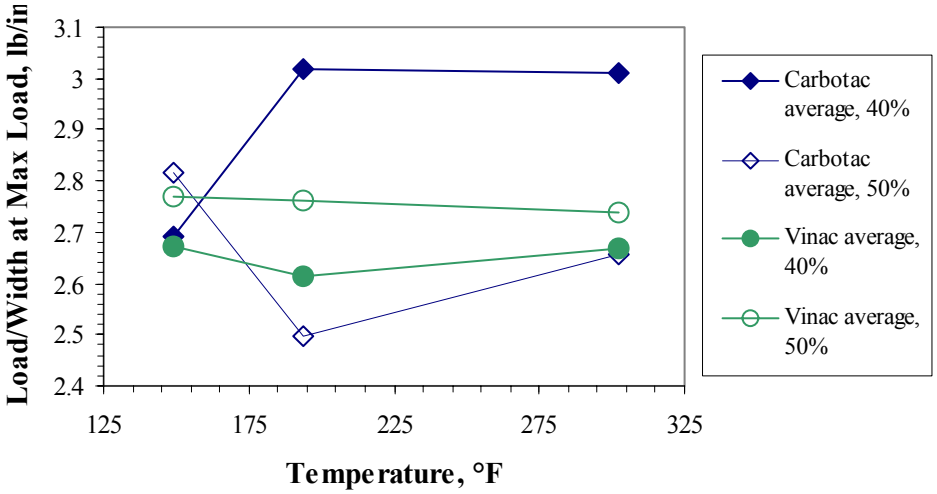

Figure 24: Tack Test Summary

The main objective of this test is to predict the results of the WADS test, that is, the work of adhesion. **Figure 25** presents a comparison of tack and work values for Carbotac, and **Figure 26** gives the comparison for Vinac. It is important to note that the dwell time of a WADS experiment is 0.17s, and the dwell time for a tack test is 0.65s. Tack and work for Carbotac appear to follow the same trend with an obvious difference in magnitude; the different dwell times of the tests may explain the magnitude difference because with an increased dwell time there is more evaporation and drying. This changes the bonding and properties of the paper including cohesion. Also, drier paper tends to stick to the adhesive more readily. The values for Vinac are less conclusive. There seems to be agreement in the trend between the 194°F and 302°F values of work and tack but not between 149°F and 194°F. Because the tack values do not change appreciably with temperature (between 149°F and 194°F at 40% solids = 0.062 lb/in and 50% solids = 0.005 lb/in) the tack test may not be an acceptable method for PVAc contamination.

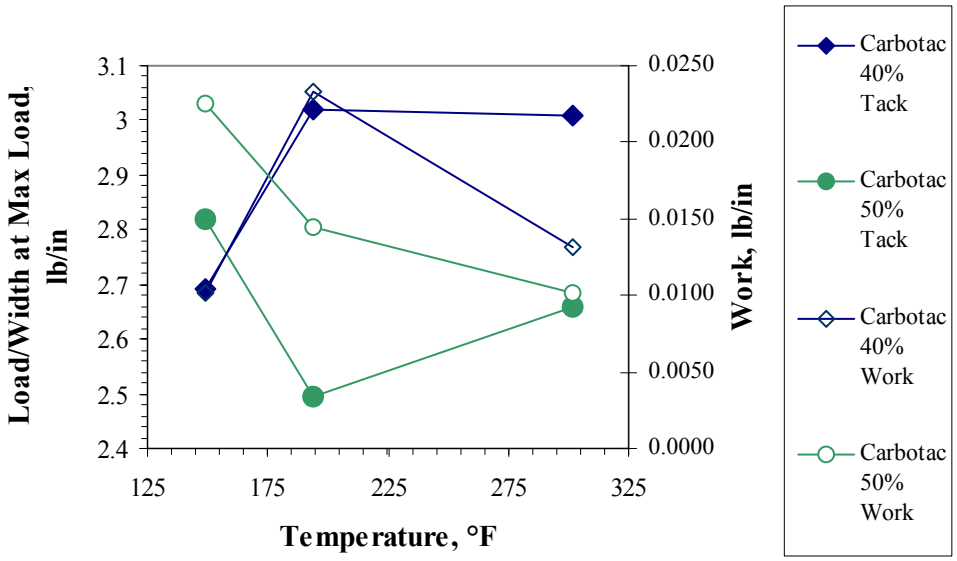

Figure 25: Comparison of Tack and Work of Adhesion for Carbotac

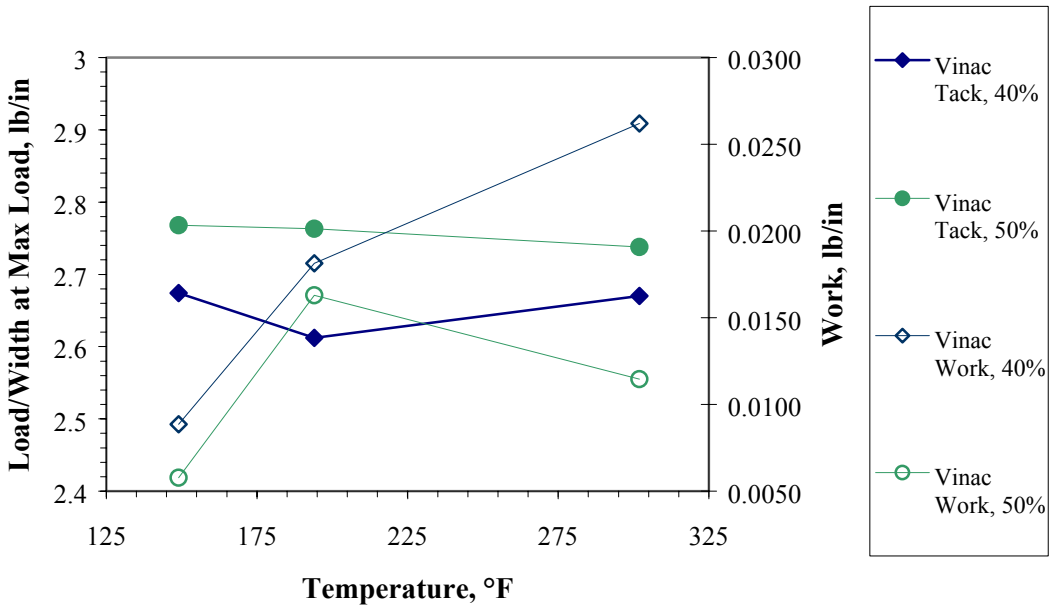

Figure 26: Comparison of Work and Tack Values for Vinac

An issue that hinders the comparison of work and tack values is the difference in the dwell times for the respective tests. At this point, there is no obvious available means of reconciling this difference as the Instron maximum speed is 20 inches per minute, a speed that would not decrease the dwell time enough. The WADS test for work of adhesion is run to simulate dryer rolls in a paper mill; therefore, the dwell time of the WADS tests should not be changed.

It was learned after these experiments were performed that the Instron was not level. This could have caused the tack testing device and contaminated plate not to be parallel, and, therefore, contact possibly was not uniform from one test square to another. This should be investigated, but it would not be helpful until the speed issue can be resolved.

Further development of the Tack Test needs to be done, but at the present time, equipment that would make this possible is not available. This development may include design of yet another device because the Instron will not provide the appropriate speed.

Conclusions

The WADS is an effective tool in evaluating the peeling of paper web samples from simulated dryer cylinder surfaces. Results from the various tests have shown that reducing picking and sticking is difficult to achieve by changing dryer operating conditions alone. On a real dryer machine, there are very few parameters that can be changed easily. For the majority of the WADS tests, only two operating parameters were varied – the surface temperature and the wetness of the sheet. The contaminated coupon runs confirmed the observations typically made by papermakers – picking and sticking were lower at low temperatures, increased at intermediate temperatures and although low at high temperatures, problems with web strain/breaks became more common. While the exact conditions that foster these results may be different from machine to machine, they nevertheless probably exist for all machines and all contaminants.

Thus, more recent work on the WADS has focused on other parameters such as the effect of pre-heating. Results from initial tests suggested that pre-heating did lead to lower work of adhesion and picking. For a contact heater such as the one used in these tests, the change in ingoing solids is the likely reason. Currently, a steam pre-heater has been designed and will be used for further testing of the pre-heating concept.

Another current project is evaluating the effectiveness of a Teflon wipe for reducing picking and sticking. This work was initiated based on empirical data from an impulse drying experiment. A Teflon® (PTFE) block was used during pilot scale impulse drying trials and was found to substantially reduce picking on the roll surface. It is believed that a thin layer of PTFE may have been deposited on the roll surface, modifying the surface adhesion forces. Work is currently underway to determine the effectiveness of a PTFE wipe for reducing/eliminating contamination build-up and/or picking of sticking of the web to these contaminants.

The tack tests performed in conjunction with WADS experiments provided much insight in understanding the different contaminants. The dry tack tests revealed trends in temperature but could not be used to predict work of adhesion as initially thought. Results of the contaminated coupon tests show the importance of tack at low temperatures and low solids. The reduction in effective tack is believed to be the reason for the low work of adhesion at these conditions. Unfortunately, the wet tack testing apparatus cannot simulate the contact times necessary to characterize the WADS runs.

For evaluating different contaminants or mixtures of contaminants, knowing the overall tack may help to predict work and picking & sticking trends.

In studying web adhesion, it is critical to also study web cohesion. The interaction between web adhesion to the roll surface and web cohesion is dependent on both roll surface and web properties. The relative magnitude of the two forces (adhesion and cohesion) determines the ease of web transfer and the amount of picking and contaminant build-up. Web cohesion plays a role in sticking which implies that optimum operating strategies depend on both press and dryer operation.

Future Work

Additional work of adhesion data is required in order to better understand the sticking and picking phenomenon. Testing of other contaminants as well as mixtures of contaminants would be extremely helpful in characterizing sticking and picking. Eventually, experiments with contaminated sheets should be performed since they will be a better simulation of the conditions on an actual dryer cylinder.

A major hurdle in understanding the WADS data has been the effect of web strain. For intermediate levels of sticking, the web curvature model is adequate in helping to elucidate the work of adhesion. But for the majority of the contaminated tests, the true work of adhesion is difficult to extract from the data as it is masked by the effects of web strain. High-speed wet strain tests will need to be performed to improve the mathematical model used to interpret the data.

A high-speed tack tester (perhaps on the same platform as the high-speed tensile tester), would be extremely helpful in obtaining more useful tack data. As mentioned above, knowing more about tack will help in classifying the different contaminants commonly found on dryer cylinders. Identifying all the various contaminants on the surface will be less important than knowing the overall tack of the surface which is basically the critical contaminant variable.

Initial web cohesion tests have been done using a prototype device. Further work on this apparatus and concept is a must in characterizing work of adhesion.

References

1. Meinecke, A, Huu, T, Loser, H. "New Knowledge on Paper Drying with Paper Cylinders," Das Papier, 42 (10A), pp159-165.

2. Mardon, J., "Theoretical and Experimental Investigations into the Peeling of Paper Webs from Solid Surfaces," *Paperi ja Puu*, No. 11, pp.797-815 (1976)

3. Mardon, J., "The Release of Wet Paper Webs from Various 'Papermaking Surfaces,"" *APPTA*, Vol. 15, No. 1, pp.14-34 (1961)

4. Douek, M.; Guo, X.Y.; Ing, J. "An Overview of the Chemical Nature of Deposits/Stickies in Mills Using Recycled Fibre,". *TAPPI Proceedings, 1997 Recycling Symposium* pp.313-330 (1997)

Task 3 & 4
APPENDICES

Appendix A: WADS Experimental Procedure, pp 3-6

Appendix B: Angle Measurements (OPTIMAS), p. 7

Appendix C: Data Analysis, pp.8-10

Appendix D: Image Analysis (Picking/% Fiber Area), p 11

Appendix E: Tack Testing Procedure, pp12-14

Appendix F: Raw Data, 15-53

Appendix G: Miscellaneous Data, 54

APPENDIX A: WADS Experimental Procedure

I. Formette Sheet Preparation
   1. Pulp Preparation
      a. Virgin Kraft Liner Board (initially)
      b. Freeness: 500 – 550 CSF
      c. Basis weight: 100 g/m^2
   2. Pressing
      a. Leave sheet in original wet blotter paper.
      b. One pass on roll press in lab 379, roll nip set at the red arrows
      c. Press to ~ 30-35 % Solids
      d. Remaining solids adjustment made under constraint in lab

II. Sample Preparation
   1. Sample Size
      a. 9 samples cut from each Formette Sheet
      b. Sample size: 2 ½" x 11"
      c. Transfer Formette sheet to dry blotter papers for ease of cutting on paper cutter in lab 351
      d. Mark sample number on wire side of paper using ink-blot pencil
      e. Minimize sample contact w/air and store between plastic
   2. Joint Section
      a. Cut joint section from Mylar sheeting using steel-rule die (pentagon shape)
         -Use hydraulic press in lab 379
         -Place 10 sheets of Mylar on die
         -Place impact-resistant cutting board on Mylar
         -Press hydraulic press to 1000 psi
      b. Cut Fiberglass tape to 105" and PRECISLY mark ½" sections from 91"-94.5"
      c. Ends of fiberglass tape (1" at each end) should be covered w/shiny Mylar tape to prevent fraying
      d. Record weight of tape
      e. Mark 1" section on paper sample and dry using constraint on hot plate (aids in adhering joint sections)
      f. Place this 1" on the wide side (sticky) of Mylar joint
      g. Place fiberglass tape directly adjacent to the paper (very important)
      h. Seal w/2nd piece of Mylar tape
      i. Press tape firmly together
      j. Store sample in plastic sheeting prior to use
   3. Adjust to Desired Solids
      a. Shortly before running test, dry sample to desired solids under constraint
      b. Place sample between blotter on hard, flat surface
      c. Place board over top blotter
      d. Place weight evenly on board (i.e. tool box @ 0.13 psi)
      e. Return sample to plastic when desired solids is reached

III. Coupon Preparation

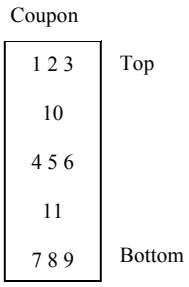

1. Drop with plastic pipette appropriate amount of adhesive on top end of coupon
2. Draw adhesive down surface of coupon using appropriate metering rod
3. Allow adhesive to air dry
4. Mark 1"x1" box centered horizontally on coupon, 6 inches from top end
5. Measure coating thickness with CMI measurement device and record
   Measure thickness in 11 areas as charted to right
6. Install coupon on WADS apparatus
7. Cure the adhesive by heating to desired test temperature for 45 minutes to 1 hour immediately prior to testing.

IV. Digital Video Camera Setup

1. Position tripod legs in three tape squares under lights
2. Mount camera to tripod
3. Attach cable from computer to back of camera

COMPUTER MUST BE POWERED OFF PRIOR TO ATTACHING CABLE!!

4. Adjust camera height to height of nip
5. Turn computer on and open Olympus Encore PCI Image Player software
6. In software, select OPEN CAMERA/CAMERA 1
   This live shot will allow you to adjust camera
7. Adjust view to include the area in which the paper will peel from the coupon, from 65^{o} to nip
8. Focus camera to front edge of paper
9. Adjust brightness with all lights turned on
10. Before running test, click REC in video software to engage recording

V. Start machine warm-up

1. Turn on power
   a. AC cord plugged in
   b. Wall breaker turned on
   c. E-stop in extended position (*Red light should be on*)
2. Set coupon heater temperature
   a. Press loop button on temperature control box, cycle display to SP1
   b. Press enter
   c. Enter desired set point using number pad
   d. Press enter
   e. Turn coupon heater power switch ON
3. Set sample heater temperature
   a. Press loop button on temperature control box, cycle display to SP2
   b. Press enter
   c. Enter desired set point using number pad
   d. Press enter
   e. Turn sample heater power switch ON
4. Allow machine to warm up to desired temperature, *(Approx. 1 hour)*

5. Start data acquisition program
    a. Click WADS Labview icon on desktop
    b. Enter experiment ID in test information field
    c. Set scan rate, buffer capacity & total number of scans
    Buffer capacity must be equal to or greater than total number of scans!
    d. Click enter button and run button on menu bar
    e. In dialog provided, save file to a place of your choosing
    f. Verify that all sensors are working and that all values are reflecting current machine conditions.
    g. DAQ will automatically start collecting when Clutch button is depressed

VI. Set machine adjustments
1. Adjust belt contact length for proper dwell time. (A function of wheel speed and arc length from leading edge of belt to peel point.) Major changes in contact length will require different belts.
2. Set peel angle.
    a. Move tension sensor away from peel arm
    b. Set peel arm to desired angle and clamp tight
    c. Position tension sensor mounting bolts directly over corresponding bolts in peel arm. Plates should be parallel.
    d. Allow approximately 0.125" clearance between plates
    e. Tighten all adjustment clamps on tension sensor frame
    f. Verify that plates are still aligned

VII. Set desired wheel speed
1. Vary speed with up/down arrows on the motor control panel. This is calibrated in feet per minute at the coupon.
2. Motor will not start unless coupon is in home position (0 degrees) and motor start button is depressed

VIII. Verify belt tension is set to proper pressure
1. Vary pressure with precision regulator mounted on idler roller blocks
2. Check alignment of belt on large rollers
3. To move belt
    a. Reduce belt tension to min. set point of regulator and shut air off to the equipment with the lock-out valve
    b. Depress tension (top) roll to create slack in the system
    c. Center belt on rollers
    d. Turn on lockout valve and increase pressure regulator to set point

IX. Load paper sample
1. Weigh sample and adjust to proper inlet solids condition by rewetting or constrained drying
2. Verify that motor is off by pressing motor stop button on control panel
3. Load paper sample into tray wire-side-down
4. Depress brake disengage

5. Rotate wheel to position cross brace on trailing edge side of coupon below paper tray (Leading edge of belt nip) Center of coupon should be between 45-190 deg.

!!!Caution!!! Do not come into direct contact with heated coupon. May cause serious burns.

6. Feed approximately 12”-18” of tape through open area of nip
7. Keeping tape centered between belt guides, rotate coupon to 330 deg. This will carry the tape to the exit side of the nip.
8. Retrieve tape
9. Rotate coupon to home position (0 deg.)
10. Position paper at start mark on sample tray. *(Paper/tape junction approximately 1” from end of paper guides)*
11. Position tape over lowest guide pin, around tension sensor, and over middle guide pin
12. Position tape through pinch roller at 91.5” tape length
13. Cover paper sample w/fiberglass tray
14. Attach spring retractor to end of tape

X. Run experiment

1. Verify that camera lights are on
2. Drape slack end of tape over tray so that it cannot interfere with the rotation of the wheel.
3. Check that tape is centered between belt guides
4. Check that operator or any coworkers are clear of the wheel
5. Press motor start switch and allow motor to accelerate to speed
6. Depress clutch engage switch, cycle will start on release of this switch
7. Depress remote camera stop as soon as wheel has completed rotation
8. Data acquisition will stop collecting data automatically
9. Remove paper sample and weigh immediately
10. Take high-resolution digital image of 1” square marked on coupon surface for picking analysis
11. Save video image
12. Turn camera lights off

APPENDIX B: Angle Measurements (OPTIMAS)

OPTIMAS 5.2 is used to measure the peel angle of a WADS experiment. A single frame is saved from the peel event video at the peel point. The peel angle is then traced using the "draw a line" tool on the DATA toolbar. One line is drawn at the edge of the paper, and another line is drawn tangent to the coupon. OPTIMAS measures the angles between each line segment and the first reference line segment, which is horizontal. The peel point is read directly from the grid seen in the figure below.

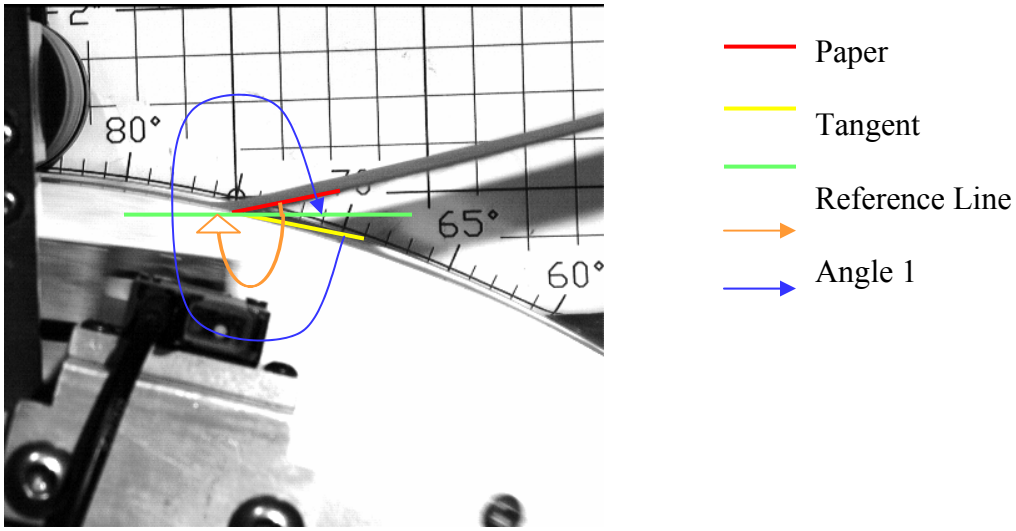

The peel angle is then calculated:

$$\text{peel angle} = \text{angle 1} - 180° - \text{angle 2} + 360°$$

APPENDIX C: Data Analysis

Although the data analysis procedure has gone through several iterations, only the most recent calculation procedure will be described here.

Data Analysis Procedure

I. Corrected Tension

1. The LabView DAQ Program collects: Speed, Pressure (belt application), Coupon Temperature, Raw Tension, and Coupon Trigger data.
2. An excel sheet is automatically created by LabView from the data file for each run
3. Scan rate and # of scans is specified before each run (usually 1000 scans/s for 4 s for a total of 4000 points per column)
4. Time is calculated in the 1st column based on the scan rate (1/scan rate)
5. Tension must be corrected for friction and zero using the following formula:

   $Tension_{zero}\ (g) = Raw\ Tension\ (g) - (base\ value + 1.0g)$

   - Base value is the value read on the tension sensor without the tape or paper connected to the system (when no load is applied). The sensor shows a non-zero value because it is at an angle and therefore the weight of the sensor apparatus itself is read by the sensor.
   - 1.0 g is added to account for the frictional drag of the tape over the tension sensor apparatus

II. Peel Start & End

1. The timing of the peel event – the *peel start* and *peel end* is determined by using the *trigger time* and a knowledge of the rotation of the wheel.
2. The trigger time is the time corresponding to a spike in a proximity sensor placed at a specific location on the wheel (75 degrees). The spike occurs when the sensor "sees" a block located on the middle of the coupon. The block is located approximately 6.03 in from the leading edge of the coupon.
3. Knowing the speed of the wheel, e.g. 100 ft/min, the start time can be determined using the trigger time. The start time corresponds to the position of the paper on the coupon (measured with video or picking evidence) which is "0 in" relative to the location of the block (6.03 in). The nip point of the tape is designed so that the leading edge of the paper lines up with the leading edge of the coupon. Usually, the first inch of paper was neglected so that the start of the peel was actually after 1 in of paper had already peeled. Converting the speed from ft/min to in/s, the time it takes for 1 in of paper to peel is determined. This value is subtracted from the *trigger time* to obtain the *peel start*.

4. The peel end is then easily calculated by using the length of the paper peeled. Since there are 9 more inches of paper (1inch is under the mylar and the first and last inch is neglected), the time corresponding to 9 in is calculated using the speed of the wheel. Subtracting the start time from this time gives the total time for the peel event. This total can be added to the start time to obtain the *peel end*.
5. A Peel Point adjustment is made to the start (and consequently end time). For each degree offset from 75, the position and therefore the time of the peel event changes. To calculate this offset, the peel point must be determined. To convert from degrees to inches, use the conversion factor $2\pi r/360$. For the WADS, the radius is 13.325 in which makes the conversion factor 0.233 in/degree. For each degree of offset (either greater or less than 75), the peel start must be adjusted which also will change the peel end.
6. Using the peel start and end, the time and tension data is extracted into a separate sheet for work analysis.

III. % Solids Ingoing and Outgoing

1. Pre and Post weight of the entire sample (paper + tape+ Mylar) are recorded during each run
2. % Solids Ingoing is calculated as follows:

$$\%\ Solids = \frac{Dry\ Weight\ (g)}{Pre\text{-}Weight\ (g) - (Tape+Mylar+Correction\ factor)} * 100$$

3. Basis Weight is checked and recorded for each formette sheet prior to sample preparation
4. Tape+Mylar+Correction = 6.59 g (based on averaging 20 different tapes); Correction is weight loss through evaporation (determined empirically) for 2 minutes (typical time from setup to run)
5. % Solids Outgoing is calculated in a similar fashion by using the post sample weight (no correction factor)

IV. Work Calculation

1. The tension data for the peel event is transferred to a new worksheet
2. Average time and tension are calculated so that the number of time & tension points equals the number of angle points
3. Tension is converted to SI units and divided by the width of the paper to get a tension per unit width
4. Following equation **3** from the main report, a calculated tension (that takes into account curvature) is calculated using the formula:

$$T' = \frac{W_s}{1-\cos\phi} + \rho v^2 + \left(\frac{R_t}{\Gamma}\right) W_g(t)$$

T' = Tension per unit width

W_s = Work of separation

ϕ = Peel Angle

R_t = Local radius of curvature (equation not shown here)

Γ = Length of curve followed by paper

W_g = Weight term

v = Velocity

5. Work (in SI units of g/s^2) is calculated using the Mardon equation:

$$W = \frac{T' - mV^2}{1 - \cos\phi}$$

6. A chart of work vs. time is created for each run

APPENDIX D: Image Analysis

Image analysis for picking quantification uses two still images taken with a Sony Mavica digital camera, one before the peel and one after. These images are then modified using ImagePro Plus 4.0, and the resulting images are analyzed using Scion Image for Windows.

First, using ImagePro Plus 4.0, an image is converted to grayscale and a rectangular area of interest (AOI) is chosen corresponding to the 1 inch square on the coupon surface. The AOI is then duplicated. A filter is used to "flatten" the image, which decreases the effect of any shadows and noise in the image. The area of the AOI is recorded in square pixels. The modified image is saved as a TIFF file.

Scion Image is then used to determine the black area, what is not covered in fiber. The modified image is duplicated; the duplicate is then put in thresholding mode (black and white). The amount of threshold is varied so that the white area on the threshold image corresponds to the fiber area on the modified image. The analysis Info Box displays the "pixels" measurement, which is the area of the AOI not covered with fibers.

The percent fiber area for this image is then calculated:

$$\%\text{Fiber Area} = \frac{\text{total area - black area}}{\text{total area}} \cdot 100$$

To quantify picking for one peel event, the percent fiber area for the "before" image is subtracted from that of the "after" image.

APPENDIX E: Tack Testing Procedure

I. Adhesive-contaminated Plate Preparation

1. Coat Test Plate with Adhesive
    f. Apply sufficient amount of adhesive to one edge of plate.
    g. Draw adhesive across surface of plate using metering rod calibrated to desired thickness.
    h. Allow adhesive to dry.
2. Mark Test Blocks on Plate
    i. Measure 1" x 1" grid covering plate (4 x 4 grid).
    j. Mark grid on plate with permanent marker.
    k. Limit contact with adhesive surface as this could affect the tack properties.
    l. Number each box in the grid with a small number on the edge of the box.
3. Measure Adhesive Thickness.
    m. Using the CMI CGX Gauge, measure the thickness of adhesive in each square on test plate.
    n. Record adhesive thickness measurements.
4. Curing and Heating
    a. Place contaminated plate on heater with divets on side lined up with screws.
    b. Tighten screws to ensure good contact with heater.
    c. Adjust temperature using control on front of heater according to calibration.
    d. Let plate heat for 1 hour before testing.

II. Sample Preparation

1. Cut paper in 4" x 0.5" strips.
2. Dry strips to 40% solids.

III. Instron Preparation

1. Install 2 pound load cell.
2. Install tack testing device.
3. Create a flat surface on bottom half of Instron by installing metal plate.
4. Place heater (with contaminated plate) on plate.
5. Using up and down arrows, position contaminated plate 1 inch below bottom surface of tack testing device.
6. Logon to Instron software
7. Edit Test Method
    a. Measure thickness of paper sample.
    b. Open test method #27.
    c. Enter thickness.
    - *Specimen – thickness: measured thickness*
    d. Save Method.
8. Setup Machine Control on Panel.
    h. Disable computer control. Make sure **IEEE488** is **OFF**.
    i. Calibrate/clear settings by pressing the following buttons in sequence:
    -S1
    -0
    -ENTER
    -CAL (in LOAD Box on control panel)
    -ENTER

    j. Input Cycle

-Check that extension is displayed in inches. ENGLISH should be lit in red on the left side of panel. If SI is lit, change to English by flipping switch on the lower backside of control panel. If the units are changed, repeat step (b) calibration.

-GL RESET
-Extension (Electronic Limits):
MAX—*1.05*—ENTER
CYCLE—ENTER
MIN—*0*—ENTER
-STOP—ENTER
-SPEED—*12*—ENTER

IV. Run Tack Tests

1. Setup Software to Collect Data
   a. From Instron software home screen, choose TEST.
   b. Create file for data.
   c. Select test method #27.
   d. Enter sample ID information.
   e. Start test.
2. Install Paper Test Strip.
   a. Squeeze tack testing device (See Figure 1) and place an alligator clip under the head of one spring screw.
   b. Clamp one end of paper strip in attached alligator clip.
   c. Wrap the paper strip around the tack testing device.
   d. Clamp free end of paper strip with the other attached alligator clip.
   e. Remove clip from spring screw. Paper strip should be taut against bottom surface of device.
3. Start Test.
   a. Press UP arrow on Instron control panel to engage test.
   b. When sample is complete, click *End Sample* and *Continue* then print data.
   c. Repeat steps 2-4.

V. After Testing is Complete

1. Reset Instron.
   -Press **GL RESET**
2. Remove tack testing device, heater/contaminated plate, and metal plate.
3. Exit Instron software.

VI. Picking Analysis

1. Take pictures of the sample squares using the Sony digital camera set on the highest resolution, macro, no flash.
2. Include 4 squares per picture.

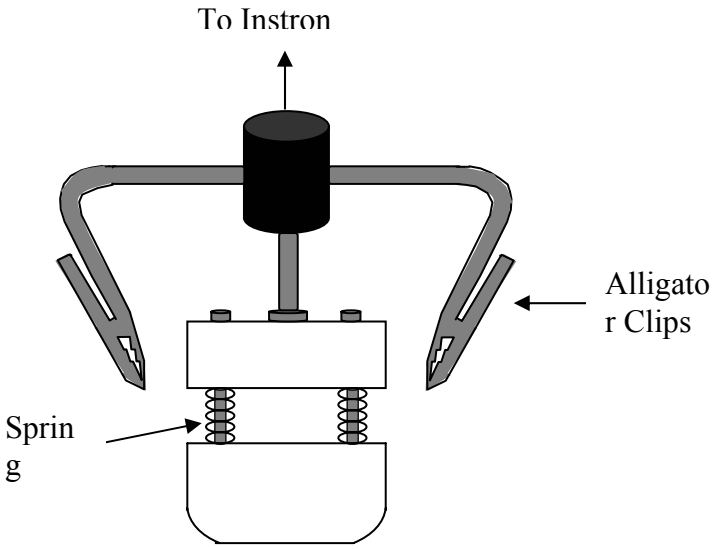

Figure 1: Tack Testing Device

APPENDIX F: Raw Data

I. Clean Coupon Tests/Roughness Tests

C drive, Folders: Matrix 1, Matrix 2, Roughness

II. Initial Carbotac Contamination Tests

C Drive, Folder: Carbotac, D drive, Folder: Carbotac Matrix II

III. Carbotac & Vinac Contamination Tests

D Drive, Folders: CM Repeats, Vinac Matrix I

IV. Consolidation Testing

D Drive, Folder: Consolidation

V. Web Separation Modeling

Various sources above (new vs. old work comparisons)

VII. Tack Testing

I. Clean Coupon/Roughness Test Raw Data

Clean coupon tests include checkout runs as well as Matrix I & II. Only Matrix II data is presented here. All graphs shows are of Work (g/cm) vs. Time unless otherwise noted.

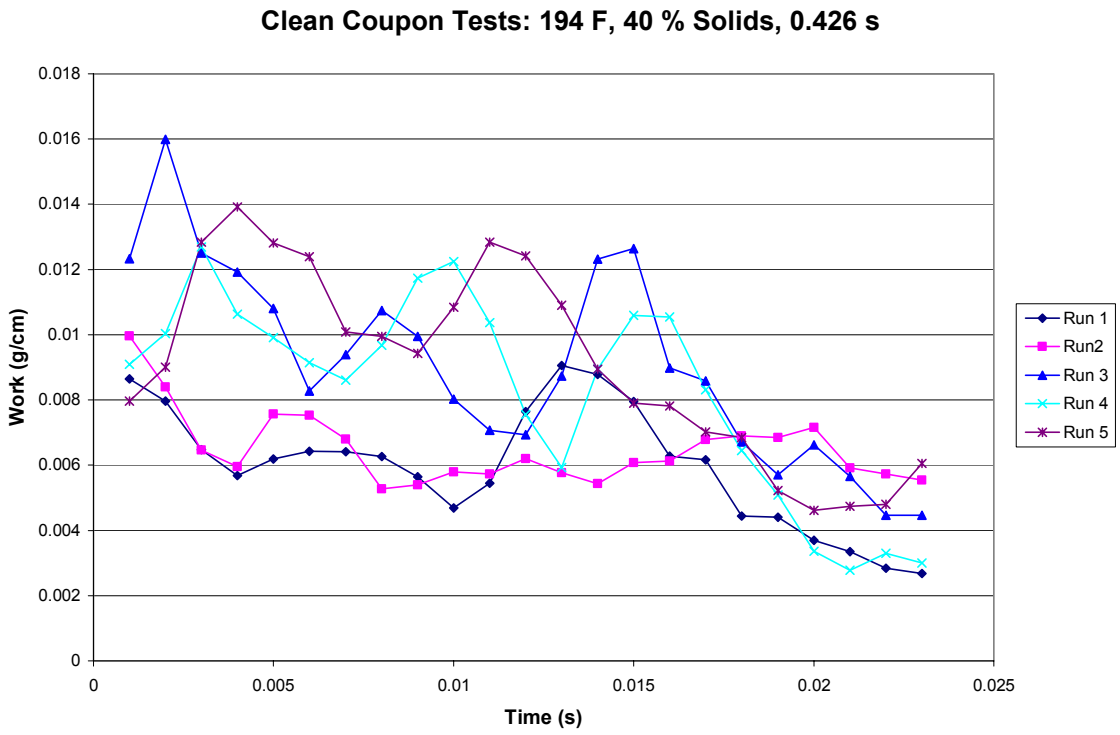

Clean Coupon Tests: 248 F, 40 % Solids, 0.426s

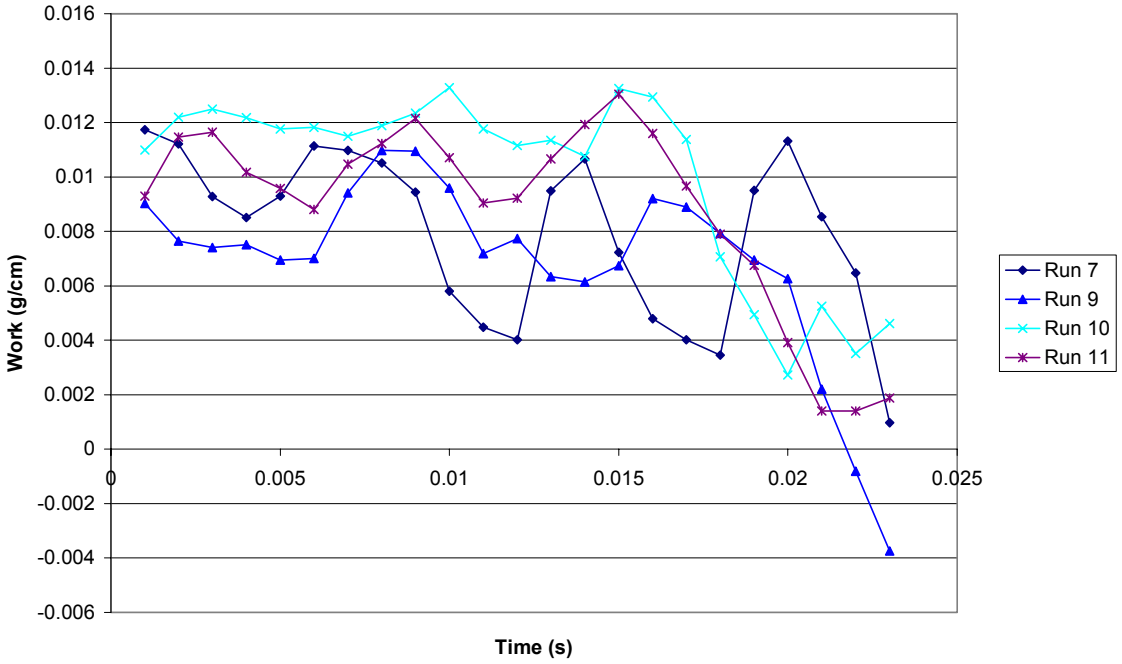

Clean Coupon Test: 194 F, 50 % Solids, 0.426s

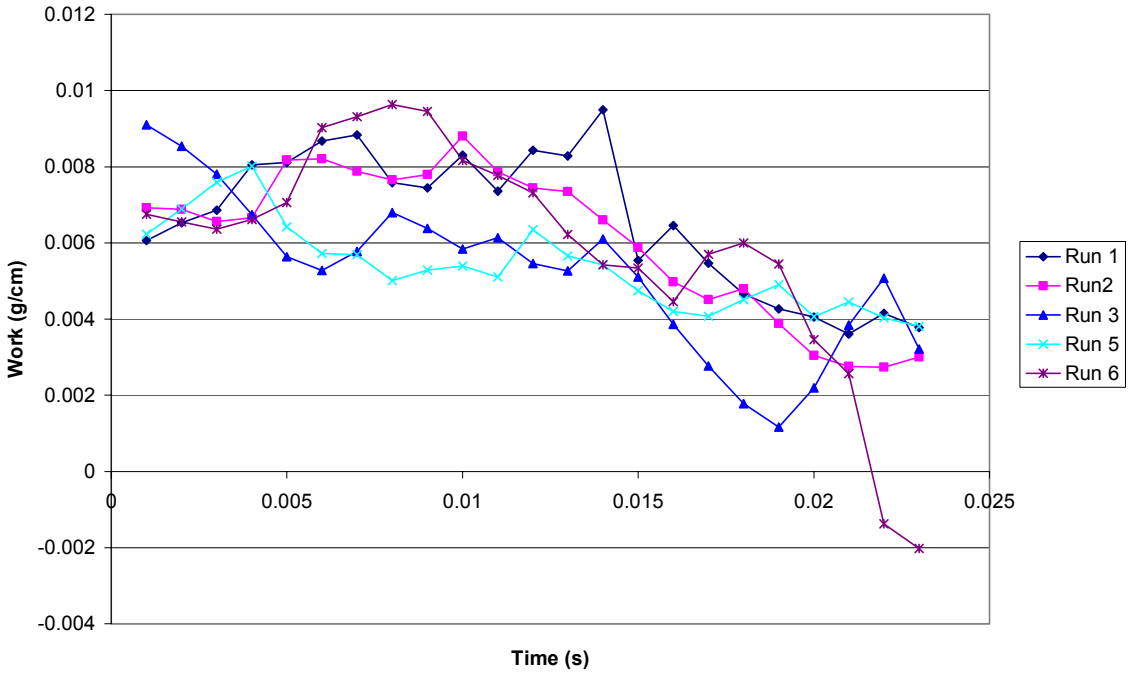

Clean Coupon Test: 248 F, 50 % Solids, 0.426s

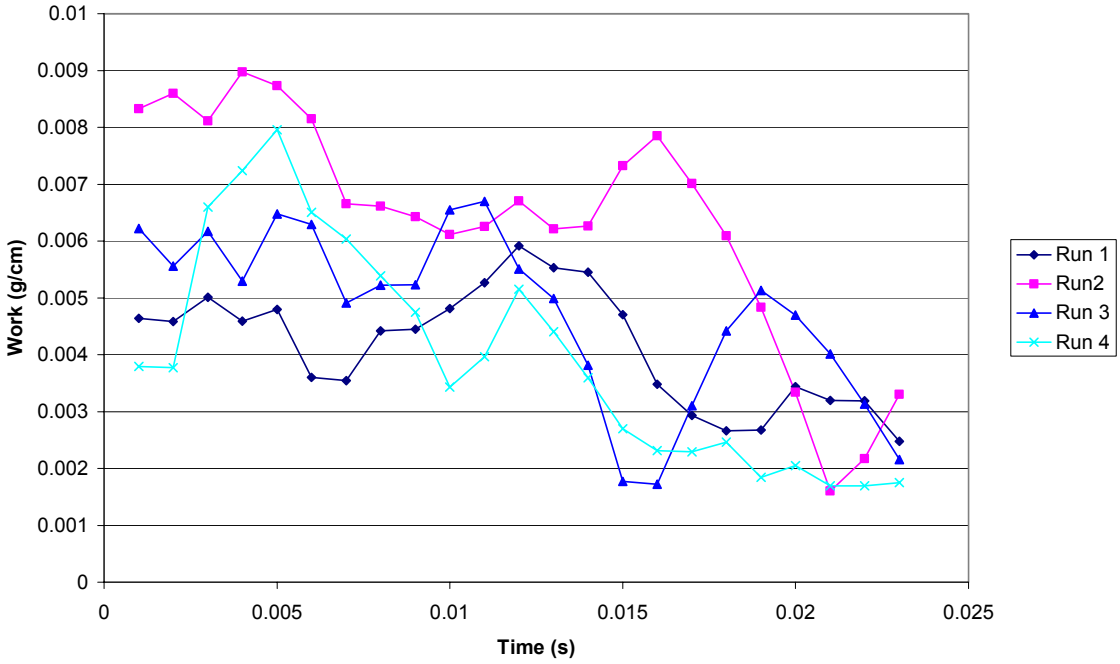

Clean Coupon Test: 302 F, 40 % Solids, 0.426s

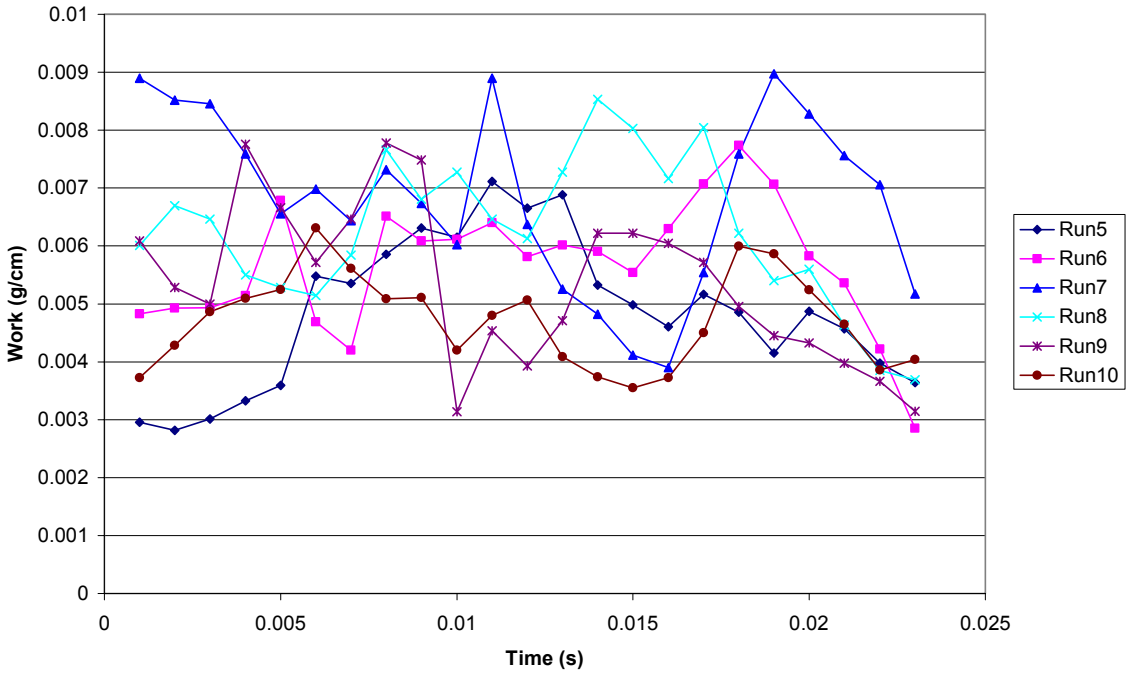

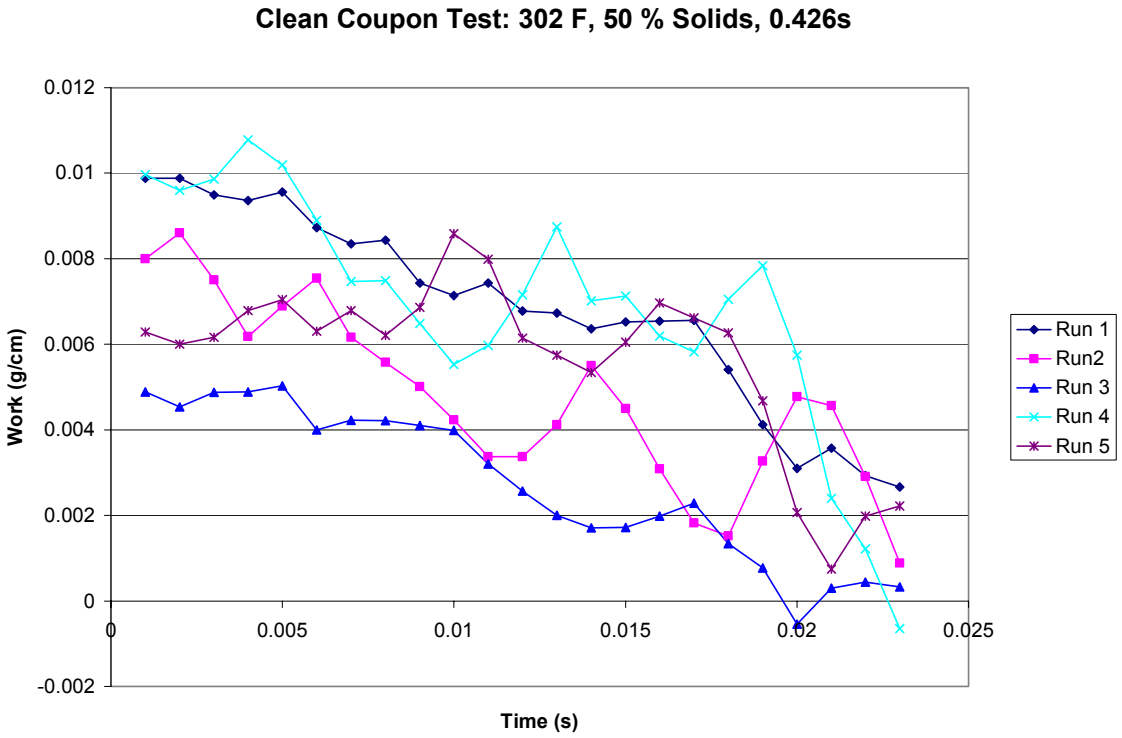
Clean Coupon Test: 302 F, 50 % Solids, 0.426s
0.012
0.01
0.008
0.006
0.004
0.002
0
-0.002
Work (g/cm)
0
0.005
0.01
0.015
0.02
0.025
Time (s)
Run 1
Run2
Run 3
Run 4
Run 5

Roughness Data was collected for two cases:

1. “sticky”: 194 F, 40% Solids, 0.426 s
2. “non-sticky”: 248 F, 50% Solids, 0.426 s

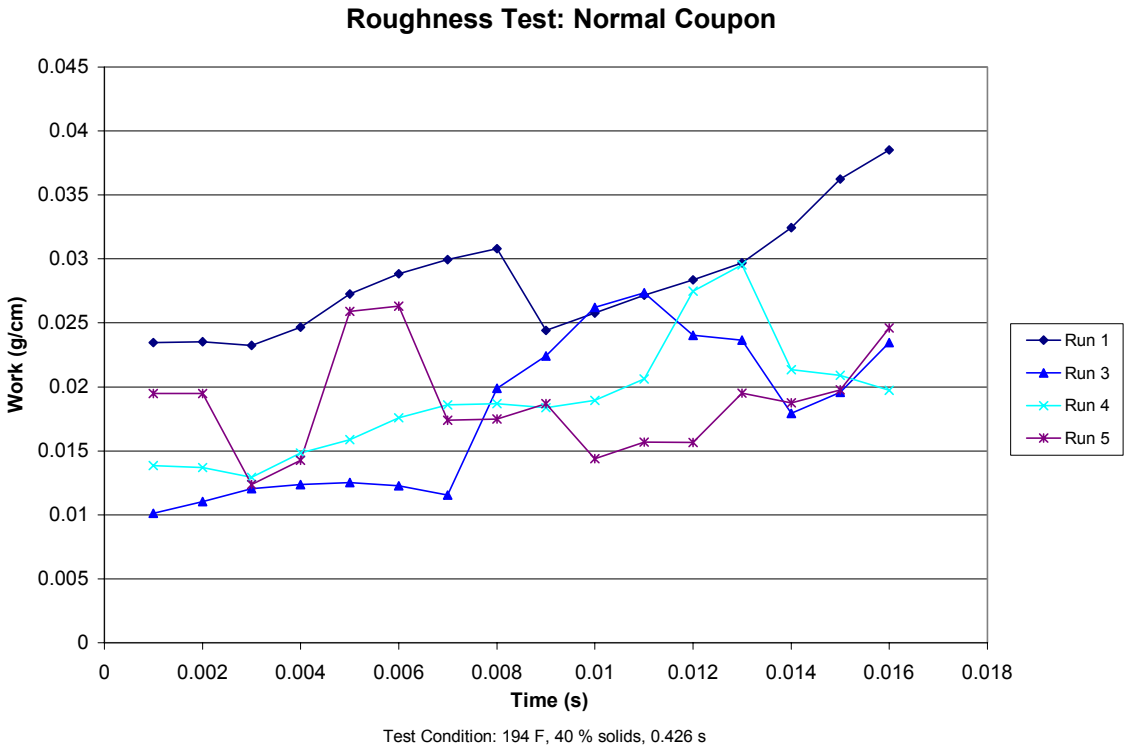

Roughness Test: Rough Coupon

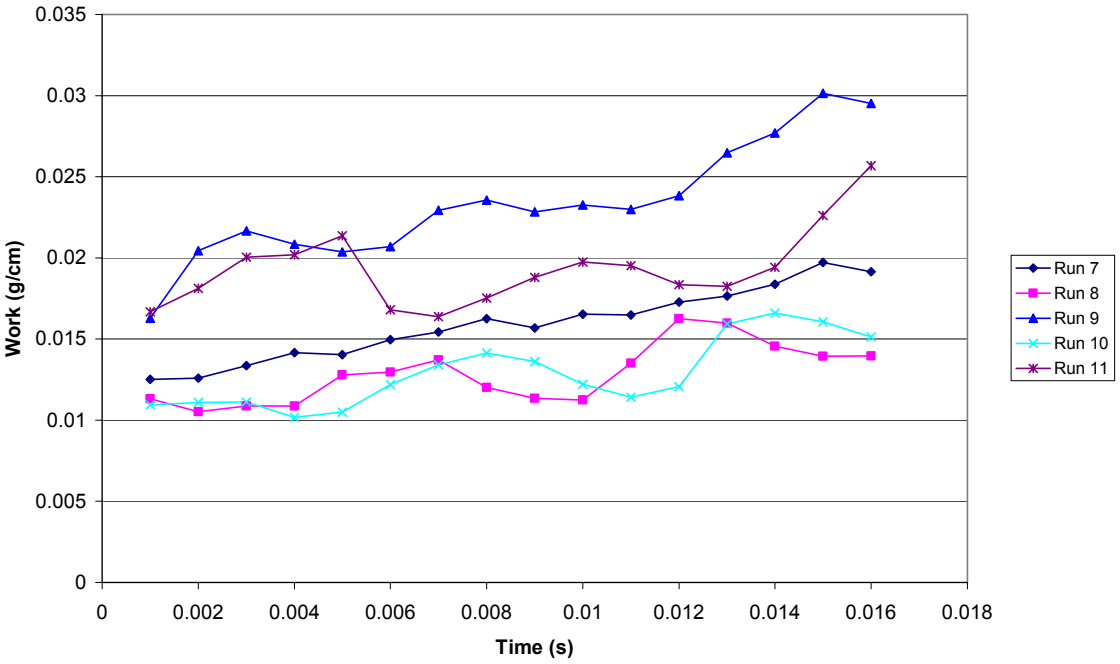

Test Condition: 194 F, 40 % solids, 0.426 s

Roughness Test: Smooth Coupon

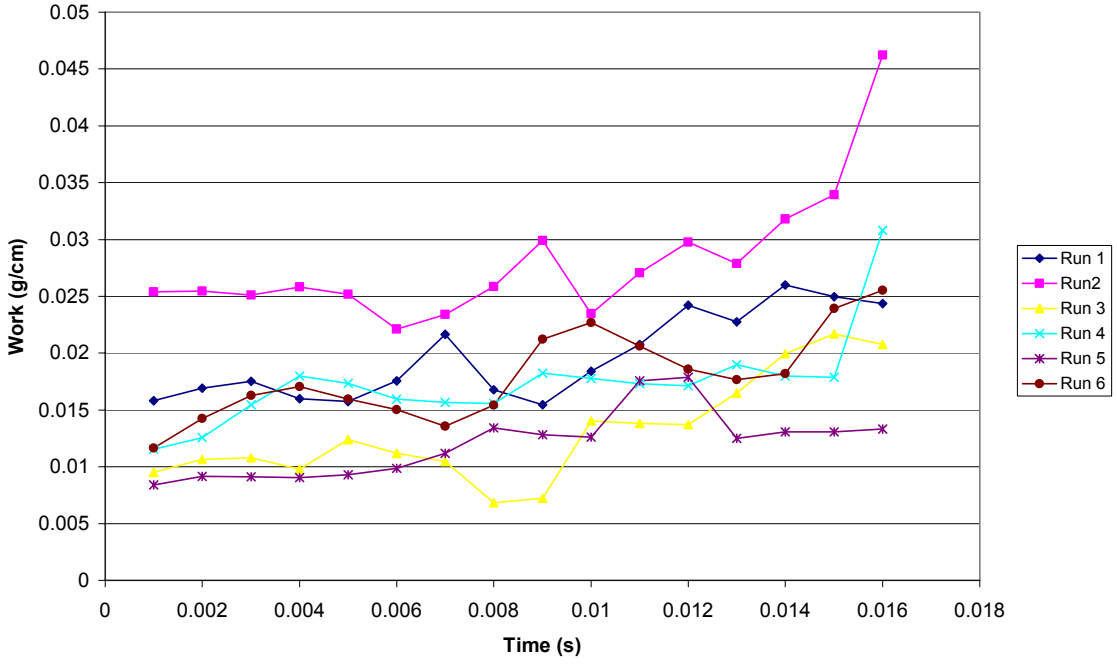

Test Condition: 194 F, 40 % solids, 0.426 s

Roughness Data for “non-sticky case”: 248 F, 50% Solids, 0.426 s

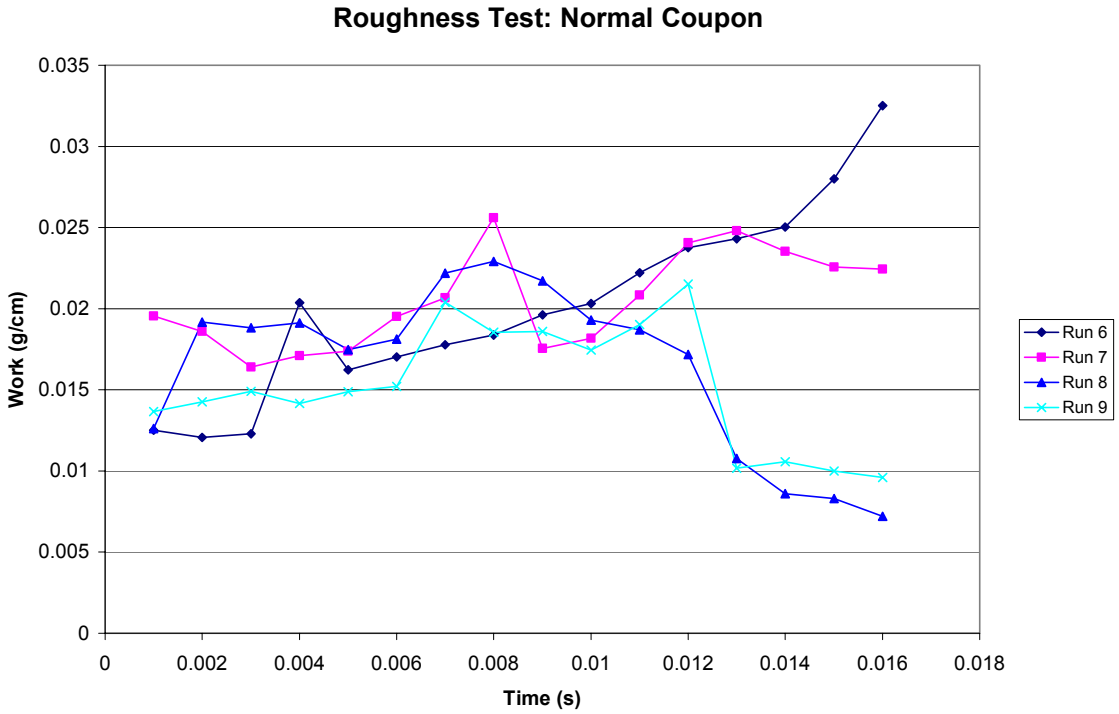

Test Condition: 248 F, 50 % solids, 0.426 s

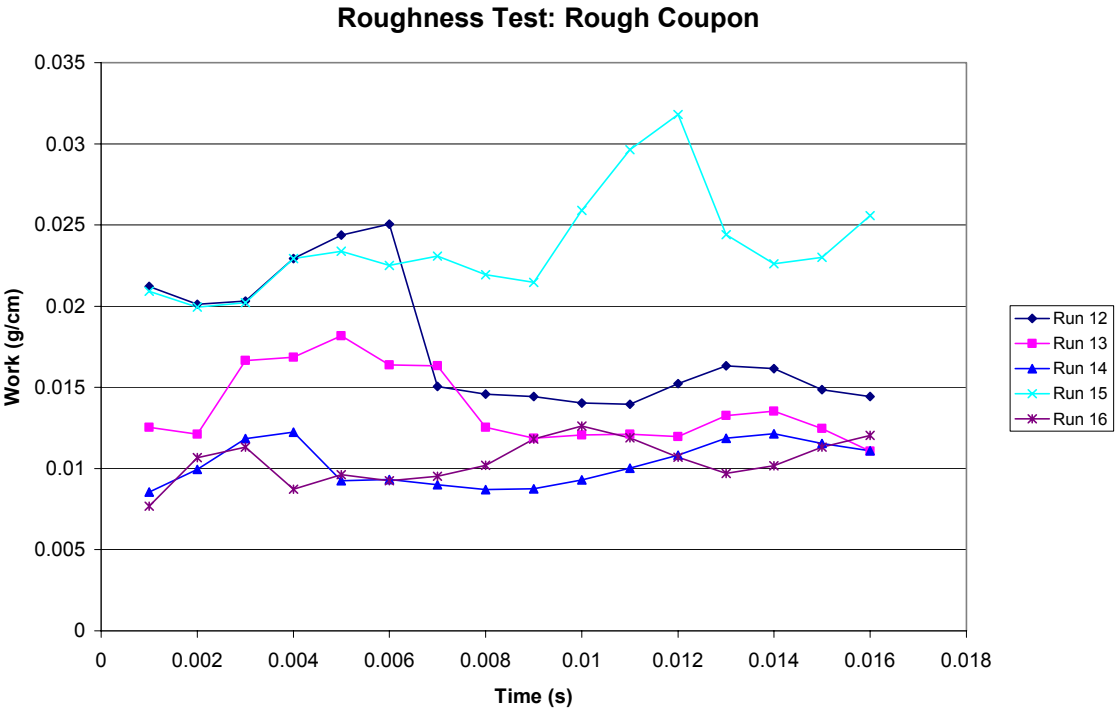

Test Condition: 248 F, 50 % solids, 0.426 s

Roughness Test: Smooth Coupon

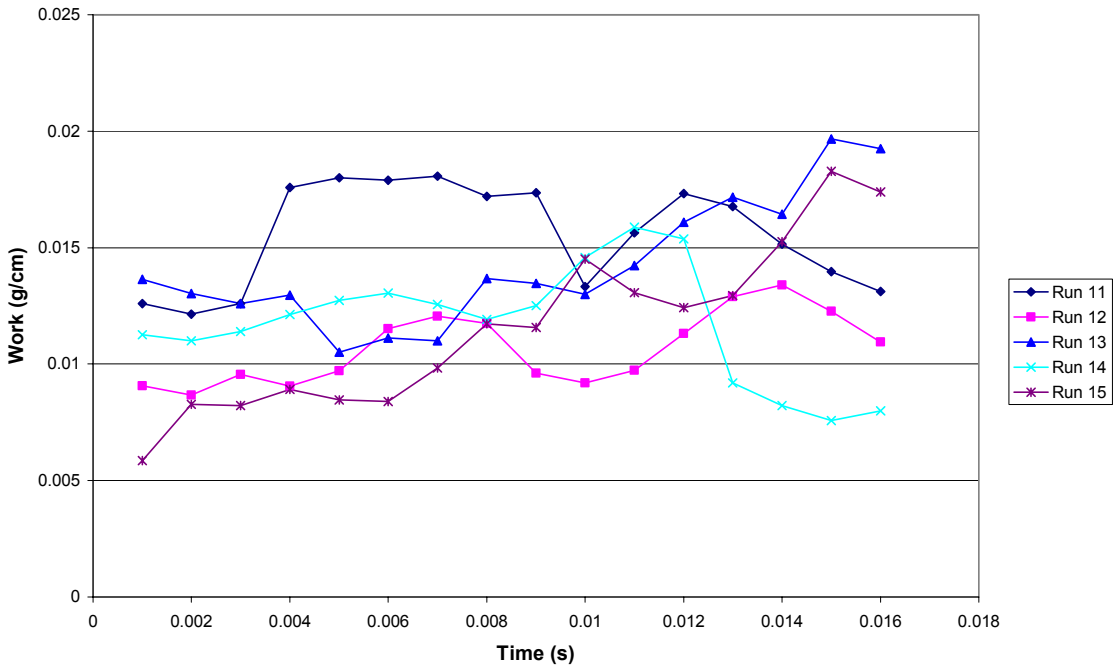

Test Condition: 248 F, 50 % solids, 0.426 s

Roughness Summary : Work of Adhesion

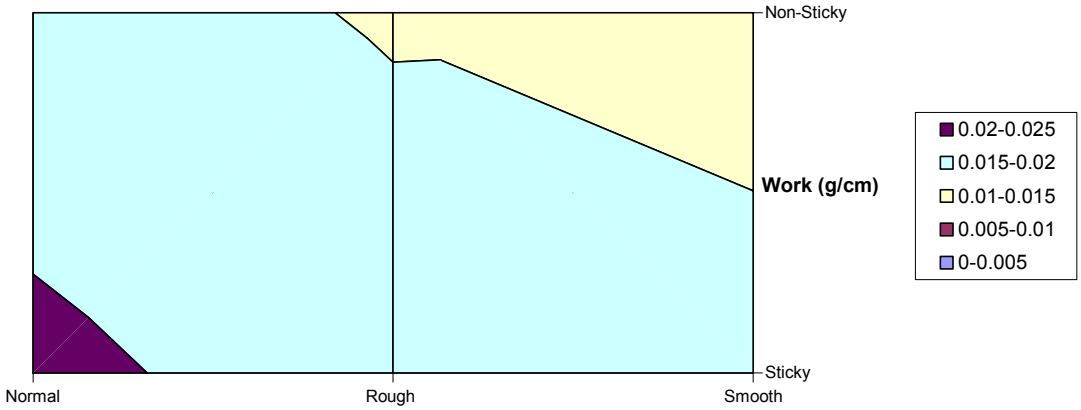

II. Initial Carbotac Contamination Tests

Carbotac Contamination Raw Data

Initial Carbotac Tests were done with 10 repeats on a single coupon. The average work values progressively decreased with run number. Conditions tested included 3 temperatures (149 F, 194 F, 302 F), two ingoing % solids (40% & 50%) and two dwell times (0.194 s & 0.484 s). For many of these tests, the tension and work values for runs 1 and sometimes run 2 exceeded the maximum level of the sensor and are therefore not included.

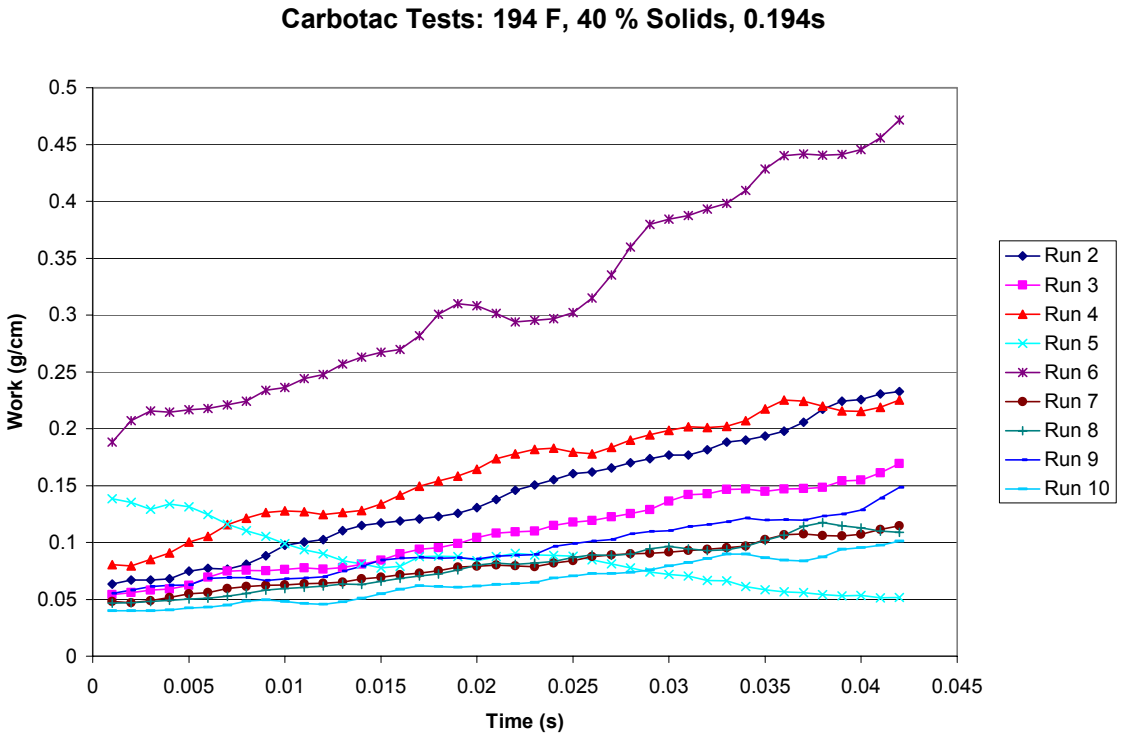

Carbotact Tests: 302 F, 40 % Solids, 0.194s

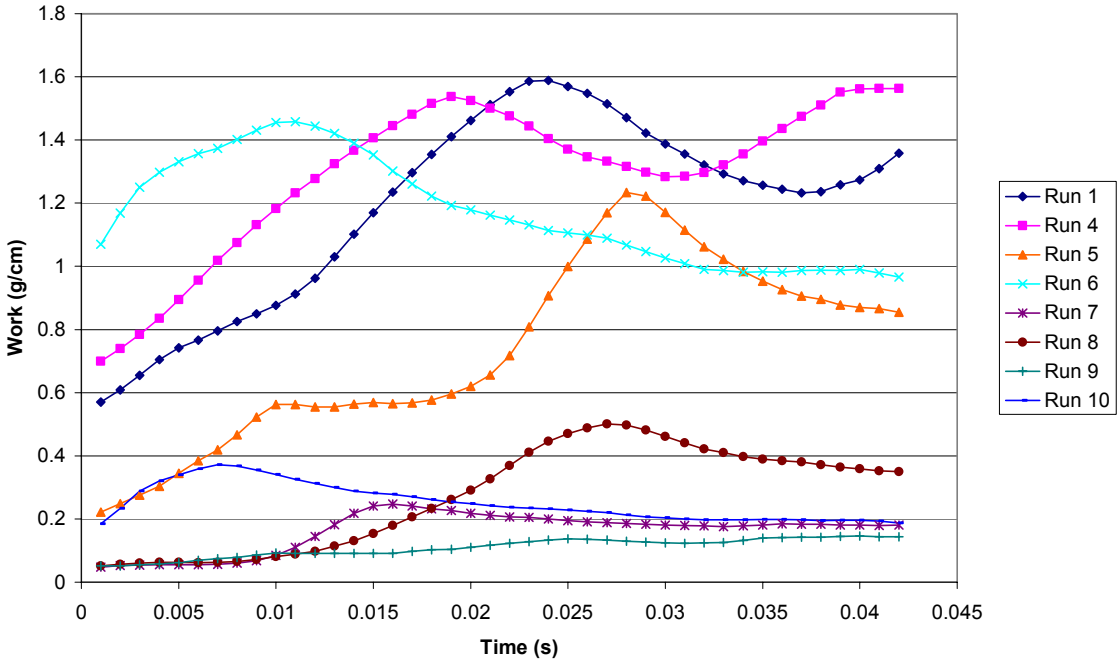

Carbotac Tests: 149 F, 40% Solids, 0.194s

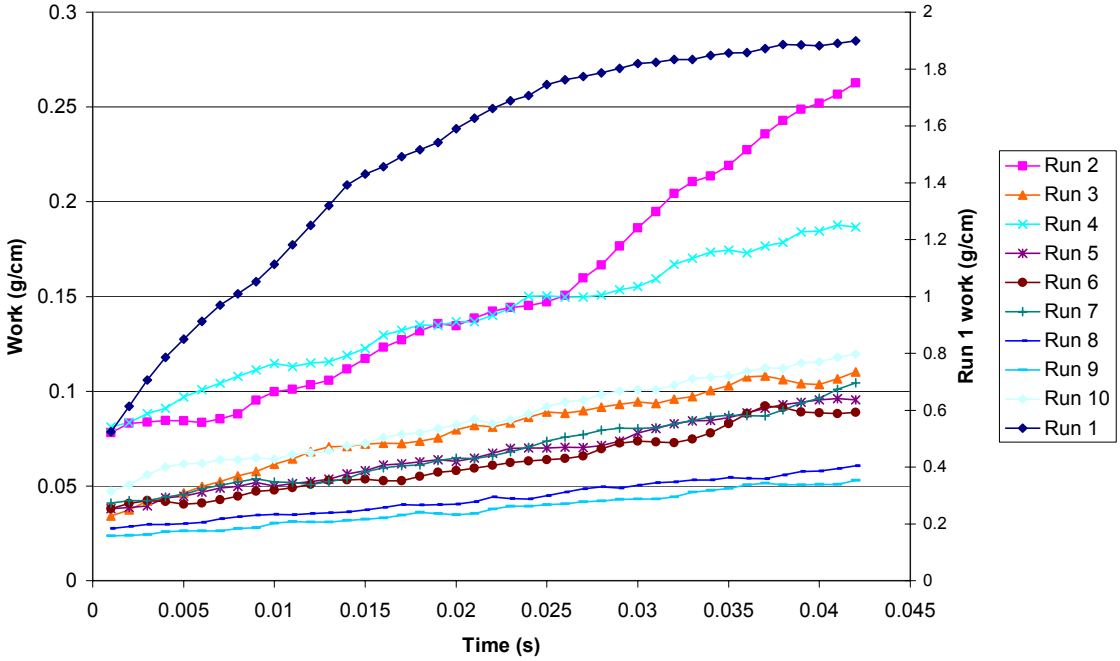

Carbotac Tests: 149 F, 50 % Solids, 0.194 s

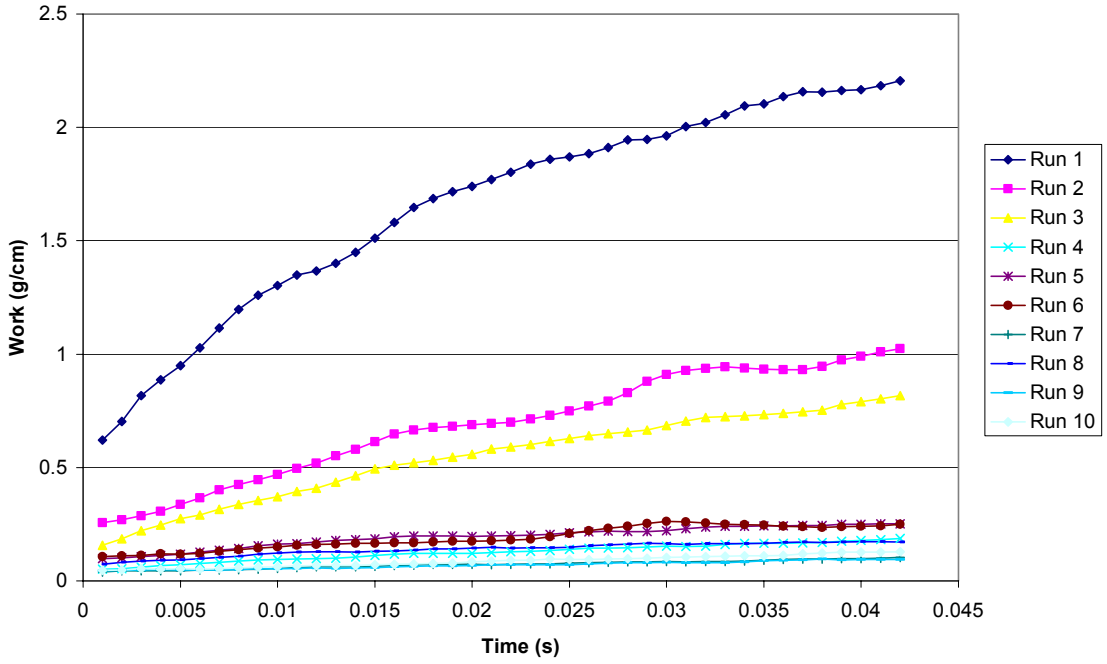

Carbotac Tests: 194 F, 50 % Solids, 0.194 s

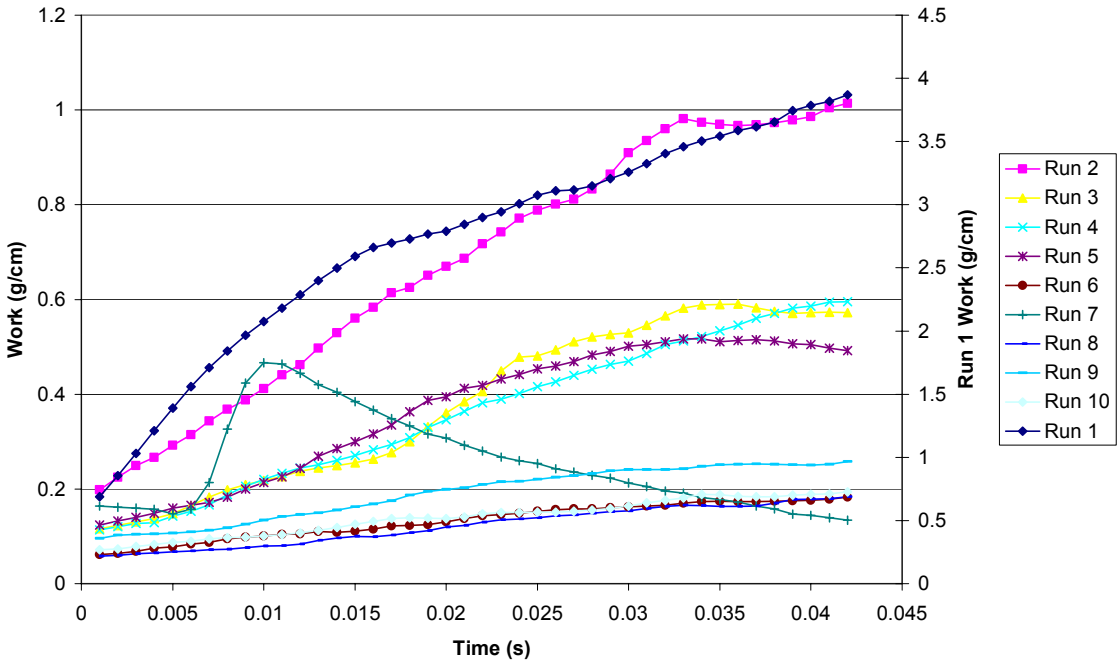

Carbotac Tests: 302 F, 50 % Solids, 0.194s

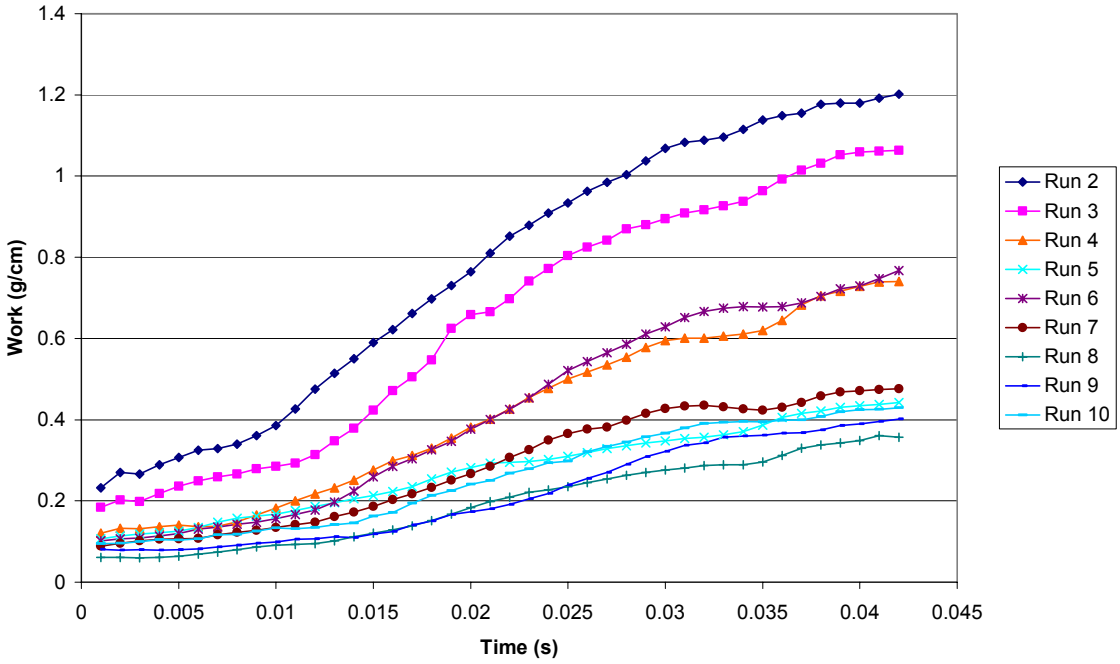

Carbotac Tests: 194 F, 40 % Solids, 0.484s

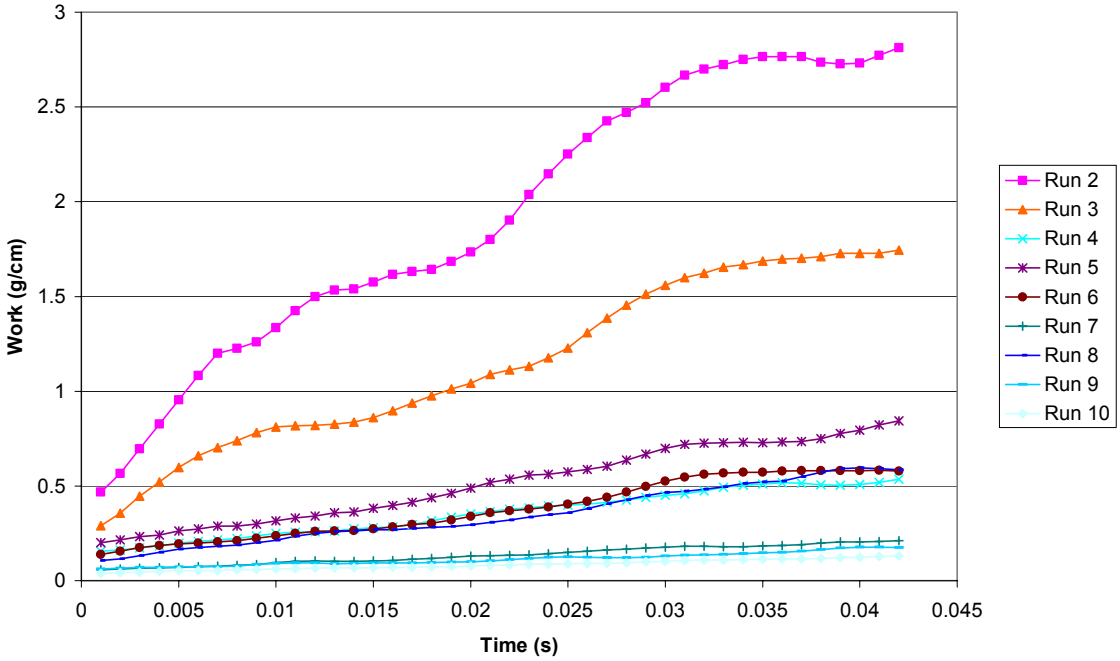

Carbotac Tests: 149 F, 50 % Solids, 0.484 s

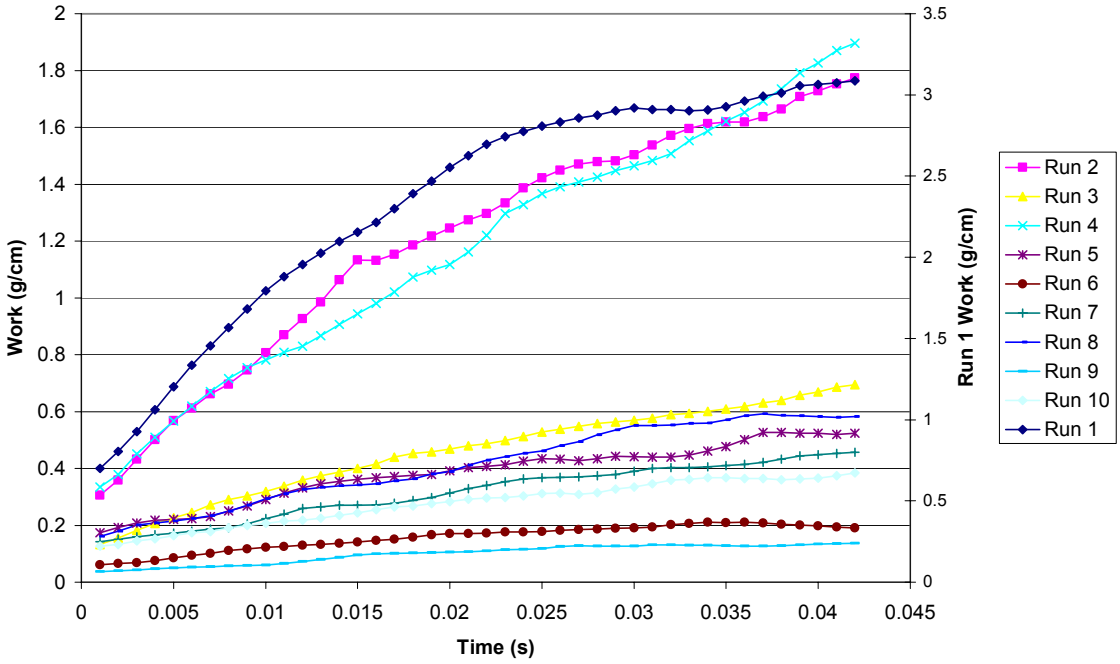

Carbotac Tests: 302 F, 50 % Solids, 0.484s

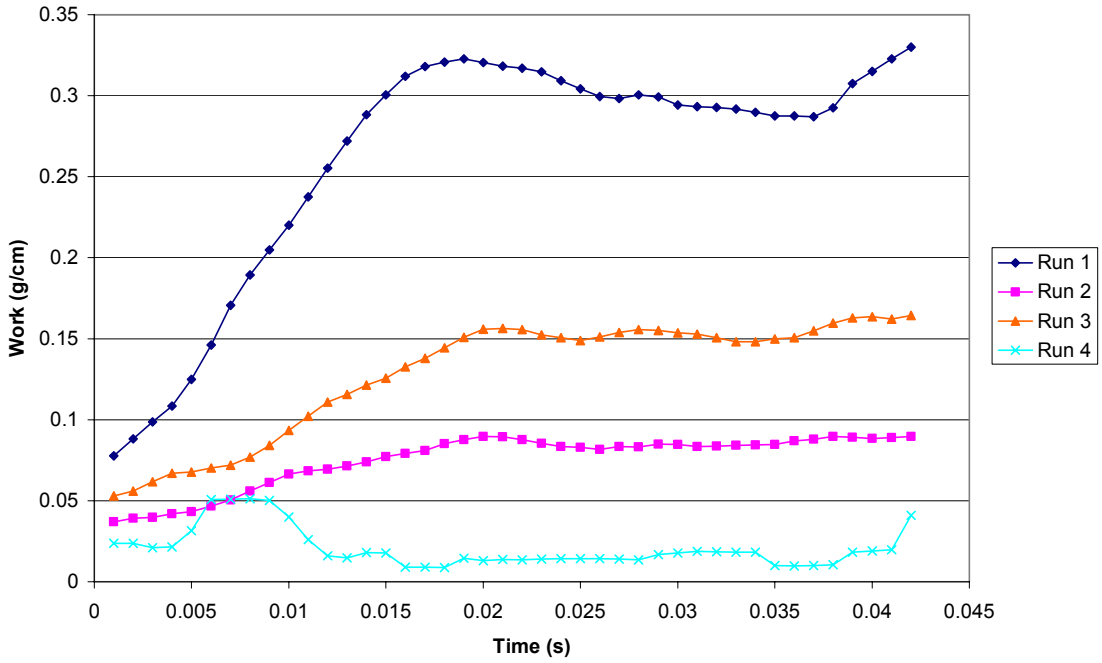

Carbotac Tests: 149 F, 40 % Solids, 0.484s

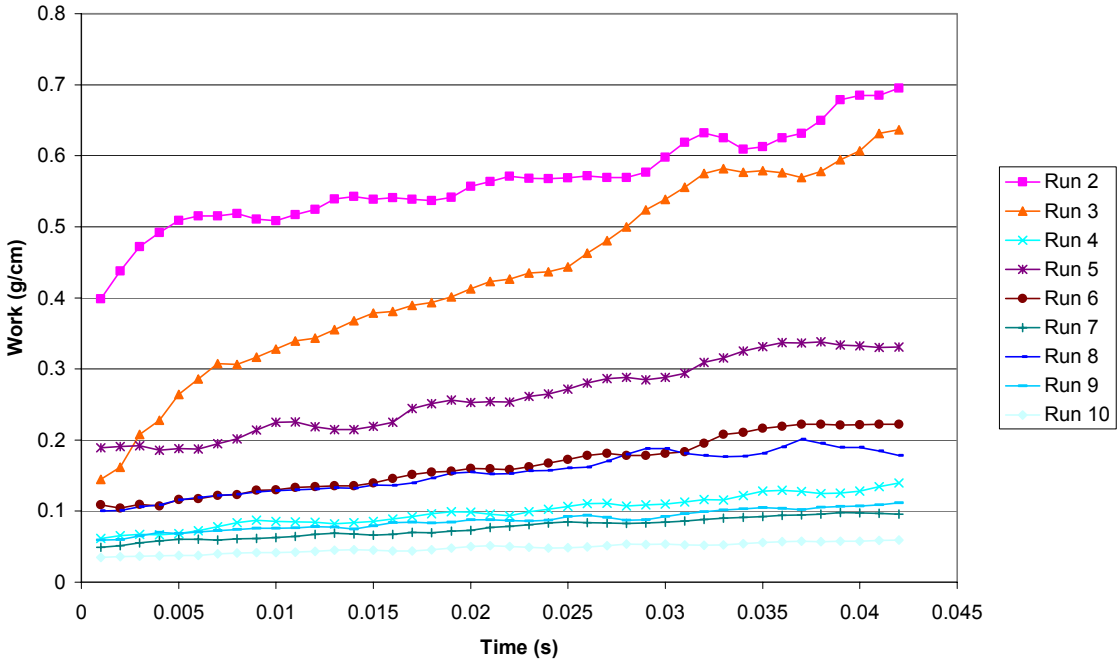

Carbotac Tests: 302 F, 40 %Solids, 0.484s

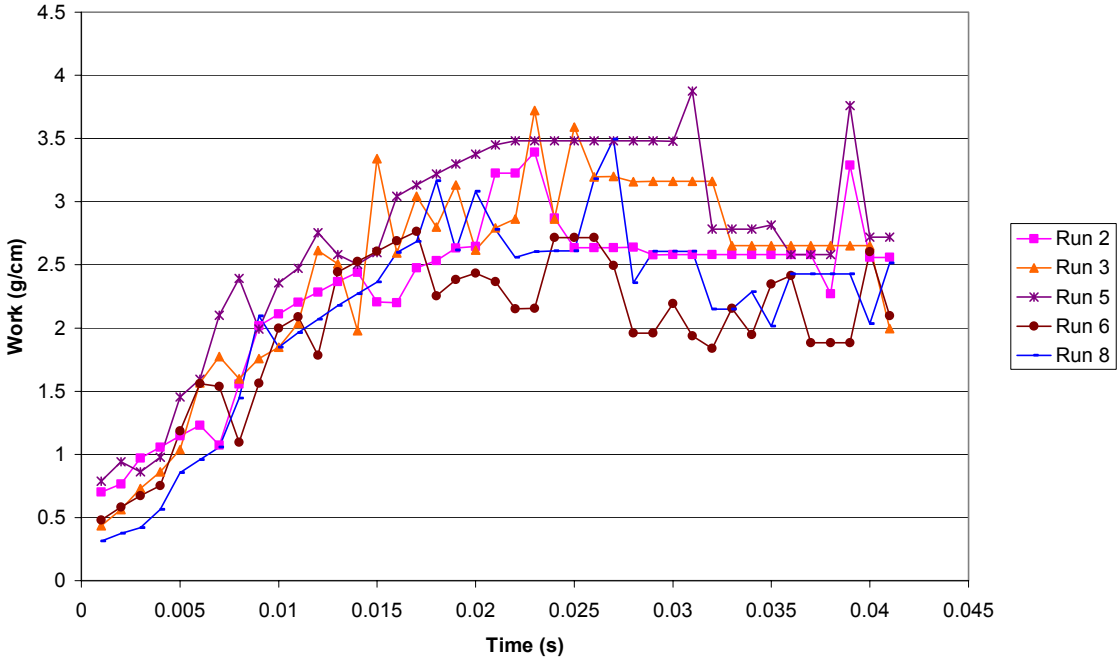

Carbotac Tests: 194 F, 50 % Solids, 0.484s

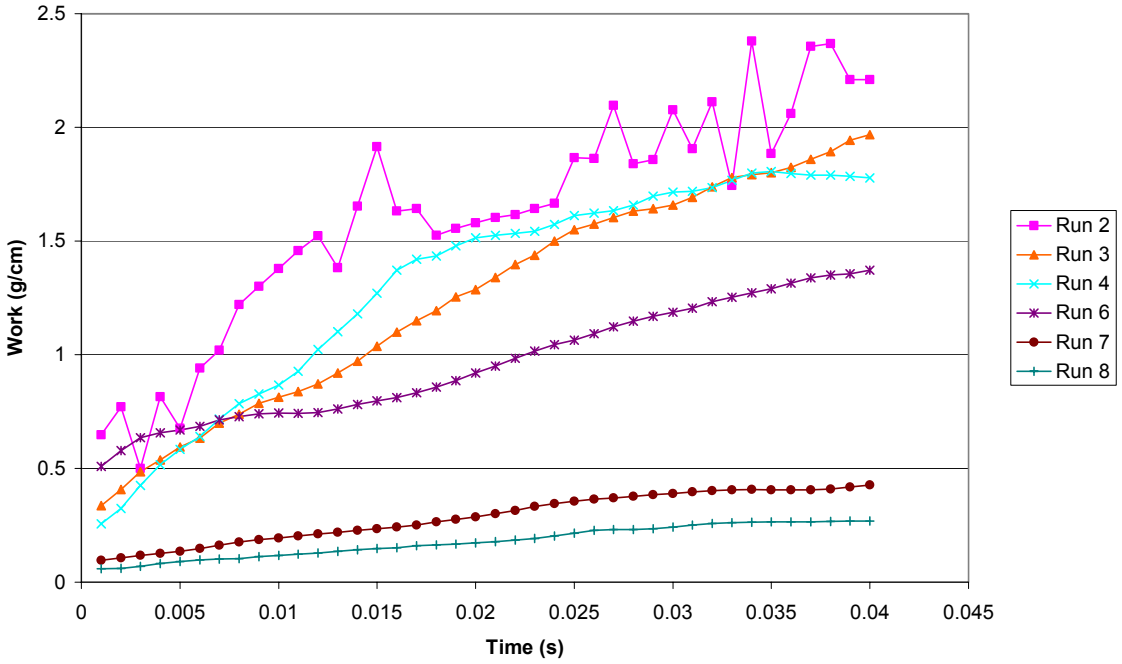

Carbotac Picking Summary : 0.194 s dwell

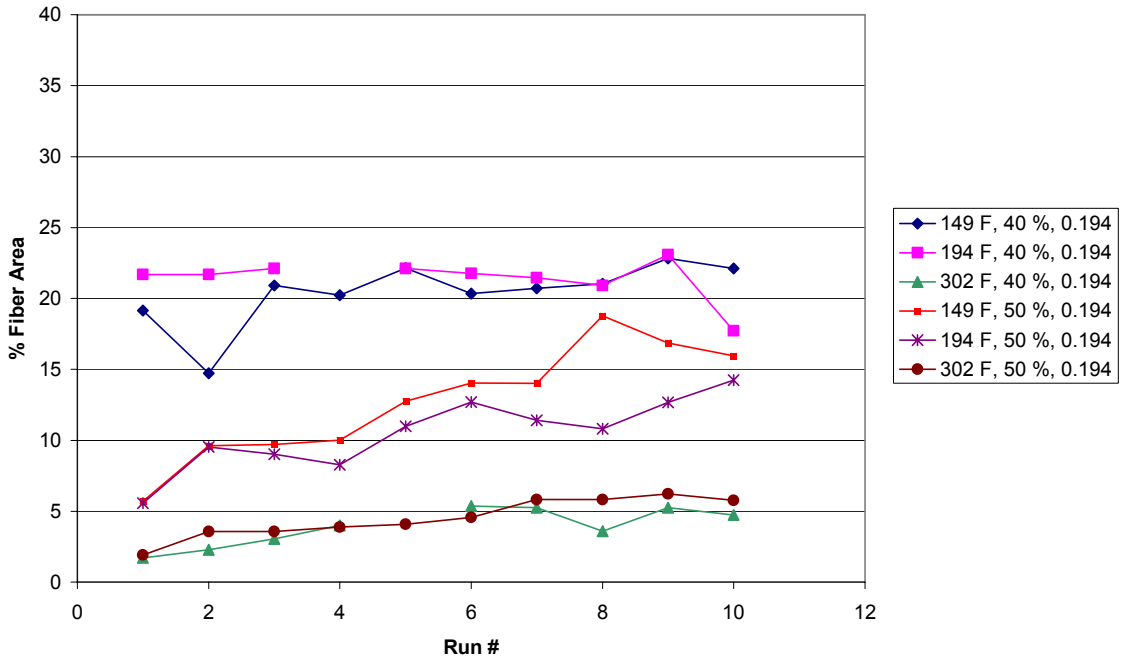

Carbotac Picking Summary: 0.484 s dwell

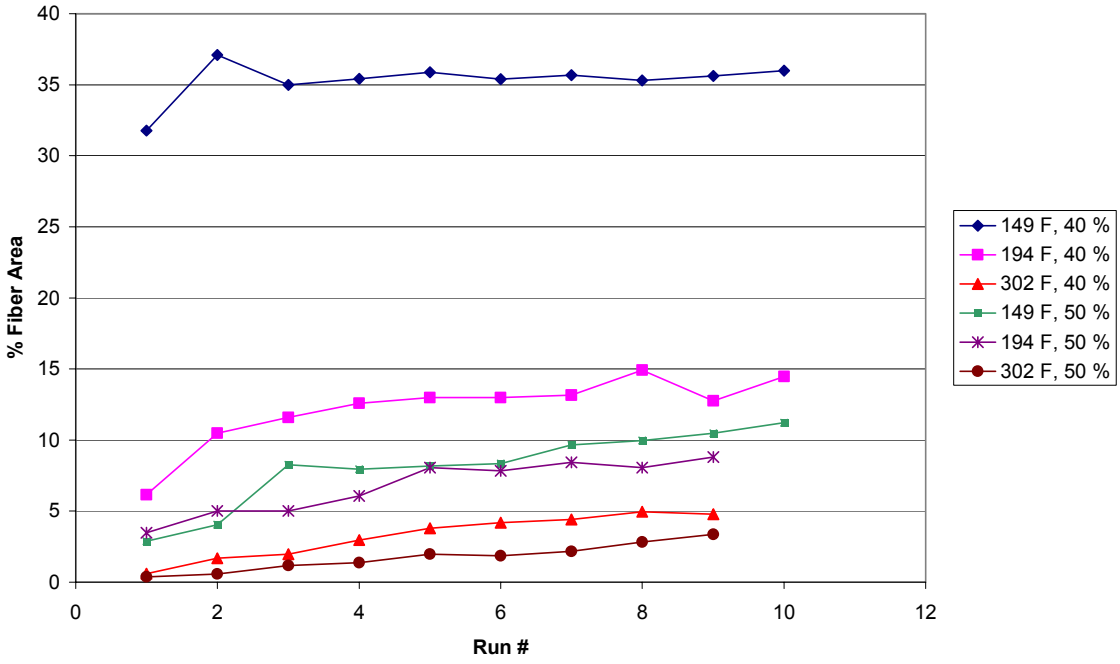

III. Carbotac & Vinac Contamination Tests

Multiple repeats of run 1 only were performed for 6 conditions (149 F, 194 F, 302 F & 40% and 50% ingoing solids). All tests were run at one dwell time – 0.194 s. A summary of the work and picking data is shown below.

Condition	Carbotac Work (g/cm)	COV/% DIFF	Carbotac Picking (% Fiber Area)	COV	Carbotac Tack (lb/in)	COV
149 F, 40 %	1.80	12.40%	11.40	48.82%	0.556	24.11%
149 F, 50%	4.01	18.85%	8.79	39.03%	0.556	24.11%
194 F, 40%	4.15	12.66%	21.30	39.65%	0.252	16.98%
194 F, 50%	2.59	4.17%	6.12	66.95%	0.252	16.98%
302 F, 40%,	2.36	28.06%	0.94	57.57%	0.181	16.28%
302 F, 50%	1.81	11.03%	0.41	34.49%	0.181	16.28%

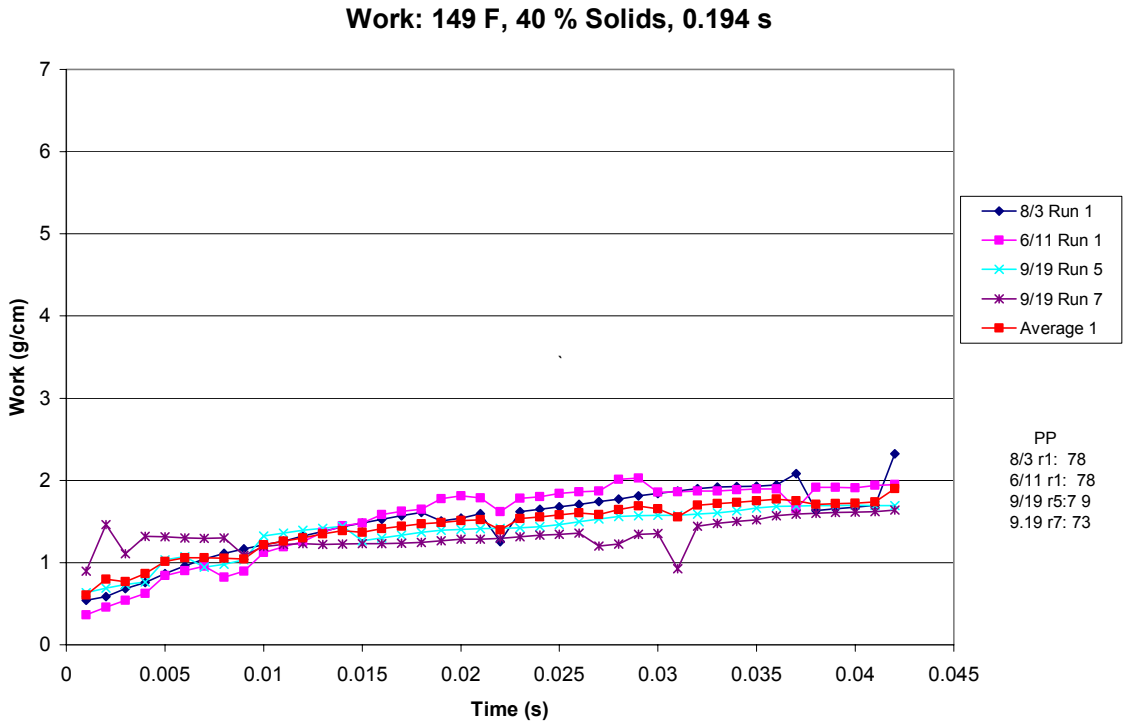

Work: 149 F, 50 % Solids, 0.194 s

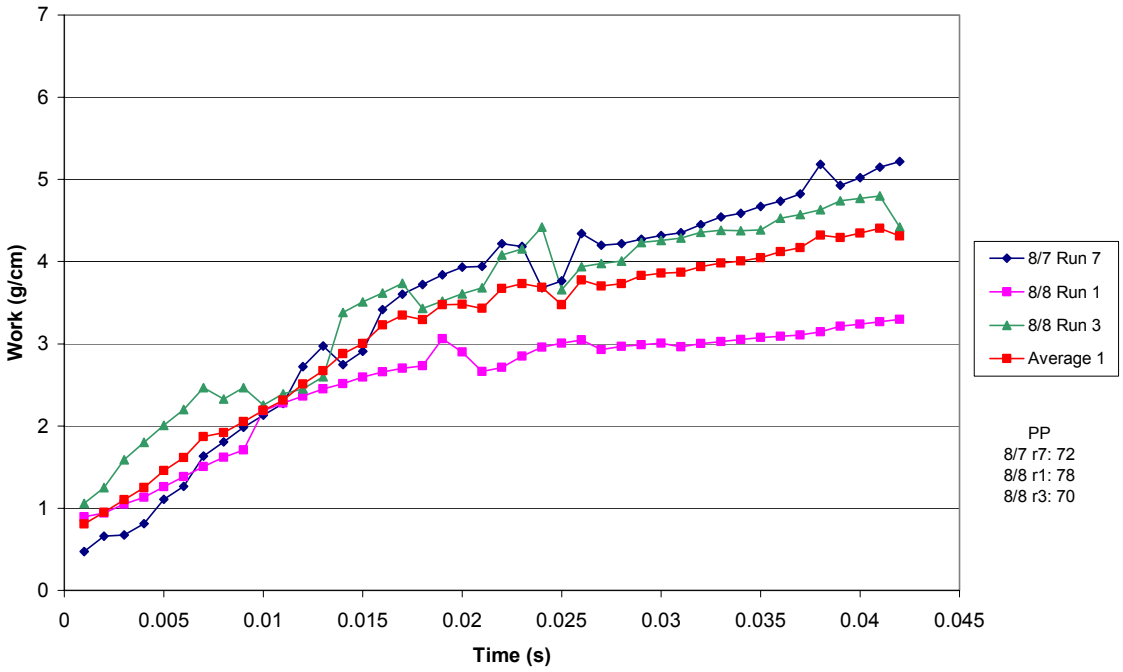

Work: 194 F, 40 % Solids, 0.194 s

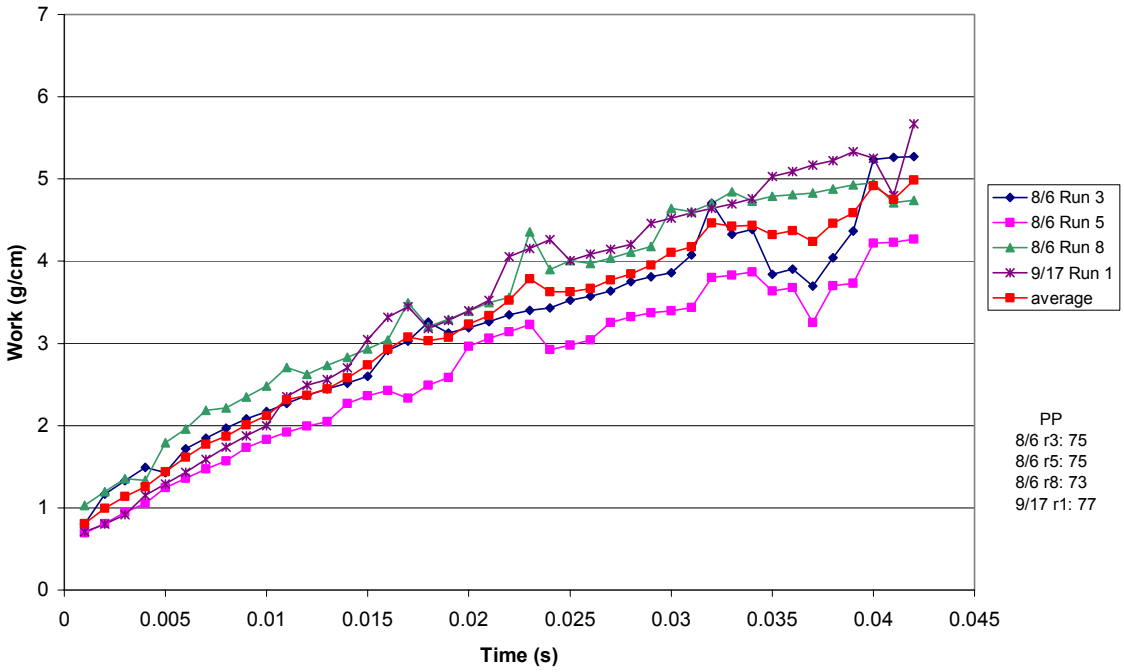

Work: 194 F, 50 % Solids, 0.194 s

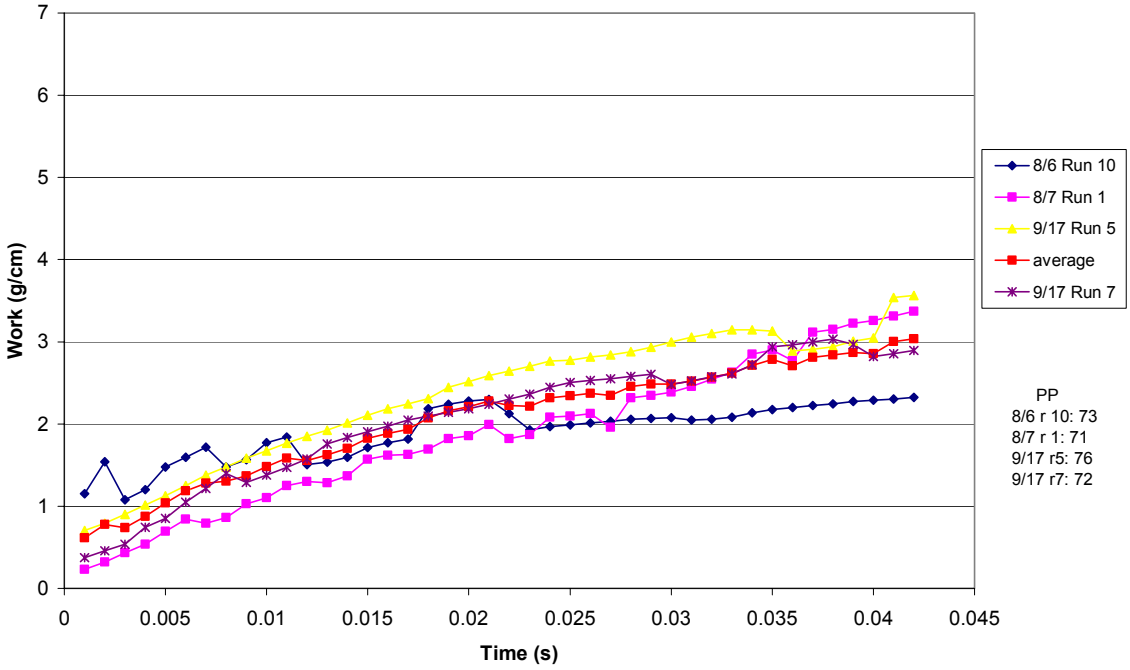

Work: 302 F, 40 % Solids, 0.194 s

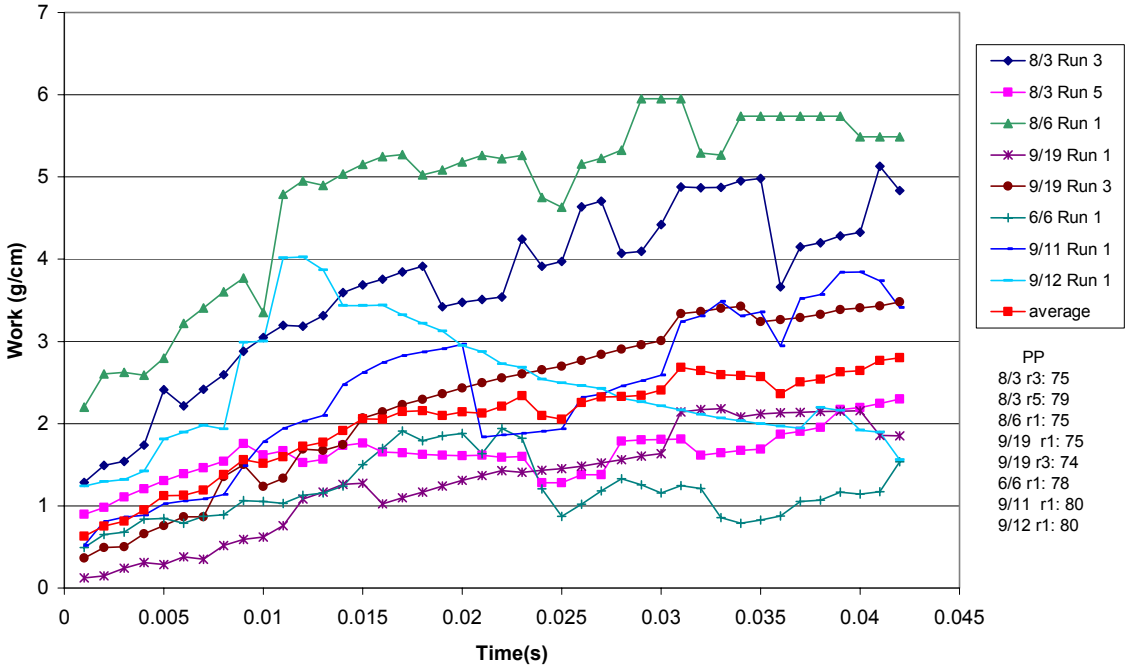

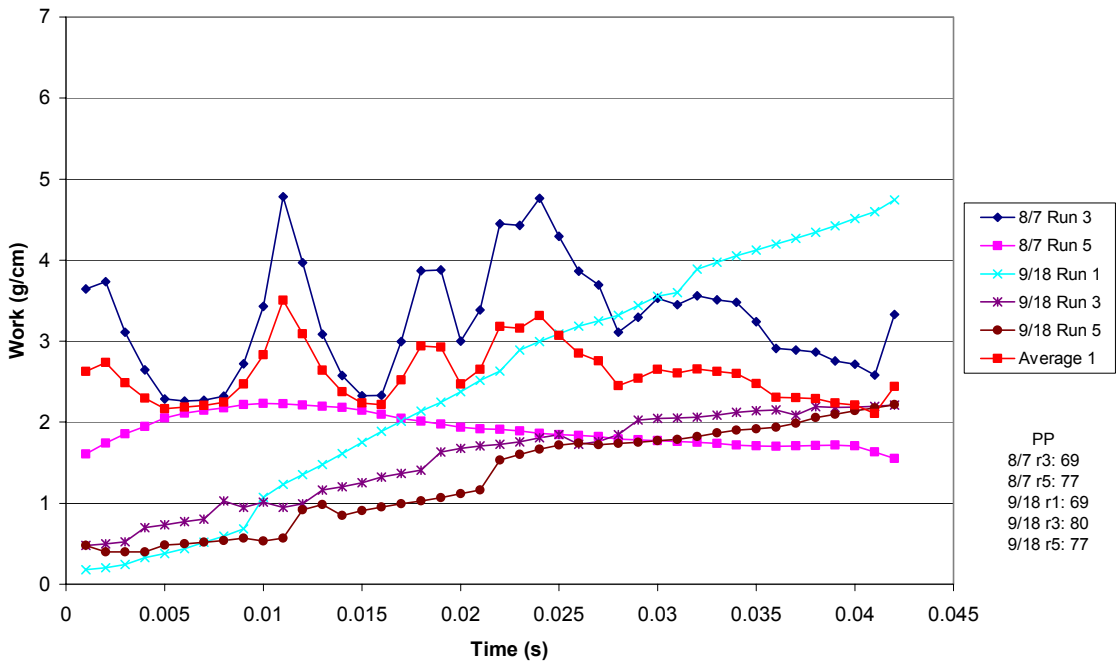
Work: 302 F, 50 % Solids, 0.194 s
Work (g/cm)
Time (s)
0
1
2
3
4
5
6
7
0
0.005
0.01
0.015
0.02
0.025
0.03
0.035
0.04
0.045
8/7 Run 3
8/7 Run 5
9/18 Run 1
9/18 Run 3
9/18 Run 5
Average 1
PP
8/7 r3: 69
8/7 r5: 77
9/18 r1: 69
9/18 r3: 80
9/18 r5: 77

Vinac Contamination Raw Data

Vinac Raw Data includes work vs. time graphs for 6 conditions (149 F, 194 F, 302 F & 40% and 50% ingoing solids). All tests were run at one dwell time – 0.194 s. A summary of the work and picking data is shown below.

Condition	Vinac Work (g/cm)	COV/% DIFF	Vinac Picking (% Fiber Area)	COV	Vinac Tack (lb/in)	COV
149 F, 40 %	1.58	12.98%	13.33	16.92%	0.2328	38.69%
149 F, 50%	1.03	13.16%	4.37	45.80%		
194 F, 40%	3.24	4.41%	13.03	17.73%	0.309	39.07%
194 F, 50%	2.91	21.76%	7.92	45.16%		
302 F, 40%,	4.68	16.92%	1.67	54.70%		
302 F, 50%	2.05	44.32%	0.70	53.77%	0.0876	29.14%

Vinac: 149 F, 40 % Solids, 0.194s

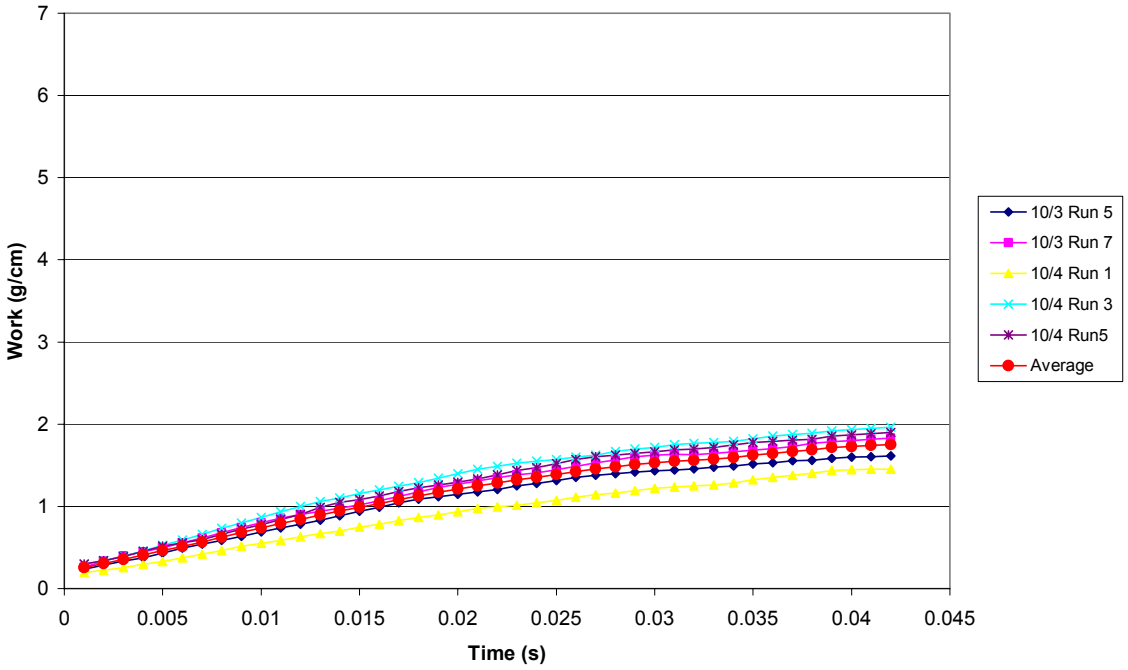

Vinac : 149 F, 50 % Solids, 0.194 s

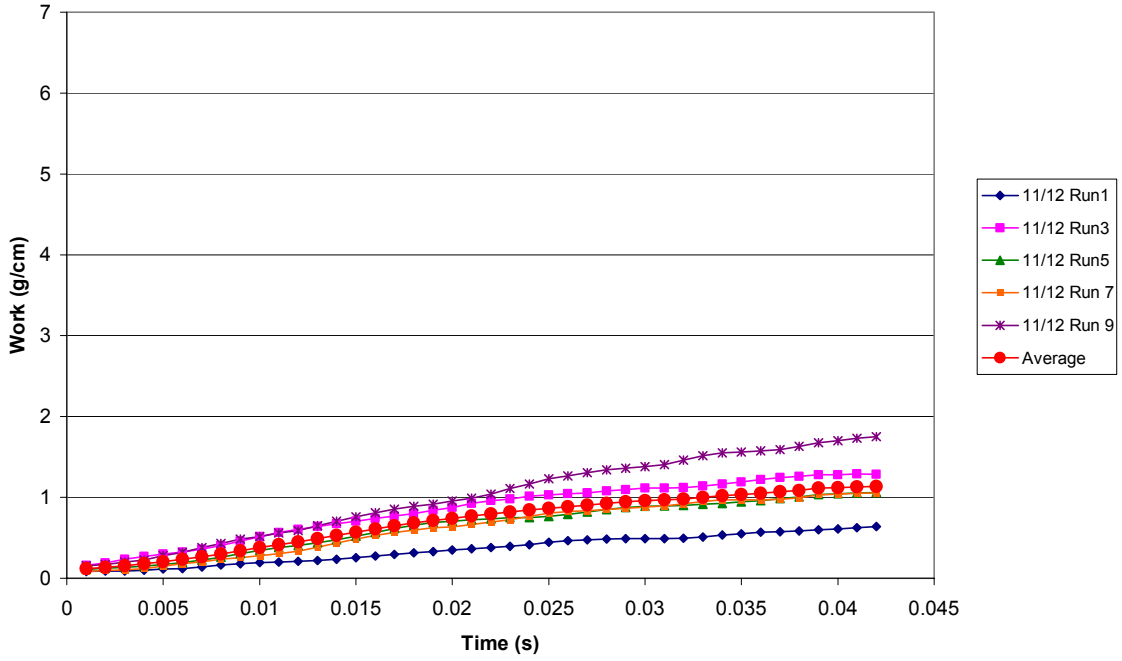

Vinac: 194 F, 40 % Solids, 0.194 s

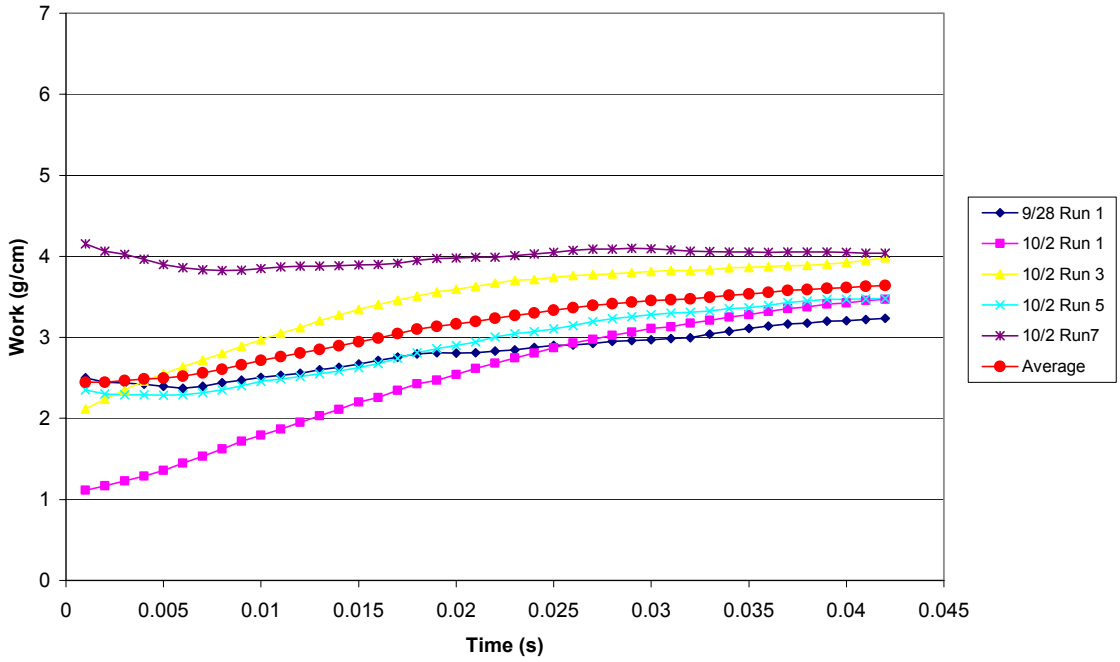

Vinac: 194 F, 50 % Solids, 0.194 s

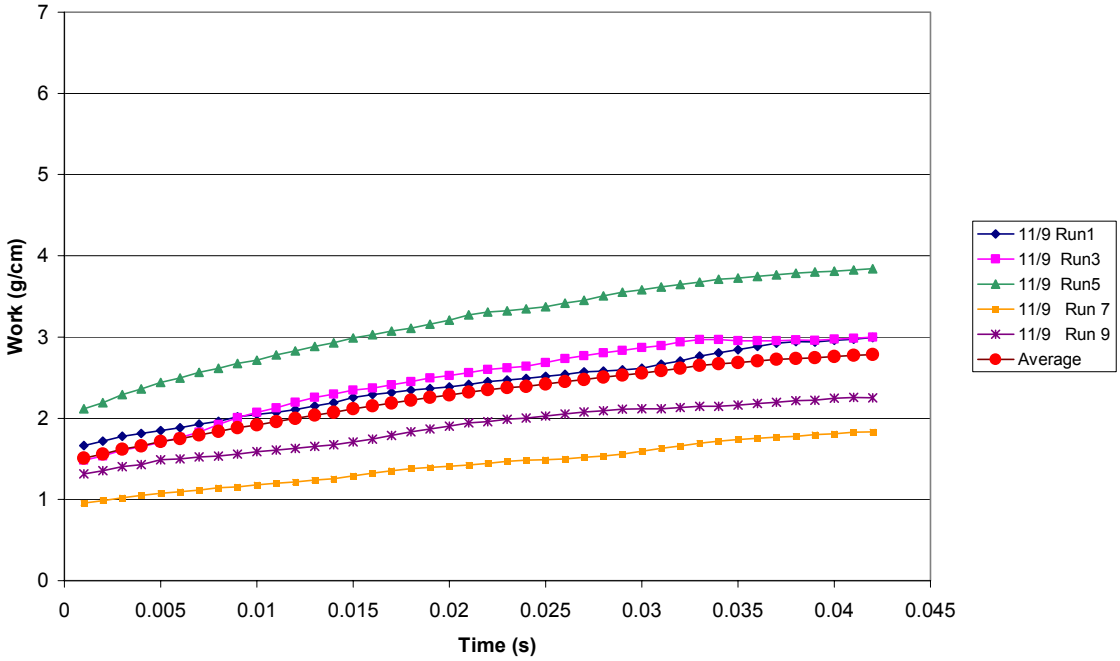

Vinac: 302 F, 40 % Solids, 0.194 s

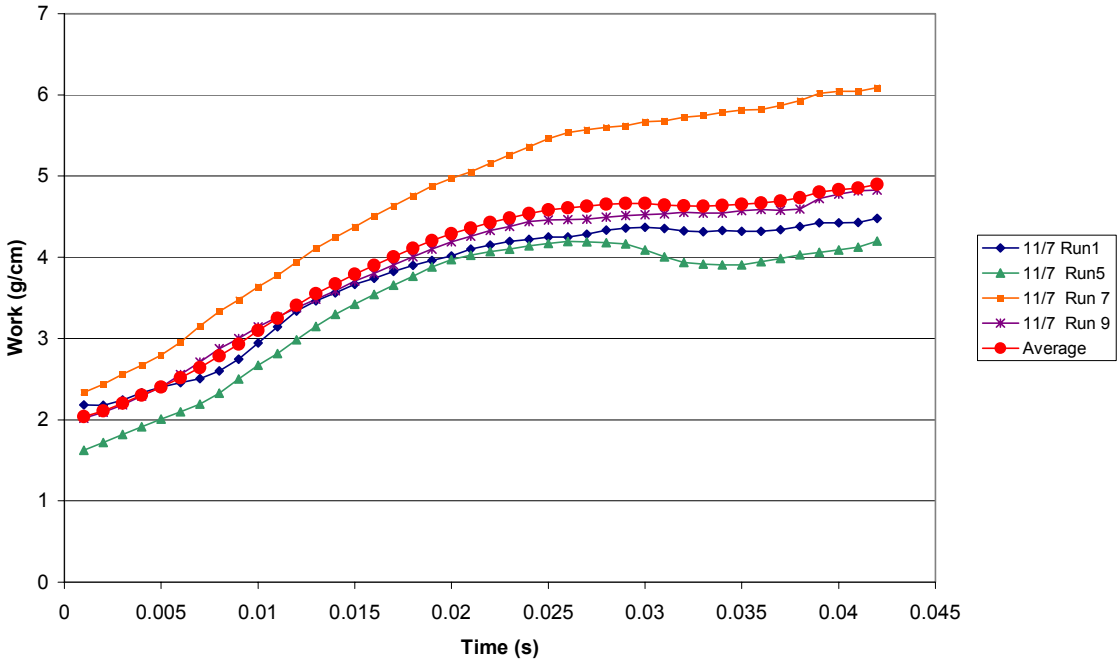

Vinac: 302 F, 50 % Solids, 0.194 s

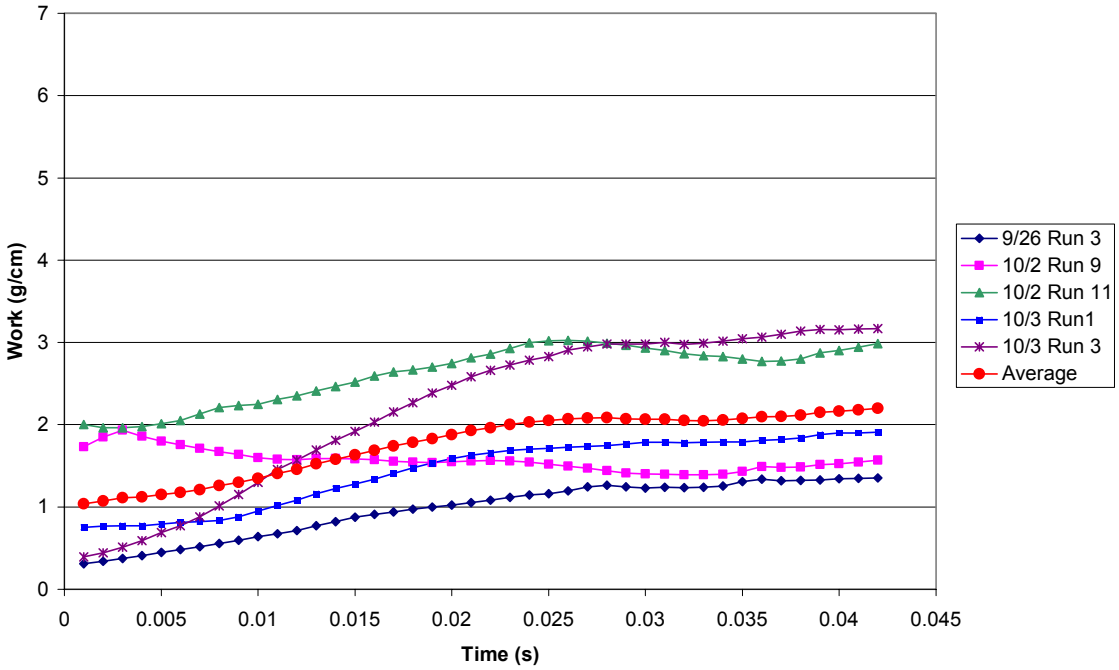

Vinac Meinicke Chart

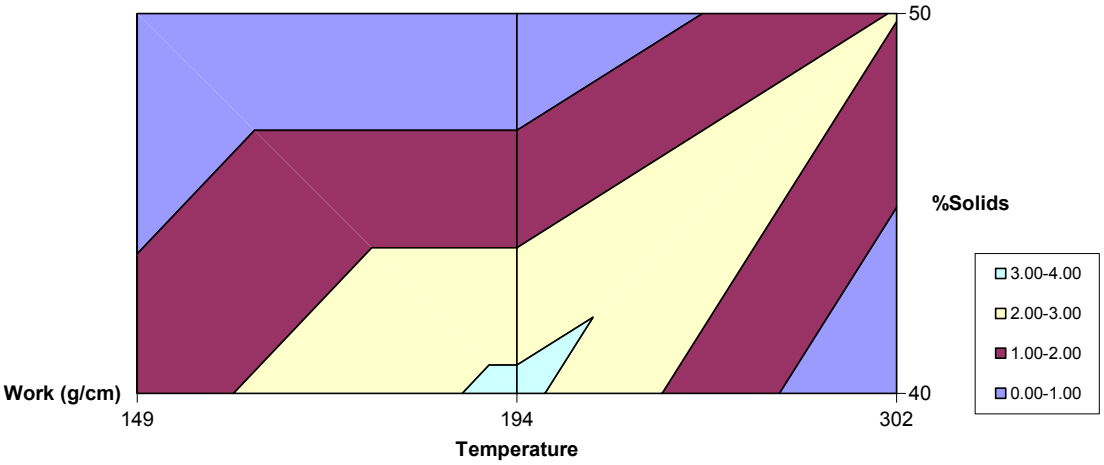

Vinac: Picking vs Work

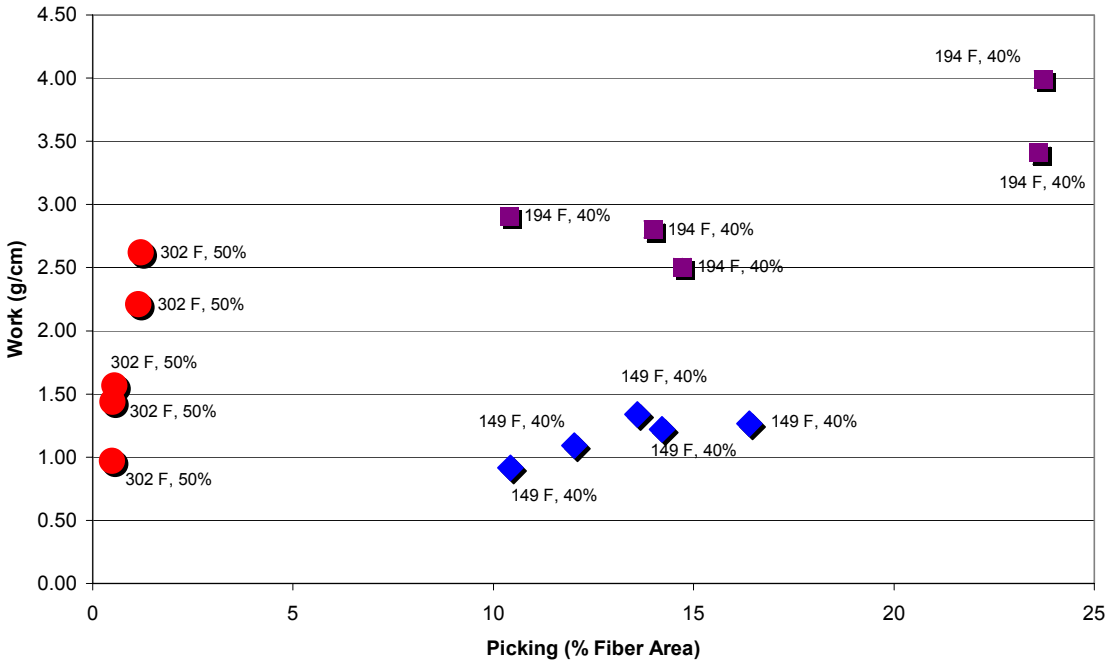

Consolidation Testing

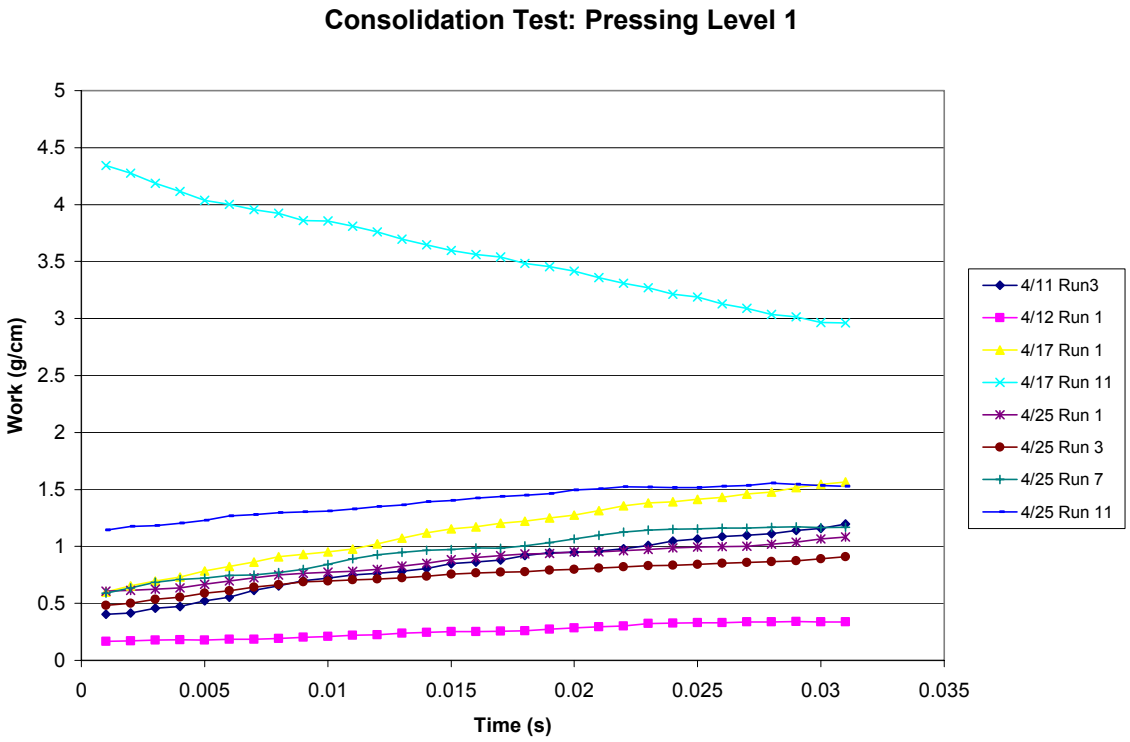

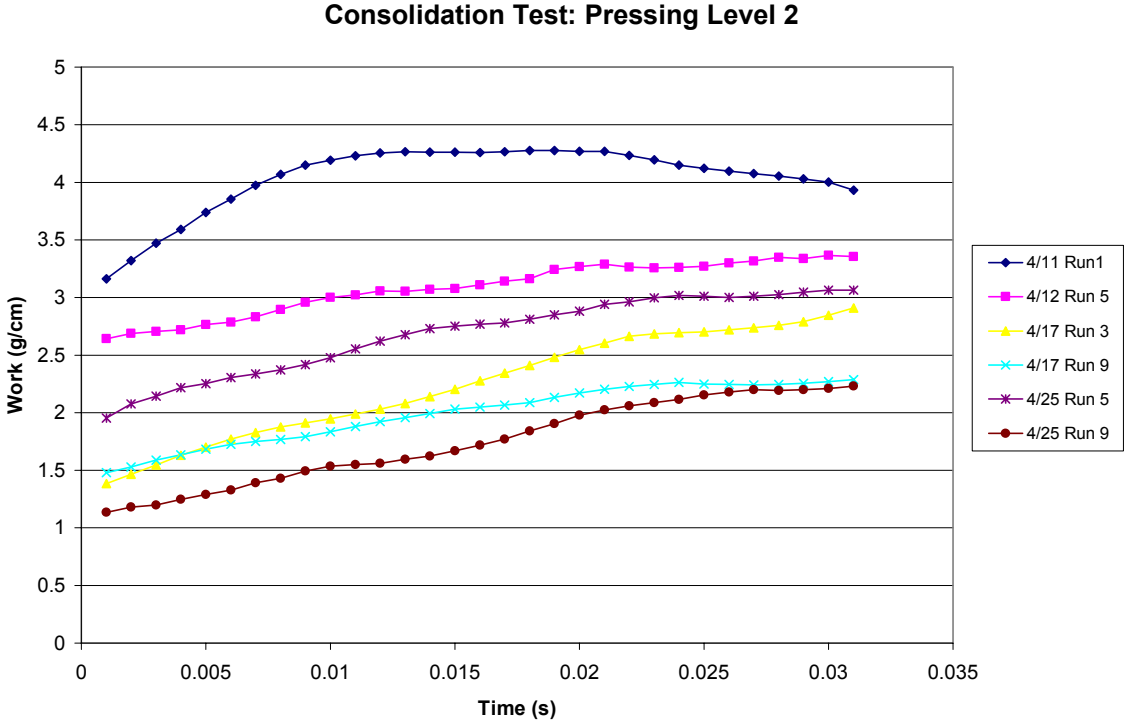

Consolidation Test: Pressing Level 3

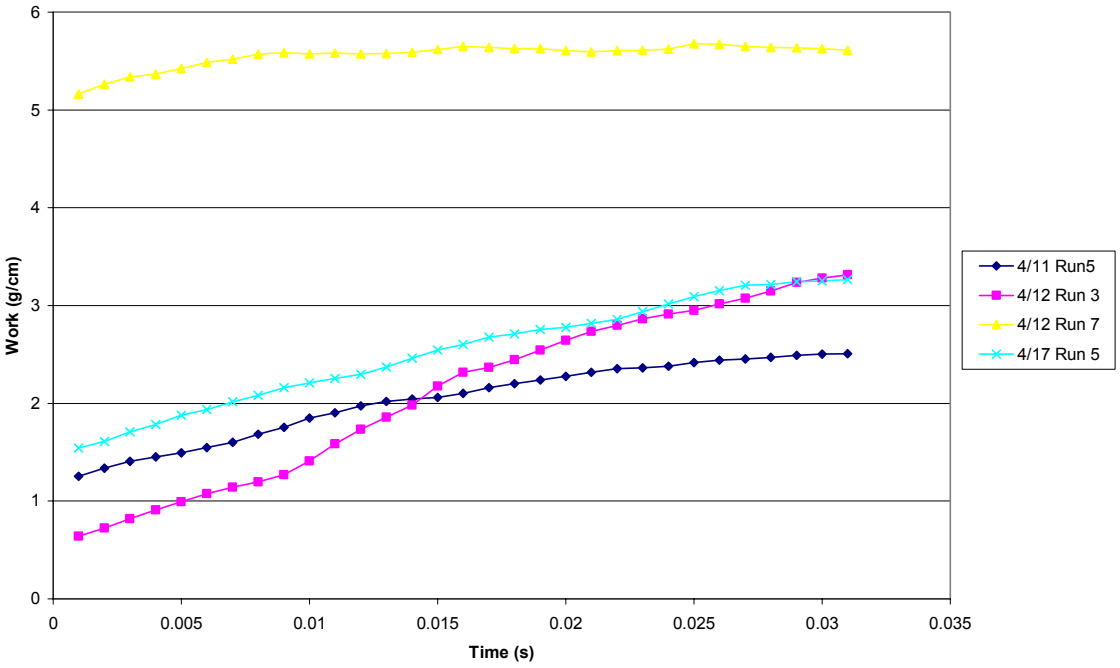

Web Separation Modeling

Presented here are the graphs of work of adhesion calculated using two different models – Old Work (Equation 2 in report) and New Work (Equation 3 in report). The data fell into 3 distinct groups in which the new work equation had different effects.

Group I: Negligible sticking

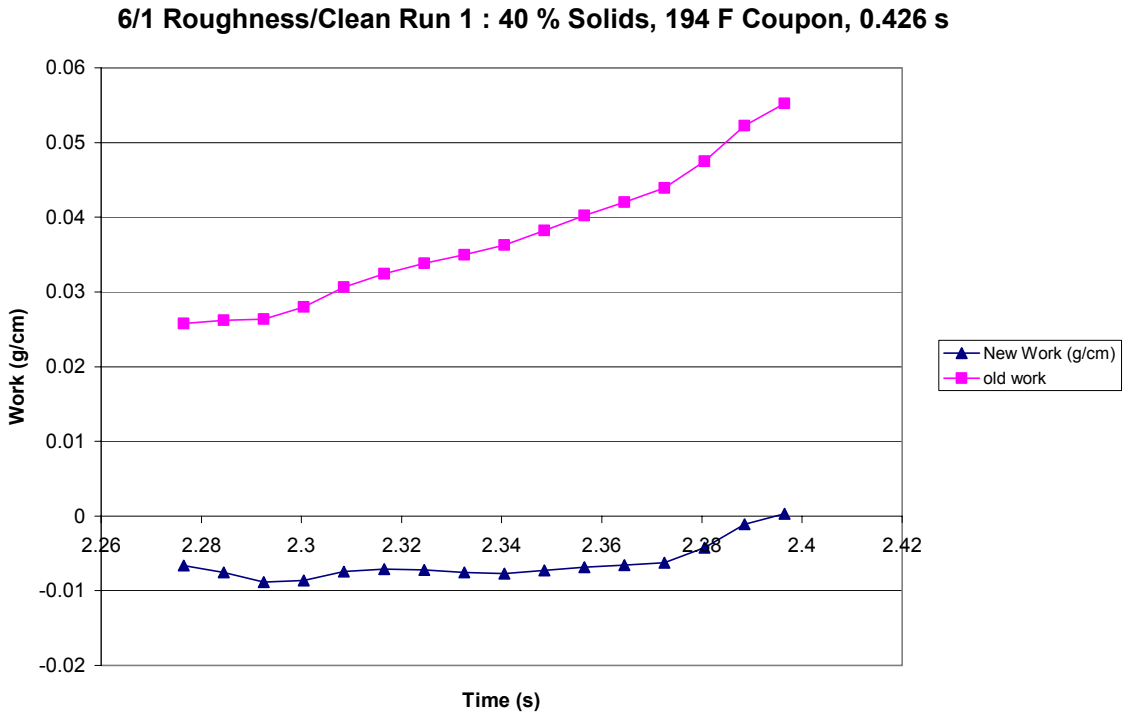

6/1 Roughness/Clean Run 4 : 40 % Solids, 194 F Coupon, 0.426 s

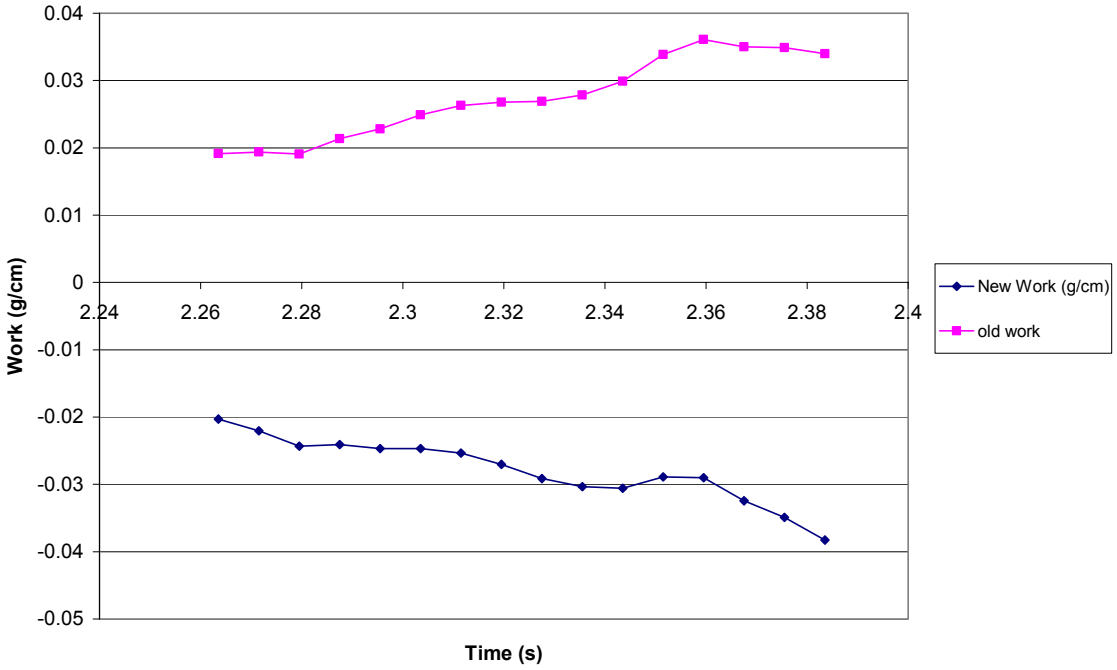

8/6 Carbotac Run 4 : 194 F, 40 % Solids, 0.194 s

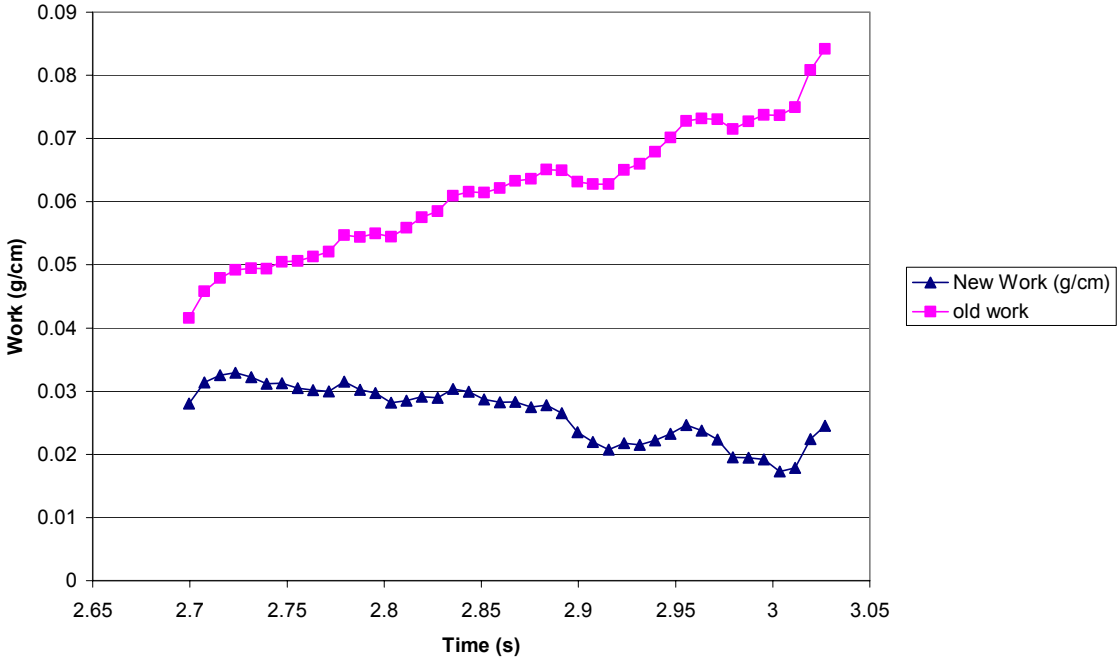

Group II: Intermediate sticking

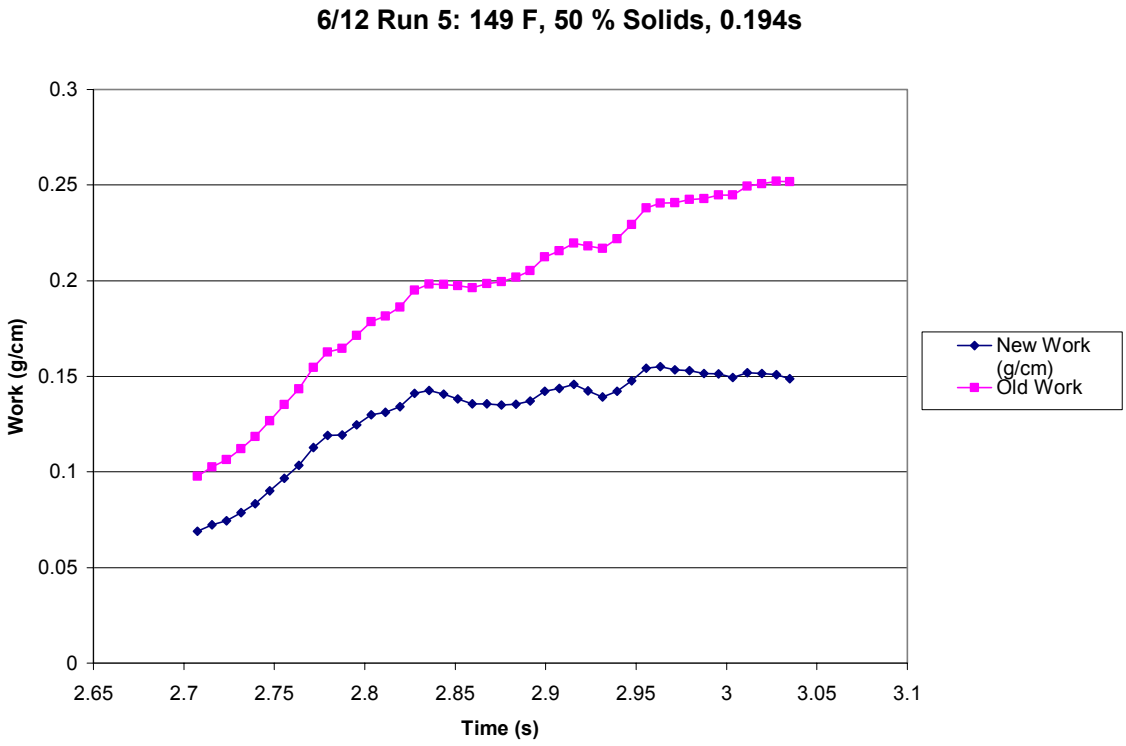

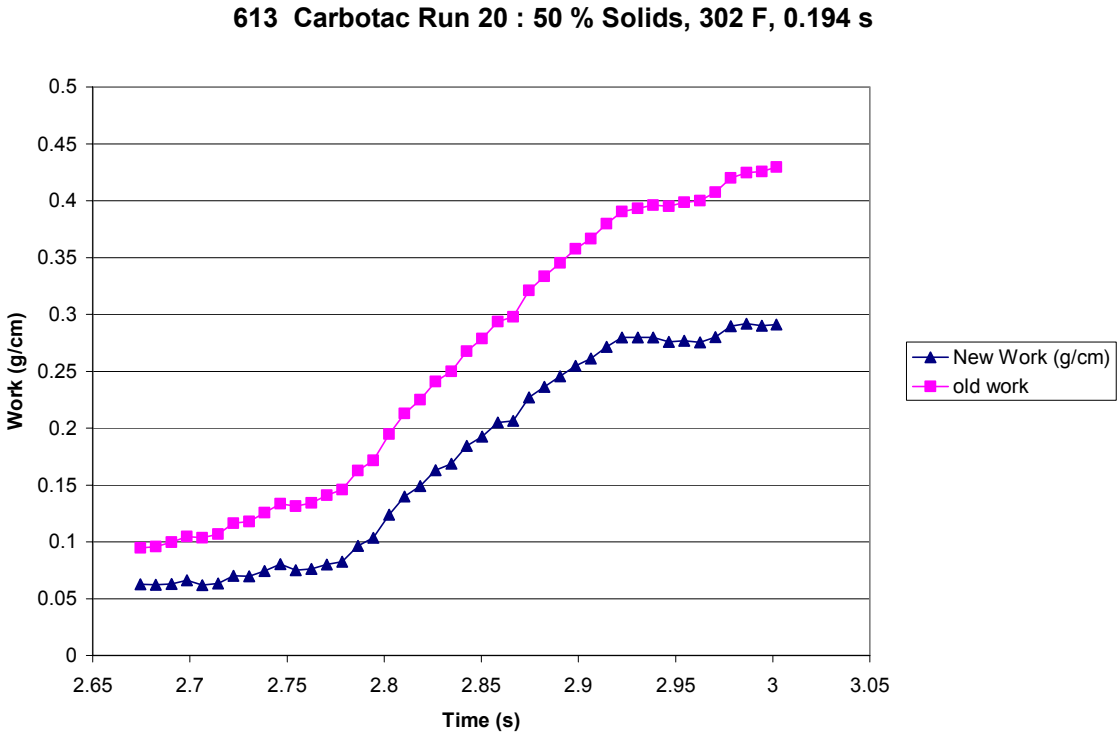

6/11 Run 4: 149 F, 40 % Solids, 0.194s

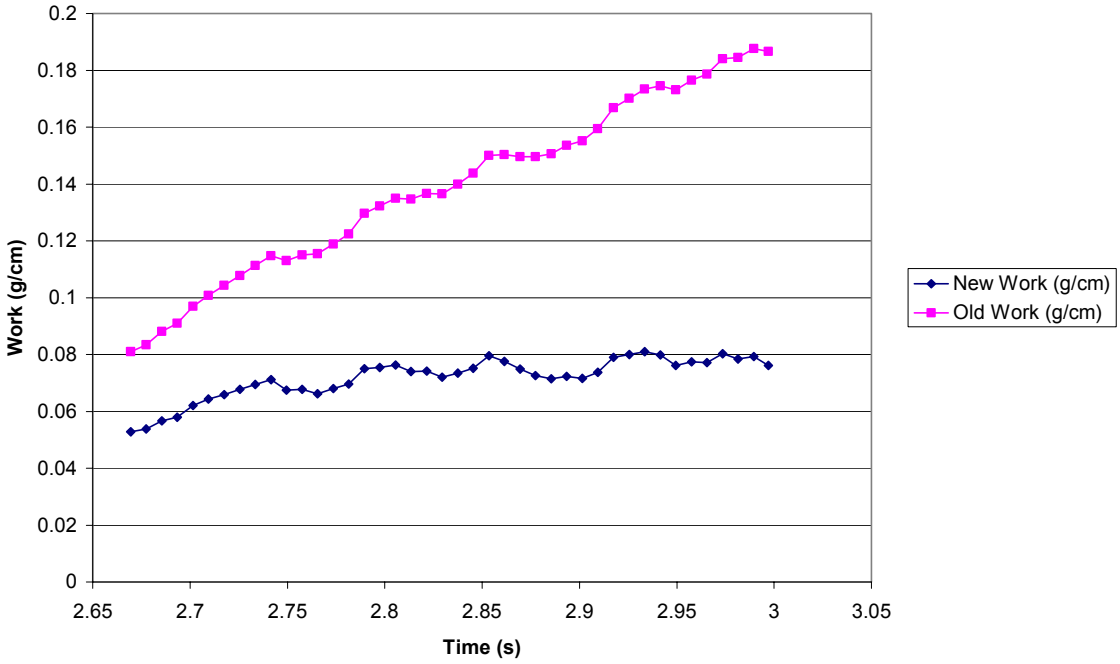

6/07 Run 4: 194F, 40 % Solids, 0.194s

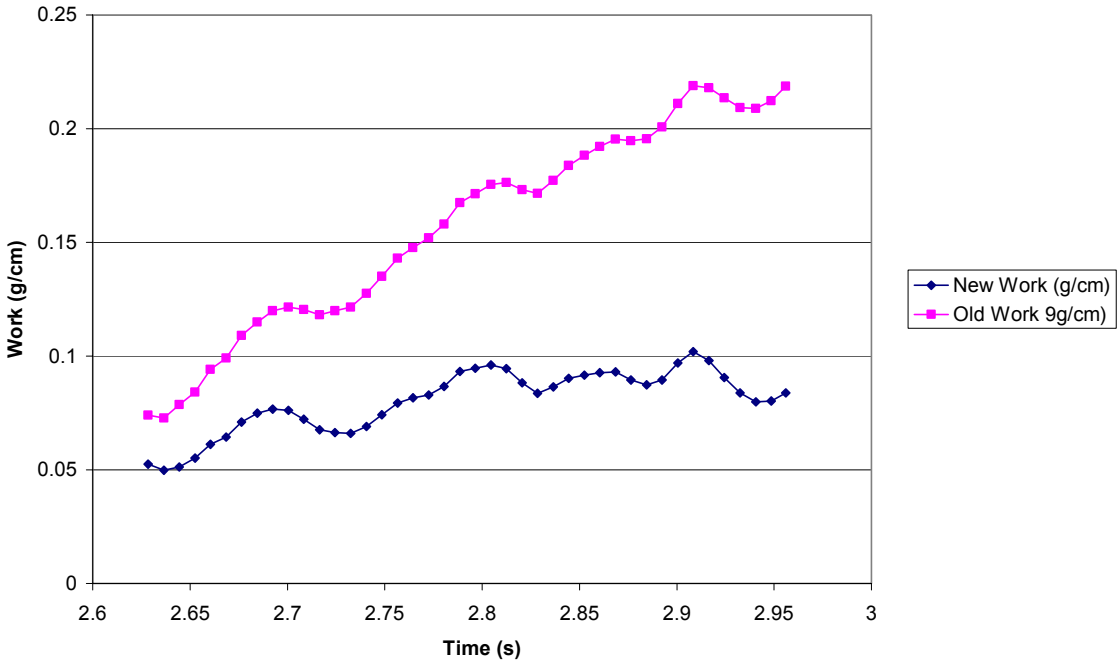

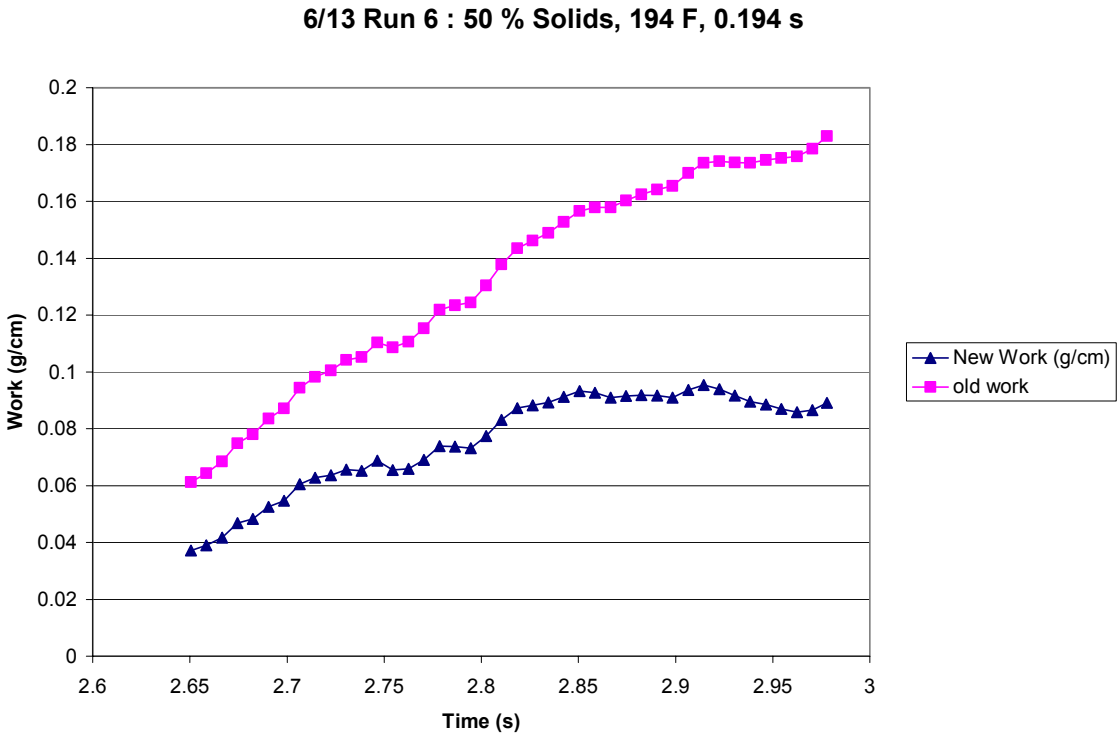

Group III: High Sticking

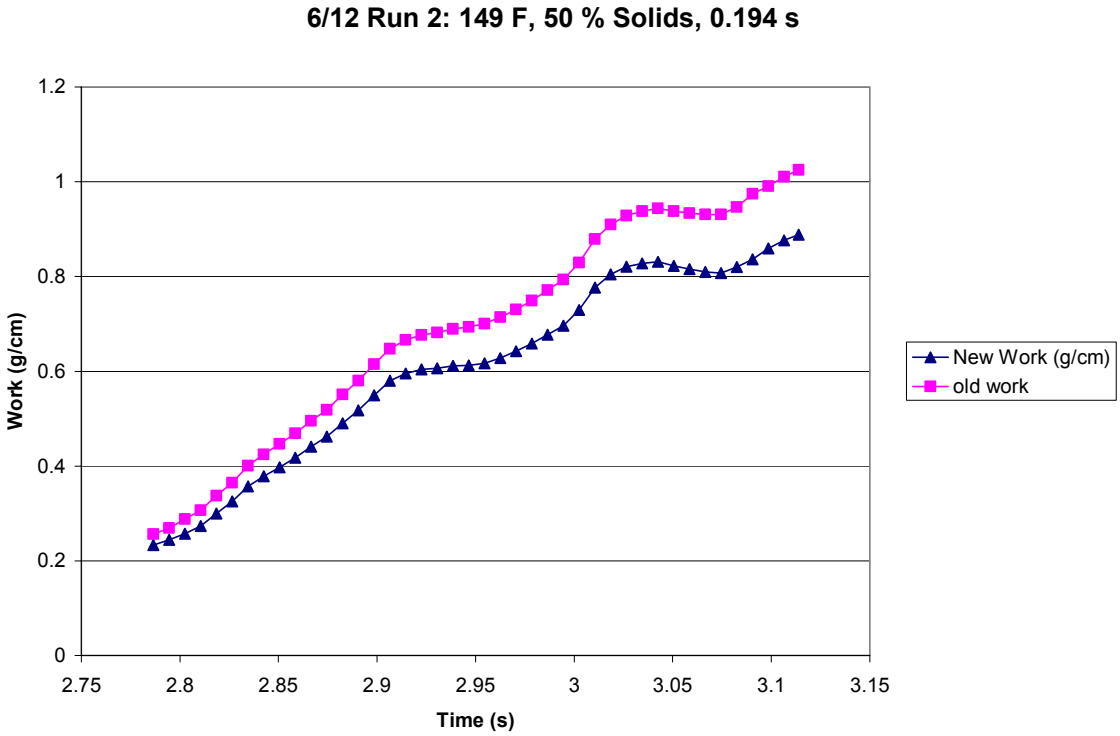

11/7 Vinac Test 1: 302 F, 40 % Solids, 0.194 s

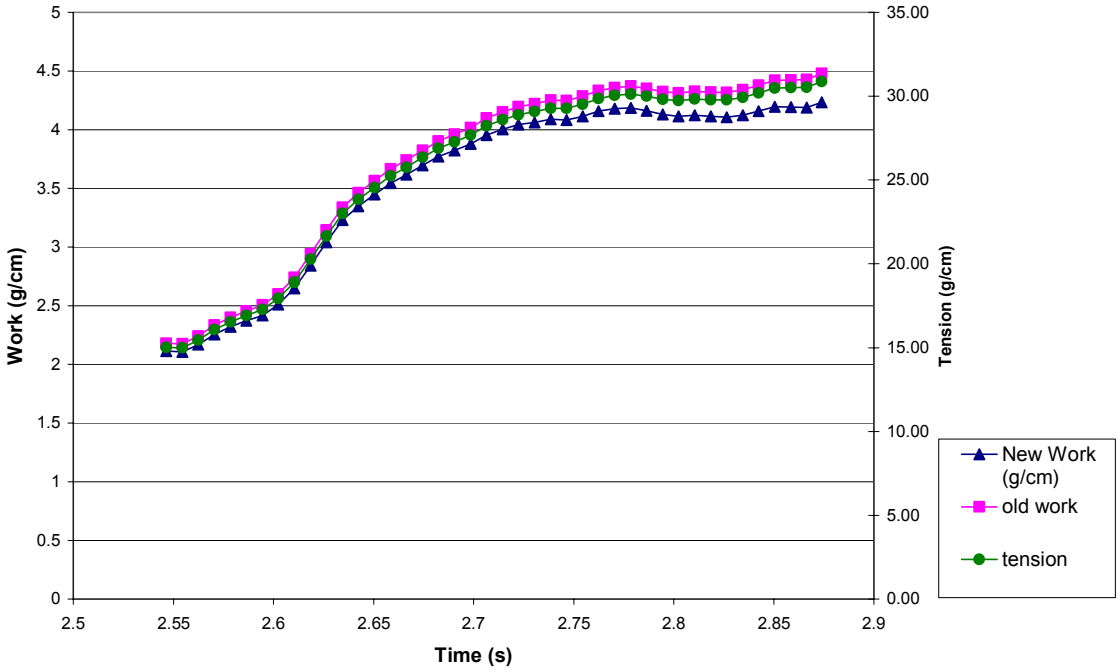

10/2 Vinac Test 1: 194 F, 40 % Solids, 0.194 s

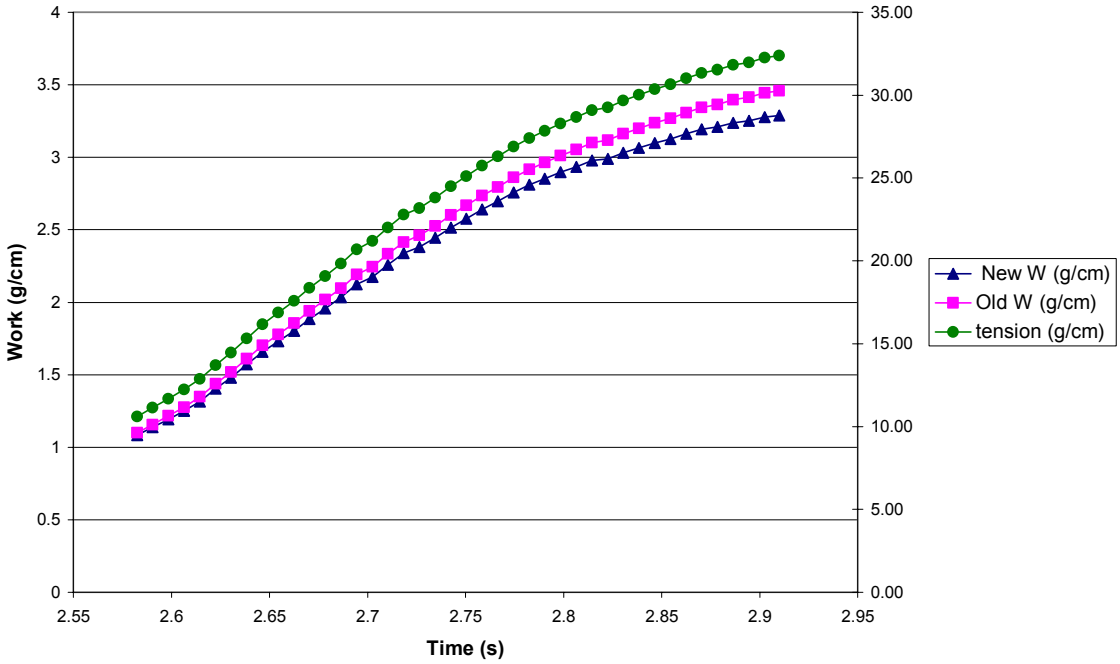

8/6 Carbotac Run 3 : 194 F, 40 % Solids, 0.194 s

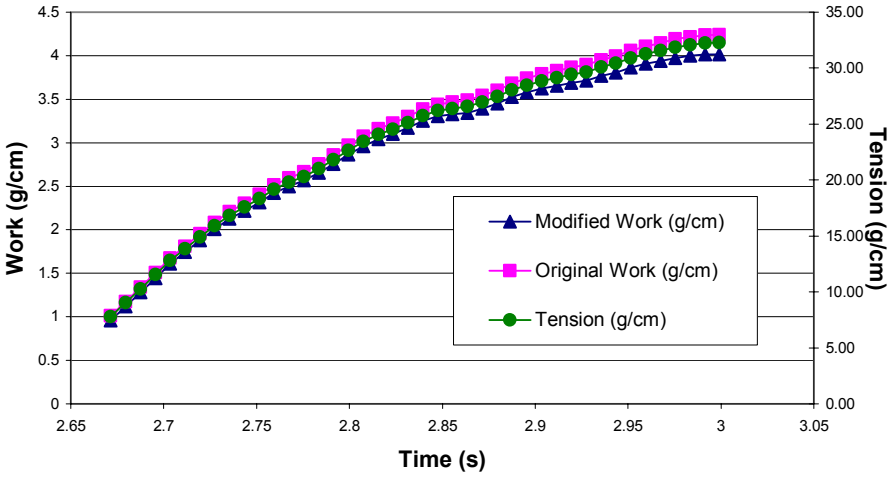

8/3 Carbotac Run 1 : 40 % Solids, 149 F, 0.194 s

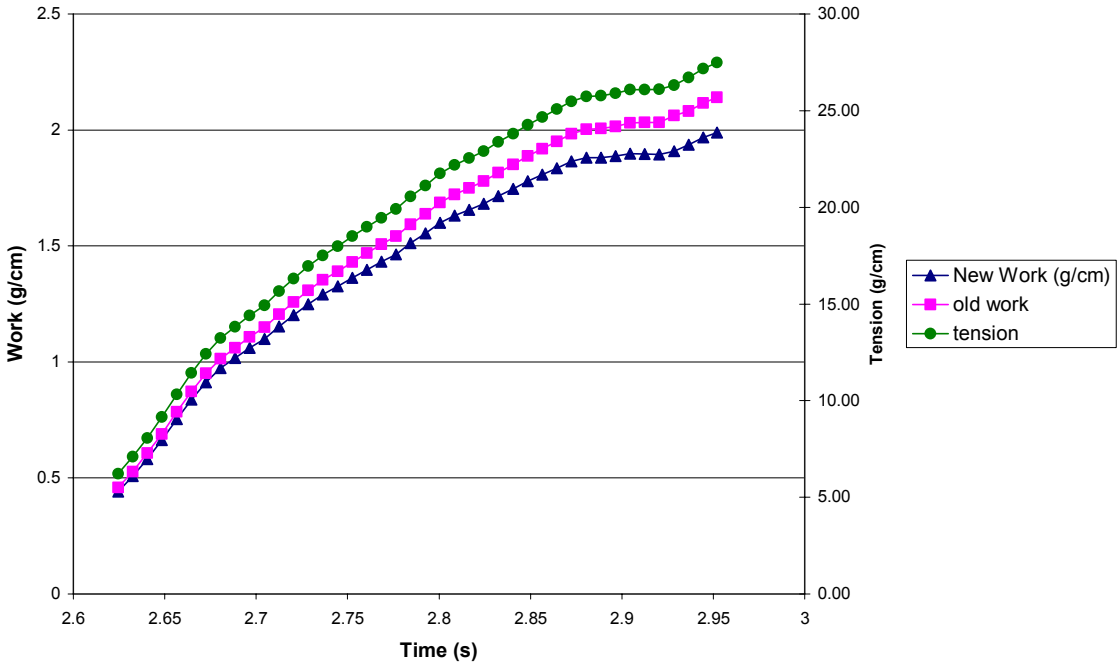

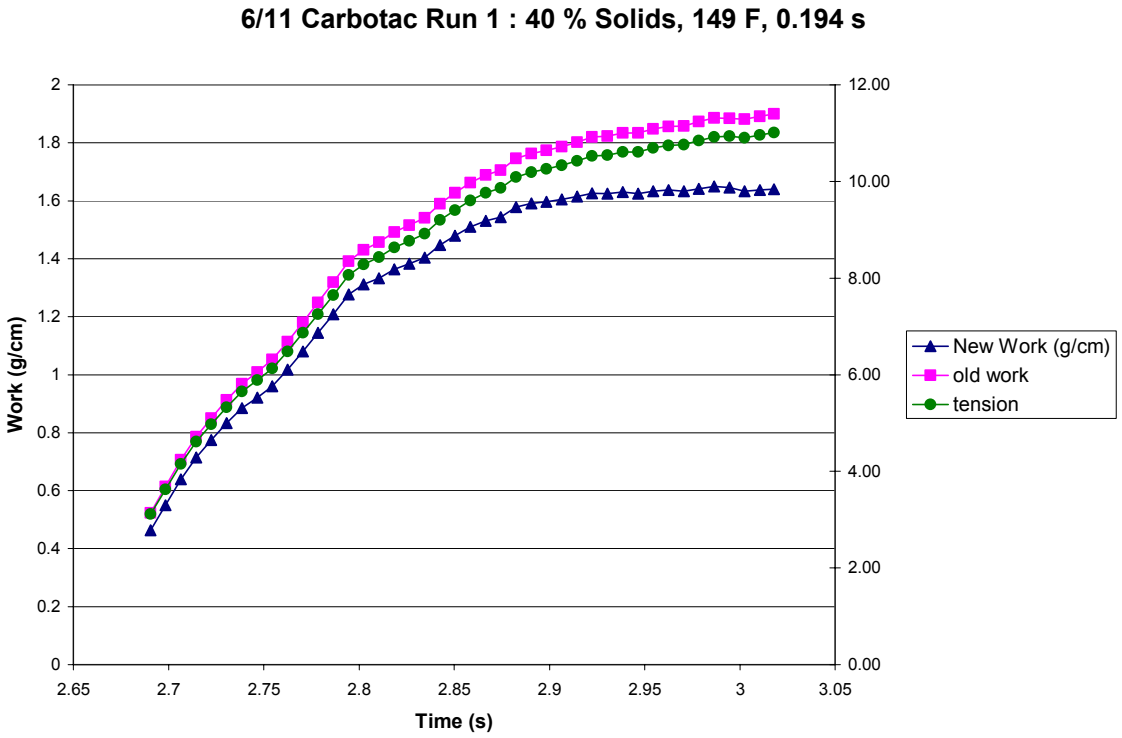

For the curvature model used to calculate work of adhesion ("New Work"), the radius of curvature term in the equation (Equation 3) breaks down to:

$$R_t W_g(t) = \kappa(\rho - \rho_t) v g t^2 + \kappa \rho_T g \Gamma t$$

The two terms of this equation (t & t^2) were plotted for the different groups of data in order to compare their relative contributions to the final work of adhesion. Term 1 is for t squared and Term 2 is for t. As shown in the graphs, there terms are more significant in the Group I & II cases than for Group III, for which the raw tension is so high that these terms have a negligible effect.

Group I: Curvature Modeling

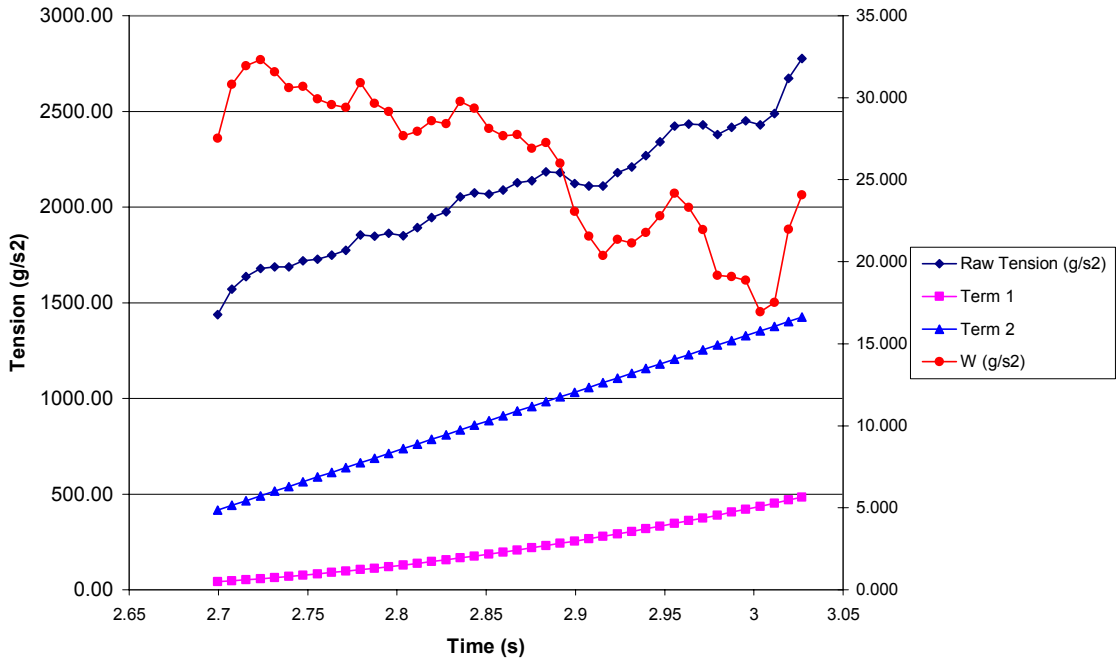

Group II: Curvature Modeling

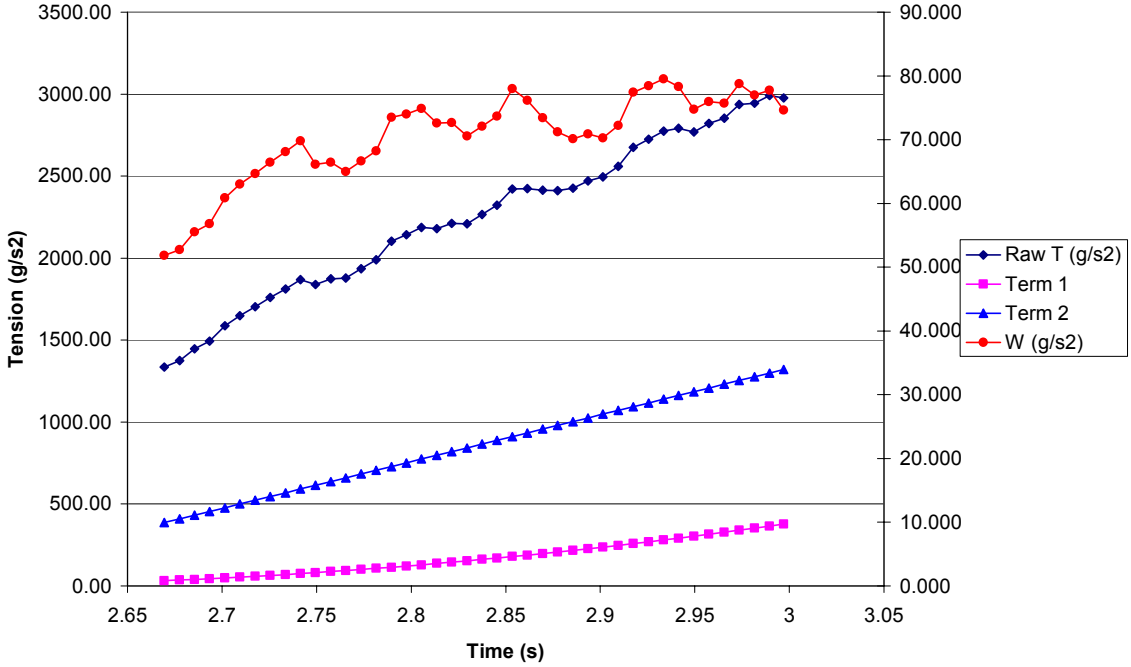

Group III: Curvature Modeling

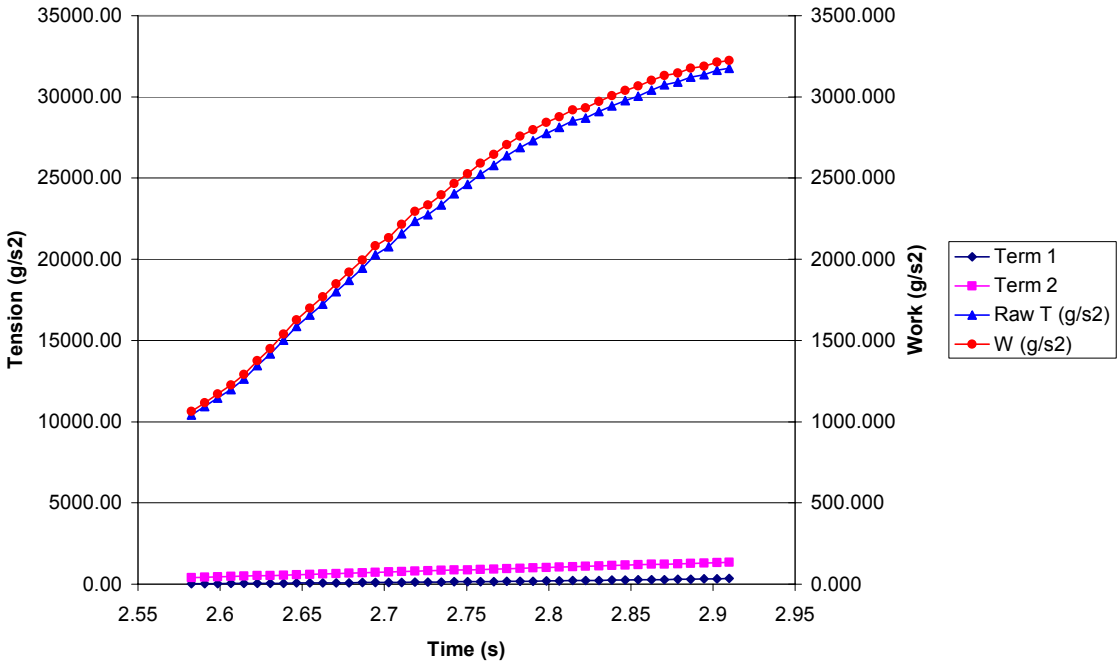

Tack Testing

For each tack test, 2 coats of an adhesive (either Carbotac or Vinac) were applied to a 4"x4" plate using an 18 um rod coater (1 hour between coats). 1" squares labeled from 1 to 16 were drawn over the adhesive. The average thickness of each square was measured using a CMI CGX Gauge thickness probe. After heating the plate for 1 hour, the tack test was performed on the INSTRON, one sample square at a time. The 'Load per Width at Max Load' is the output of the INSTRON, and the sample width was 0.5". The % Solids is the solids content of the sample prior to testing.

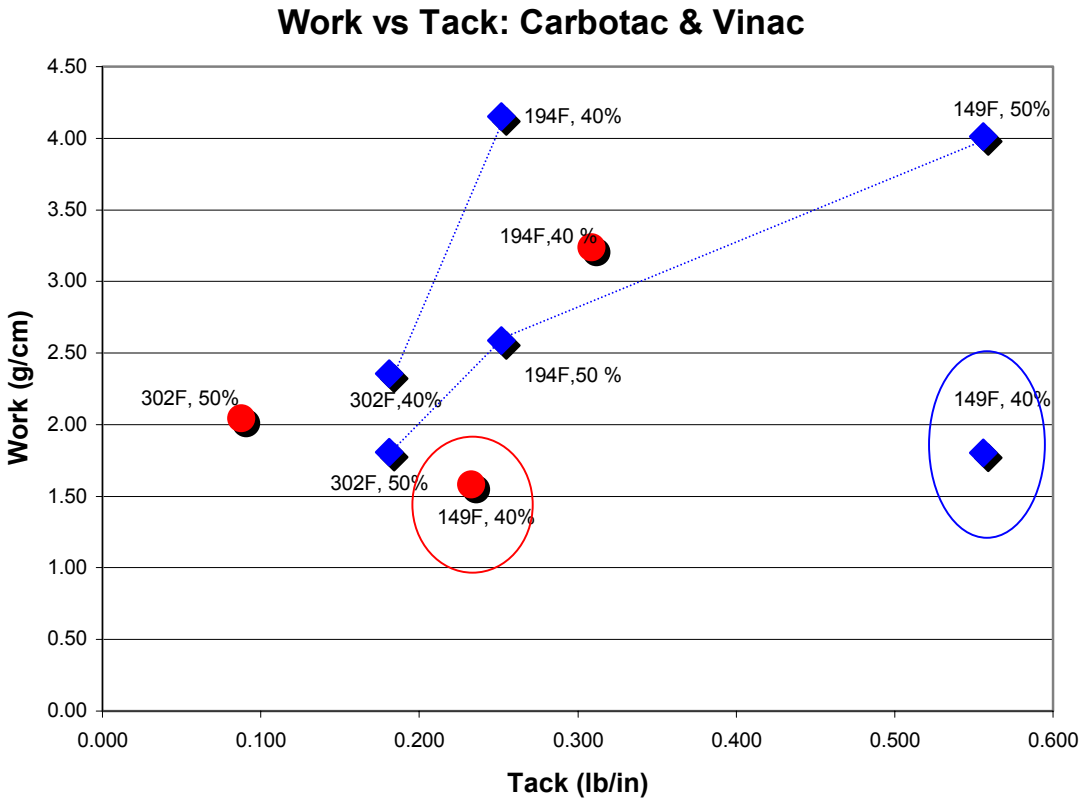

For the wet tack tests, it was found that there was a repeating pattern to the data, as shown below:

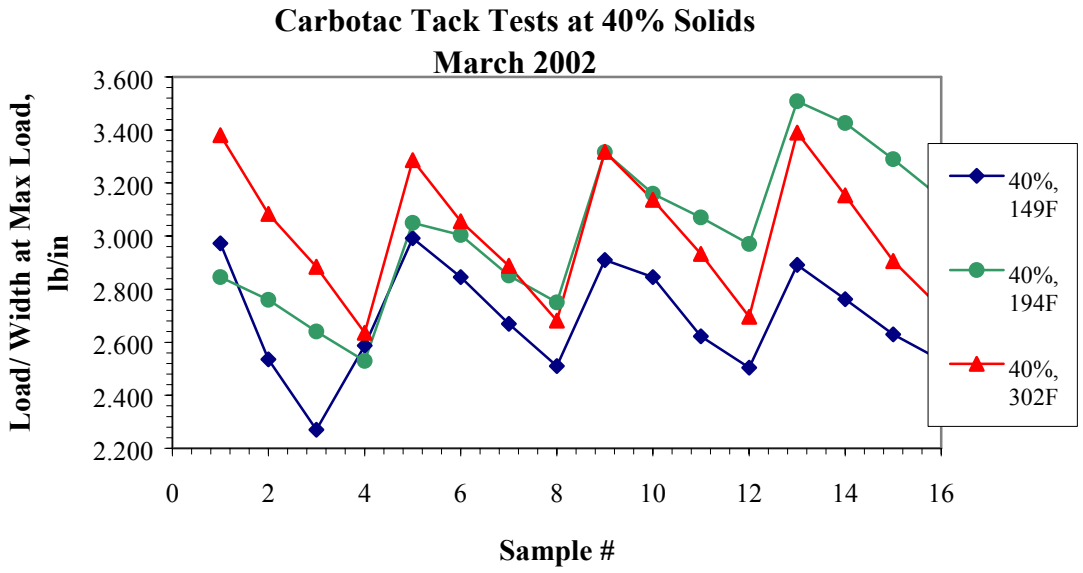

Thus a series of tests were undertaken to check whether it was the varying time of the test that made the difference or whether it was a pattern in the thickness across the surfaces (samples were tested from left to right across the plate).

Results of pattern tests for tack test: 8 random squares & 8 squares in one set (rows), varying time:

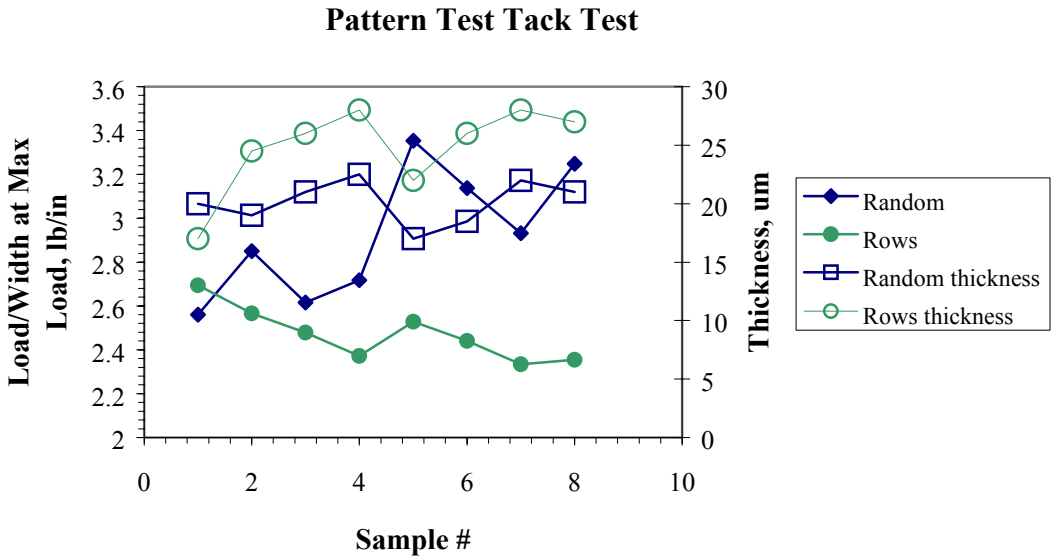

6 random squares & 6 squares in one set (rows), printing after 3, keeping time constant:

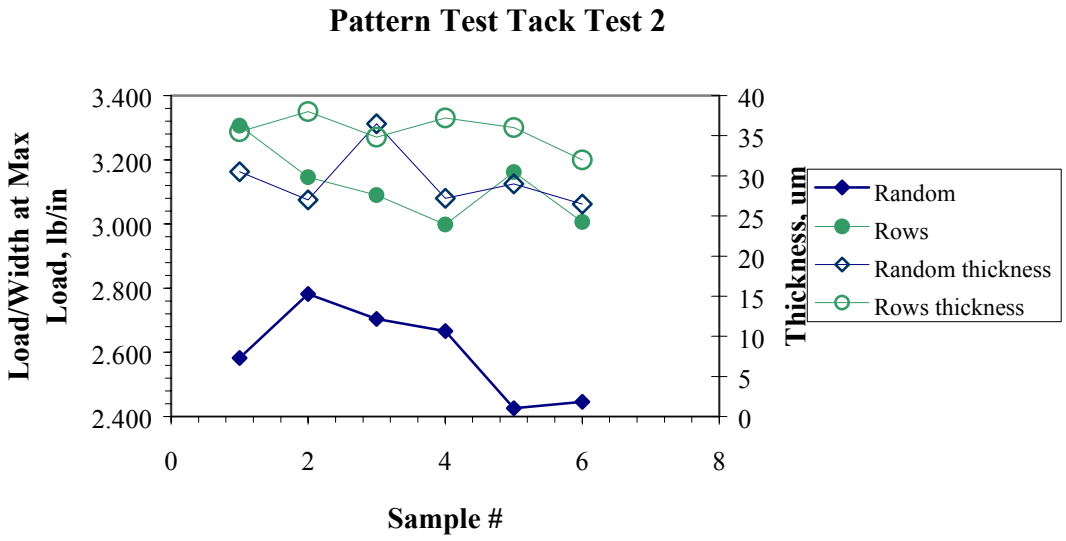

APPENDIX G: Miscellaneous Data

I. Initial Work Analysis

An examination of initial work values for high tension runs was undertaken based on the hypothesis that the initial work (before the steep increase in slope typical of high tension runs) may represent the true work of adhesion. The idea being that the sharp incline in the graph of work of adhesion vs. time for high tension runs was due to web strain.

To test this hypothesis, initial work values (work for the 1st 5 points or 12% of the peel event) for high strain cases (run1 with Carbotac & Vinac) were calculated and used to create Meinecke graphs of work of adhesion as a function of temperature and % ingoing solids. The results are not conclusive – there is not much repeatability from run to run and the coefficient of variation is very high from some of the runs. The data is presented in the graphs below.

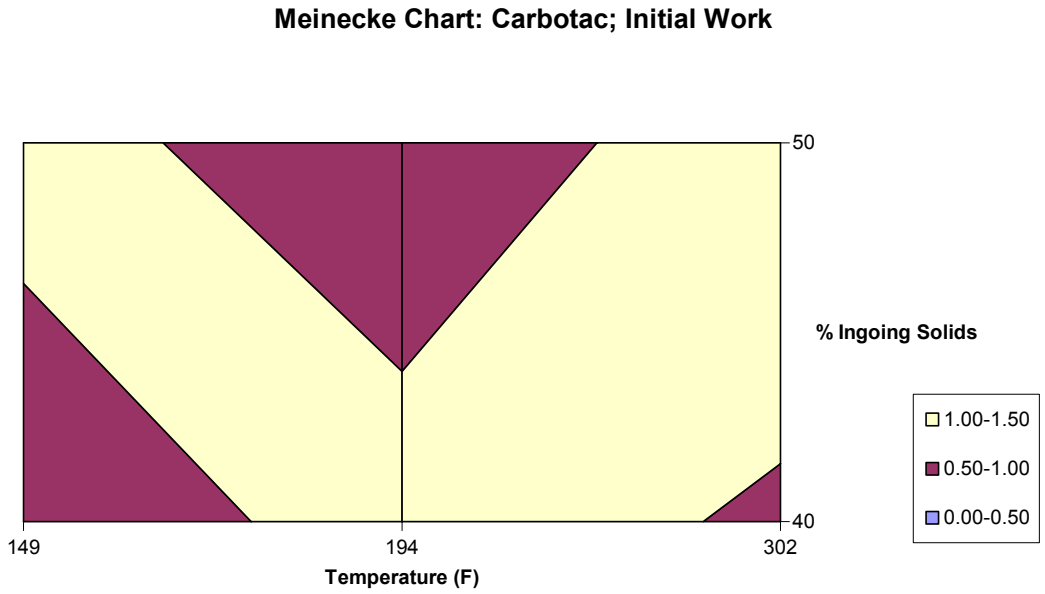

Meinecke Chart: Vinac; Initial Work

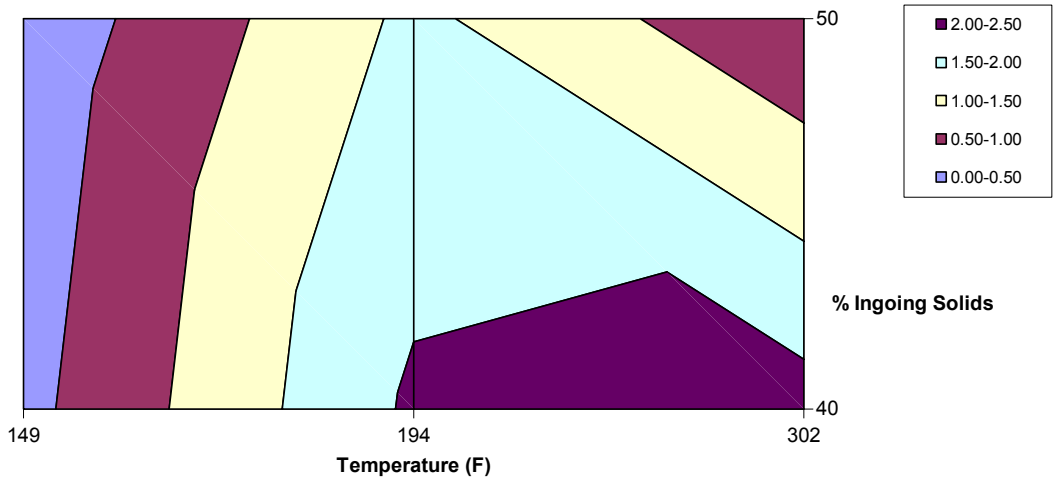

RAW DATA: Carbotac (includes original work data summary for comparison)

Condition	Run	Initial Work (g/cm)	Notes	Summary Initial W		Summary Original Work	
302,40%,0.194	8/3 run 3	1.69					
	8/3 run 5	1.1					
	9/19 Run 1	0.222					
	9/19 Run 3	0.555		Average	0.97	Average	2.12
	6/6 Run 1	0.702	sheet split	Std Dev	0.55	Std Dev	0.99
	9/11 Run 1	0.819		COV	56.46	COV	46.70
	9/12 Run 1	1.42					
194,40%,0.194	8/6 Run 3	1.24					
	8/6 Run 5	0.949		Average	1.13	Average	3.20
	8/6 Run 8	1.34		Std Dev	0.19	Std Dev	0.36
	9/17 Run 1	0.974		COV	17.26	COV	11.25
149,40%,0.194	8/3 Run 1	0.686					
	6/11 Run 1	0.565		Average	0.81	Average	1.43
	9/17 Run 3	0.842	tape twisted	Std Dev	0.29	Std Dev	0.09
	9/19 Run 5	0.77		COV	35.28	COV	6.42
	9/19 Run 7	1.22					
149,50%,0.194	8/7 Run 7	0.745		Average	1.11	Average	3.15
	8/8 Run 1	1.05		Std Dev	0.40	Std Dev	0.53
	8/8 Run 3	1.54		COV	36.08	COV	16.78

Condition	Run	Initial Work (g/cm)	Notes	Summary Initial W		Summary Original Work	
194,50%,0.194	8/6 Run 10	1.29		Average	0.81	Average	1.95
	8/7 Run 1	0.443		Std Dev	0.37	Std Dev	0.10
	9/17 Run 5	0.908		COV	46.38	COV	5.27
	9/17 Run 7	0.593					
302,50%,0.194	8/7 Run 3	3.08	problem	Average	1.18	Average	1.58
	8/7 Run 5	2.52		Std Dev	1.16	Std Dev	0.31
	9/18 Run 1	0.268	problem	COV	98.56	COV	19.34
	9/18 Run 3	0.587					
	9/18 Run 5	0.433					

RAW DATA: Vinac (includes original work data summary for comparison)

Condition	Run	Initial Work (g/cm)	Notes	Summary Initial W		Summary Original Work	
194,40%,0.194	9/28 Run 1	2.44					
	10/2 Run 1	1.23					
	10/2 Run 3	2.34					
	10/2 Run 5	2.30		Average	2.08	Average	2.91
	10/2 Run7	0.33	bad graph	Std Dev	0.57	Std Dev	0.38
				COV	27.31	COV	12.99
149,40%,0.194	10/3 Run 5	0.33					
	10/3 Run 7	0.39		Average	0.36	Average	1.16
	10/4 Run 1	0.26		Std Dev	0.06	Std Dev	0.16
	10/4 Run 3	0.40		COV	17.12	COV	13.79
	10/4 Run5	0.40					
302,50%,0.194	9/26 Run 3	0.38					
	10/2 Run 9	1.83	problem	Average	0.56	Average	1.54
	10/2 Run 11	1.98	problem	Std Dev	0.20	Std Dev	0.63
	10/3 Run1	0.77		COV	35.85	COV	40.71
	10/3 Run 3	0.52					
149,50%,0.194	11/12 Run1	0.10		Average	0.16	Average	0.71
	11/12 Run3	0.23		Std Dev	0.06	Std Dev	0.24
	11/12 Run5	0.14		COV	37.61	COV	34.47
	11/12 Run 7	0.11					
	11/12 Run 9	0.21					
194,50%,0.194	11/9 Run1	1.77		Average	1.61	Average	2.27
	11/9 Run3	1.60		Std Dev	0.47	Std Dev	0.66
	11/9 Run5	2.28		COV	28.92	COV	29.16
	11/9 Run 7	1.02					
	11/9 Run 9	1.40					

Condition	Run	Initial Work (g/cm)	Notes	Summary Initial W		Summary Original Work	
302,40%,0.194	11/7 Run1	2.27	sheet split	Average	2.21	Average	4.51
	11/7 Run3	4.42	max	Std Dev	0.31	Std Dev	1.36
	11/7 Run5	1.82	sheet split	COV	13.85	COV	30.16
	11/7 Run 7	2.56	sheet split				
	11/7 Run 9	2.20					

Task 6

Develop and demonstrate new roll surface conditioning technologies, including PTFE roll wiping technology for use on dryer cylinder rolls.

a. **Develop contamination control options on CTS.**
b. **Develop options for controlling roll surface topology on CTS.**
c. **Evaluate desirable options on pilot machine.**

Final Status:

Sub-Task a. – Various polymer roll wipe tested using pilot machine equipment provided by AstenJohnson. (work was initiated and completed after the no cost extension had ended. This work was funded by the IPST Member Companies)

Sub-Task b. – not completed, apparatus did not produced required data

Sub-Task c. – A Fluro-Polymer roll wipe was tested and its viability verified using pilot machine equipment provided by AstenJohnson. (work was initiated and completed after the no cost extension had ended. This work was funded by the IPST Member Companies)

Teflon Doctor Blade Testing

Pilot-Scale Studies

J
Shana Mueller
James Loughran

Objective

The objective of this work is to determine the effectiveness of a polymer doctor blade for reducing/eliminating contamination build-up on dryer cylinders and to identify the mechanisms behind this reduction. To achieve these goals, experiments with various polymer materials were conducted on a pilot-scale dryer cylinder at Asten-Johnson's facility in Walterboro, SC.

Background

Dryer can contamination can cause runnability problems such as picking and sticking of the web, which result in lowered productivity. Reducing and/or eliminating dryer contamination (picking) will permit the use of higher steam temperatures in the first dryer section and higher machine speeds in dryer limited machines.

This work was initiated based on empirical data from an impulse drying experiment. A Teflon® (PTFE) doctor blade was used during pilot scale impulse drying trials and was found to substantially reduce picking/sticking on the roll surface. The effectiveness of the Teflon® doctor blade was reported to be superior to blades that simply scrape the roll clean. It is believed that a thin layer of PTFE may have been deposited on the roll surface, modifying the surface adhesion forces. This concept is also applicable to traditional dryer cylinder rolls which face similar problems with sticking and picking.

In order to better understand these phenomena, a pilot-scale trial at AstenJohnson was undertaken to test a number of polymer materials (including virgin PTFE/Teflon®) on a heated dryer roll surface. Surface friction was the primary parameter used to judge the effectiveness of the polymer treated surface. Physical observations of the roll as well as the wear of the polymer block were also made.

Equipment/Procedures

The pilot dryer machine at Asten Johnson's Walterboro, SC facility was used for the experiments. The apparatus, shown below in **Figures 1 & 2**, consists of a steel cylinder that is 1 meter wide and with a diameter of 1m. The cylinder can be heated with two induction heaters to a maximum temperature of approximately 270º F (after 1 hour). A third induction heater that is normally positioned at the top of the roll was removed to

house the sample rig. The speed of the cylinder, verified with a tachometer (see Appendix B for data) can be adjusted from 70 ft/min to a maximum of 2110 ft/min.

A special assembly was constructed in order to apply the polymer materials to the surface of the cylinder. It features a slotted frame in which samples are placed in contact with the roll. Weights are then placed on top of the samples within the slots to provide the necessary load. Loads of 5 PLI and 10 PLI are achieved using 25 and 50 lb weights.

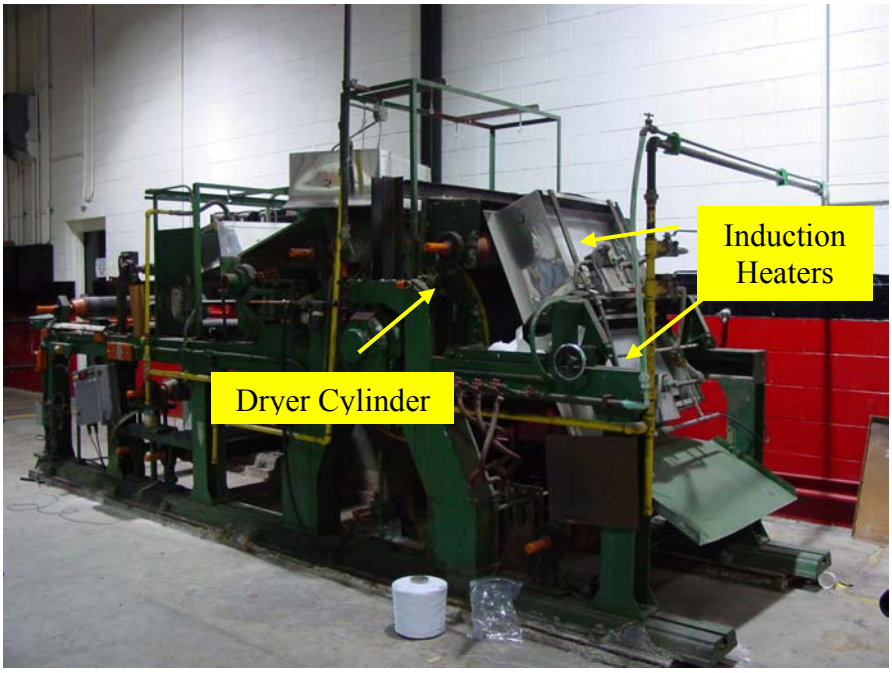

Figure 1: Pilot Plant Dryer Cylinder

The polymers that were investigated included: virgin Polytetrafluoroethylene(PTFE), Polyvinylidene fluoride (PVDF) and Ultra-high-molecular weight polyethylene (UHMW PE). For a detailed description of these materials, see Appendix A. Samples, as pictured in **Figure 3,** consisted of a machined block of the individual polymers. The top surface that is in contact with the roll was actually machined from a rod (except PE) and was therefore curved rather than flat in shape. Consequently, the actual area in contact with the roll was not the entire width of 1". Rather, the initial contact was probably a line with the area increasing continuously as the top surface was worn down.

Figure 2: Close-up of Dryer Cylinder

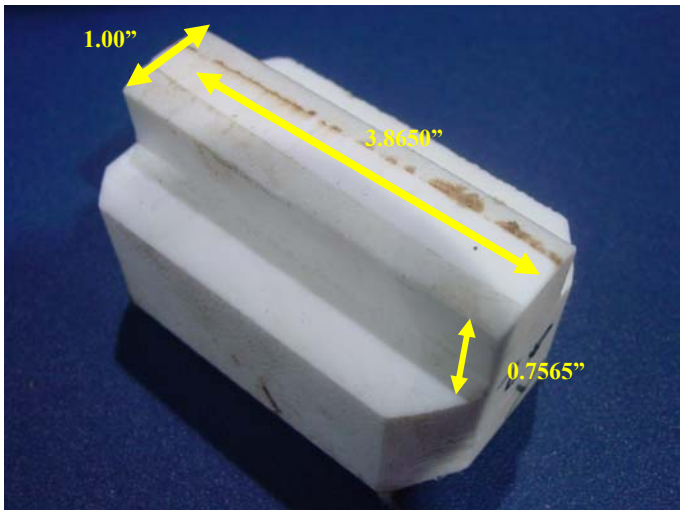

Figure 3: Polymer Sample

In order to reach the operating temperature, the heaters were turned on for approximately 1 hour prior to testing with the cylinder rotating at the lowest speed. Once the testing

temperature was attained, the speed was set at the maximum (2110 ft/min) for the experiments. Temperature was recorded with an IR sensor pointed at the center of the roll as well as with an IR camera that periodically recorded images of the entire roll. During the experiments, the heaters were manually turned off or on to maintain the test temperature.

The primary analysis technique employed was friction testing. This was accomplished by using a dryer felt, cut to 1ft width, which was draped over the roll. The felt was positioned so that it made contact with the appropriate test areas on the cylinder. One end was affixed to the floor while the other end was attached to a fish-tail weight. The value on the fish-tail was read while the cylinder was rotating at operating speed to obtain a "kinetic" value for the friction. When the roll was not in motion, the static value was recorded. Both pre- and post-polymer deposition values were measured.

The weight change of the polymer blocks was also measured and recorded. All samples were weighed prior to testing and again after each experiment. Photo documentation was made of the wear of each block and physical observations during the testing were noted.

The test plan is detailed in **Table 1**.

Samples	Test Temperature (F)	Load	Duration of Test
PTFE	170 F, 270 F	5 PLI, 10 PLI	10 min
PTFE	170 F, 270 F	5 PLI, 10 PLI	10 min
PVDF	170 F, 270 F	5 PLI, 10 PLI	10 min
UHMW PE	170 F, 270 F	5 PLI, 10 PLI	10 min

Table 1: Experimental Conditions Planned

For each sample, the friction was measured at the test temperature/speed and recorded in addition to the initial weights. The felt was removed and the sample was then installed in the sample rig with the appropriate load. The machine was brought up to full speed for 10 minutes for the run. After each experiment, the sample was removed and its post-experimental weight was recorded. Friction was tested again using the same felt (same side) as was used for the initial measurement. A new felt was used for each test.

Once these conditions had been evaluated, the initial plan called for a contaminated felt, obtained from a recycle mill experiencing picking/sticking problems, to be installed on

the machine. The idea was to examine whether any transfer of material from the felt to the roll would occur.

Analysis/Discussion

The initial trial plan was modified after the first set of tests, and not all tests in the initial plan were performed. Initially, PVDF and PE were scheduled to be tested at both 5 and 10 PLI and both temperature conditions. After just a minute or so of running both at the low temperature, low load condition, it became obvious that these materials could not withstand the test. A loud grinding noise was heard coming from the rig and the samples began shredding off flakes of material. No visible deposition was observed. The PE sample actually showed some blistering at the contact surface indicating that the temperature (due to both the heating of the surface as well as friction) was simply beyond the operating range of the material. The PVDF block showed similar results with large flakes of the sample coming off as the block was applied to the surface. Pictures of both samples are shown below in **Figure 4 & 5**.

Figure 4: UHMW PE

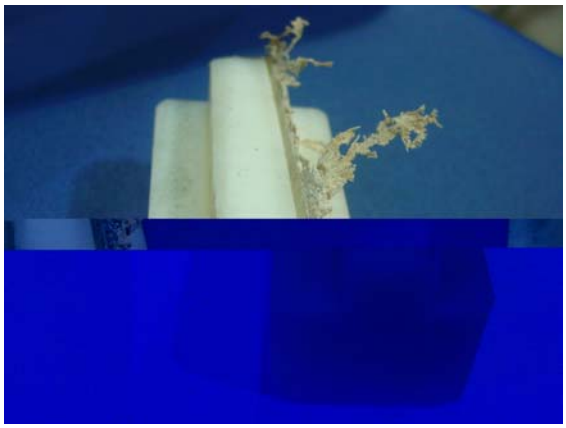

Figure 5: PVDF

PTFE was applied to the cylinder at both temperatures, under both loads and deposited a visible (the surface appeared shinier in this area) layer of material on the cylinder. The low temperature runs with PTFE sample did not indicate any of the same issues that were observed with PE and PVDF. At the high temperature/high load condition (see **Figure 6**), some shredding of the material was seen after 10 minutes of application.

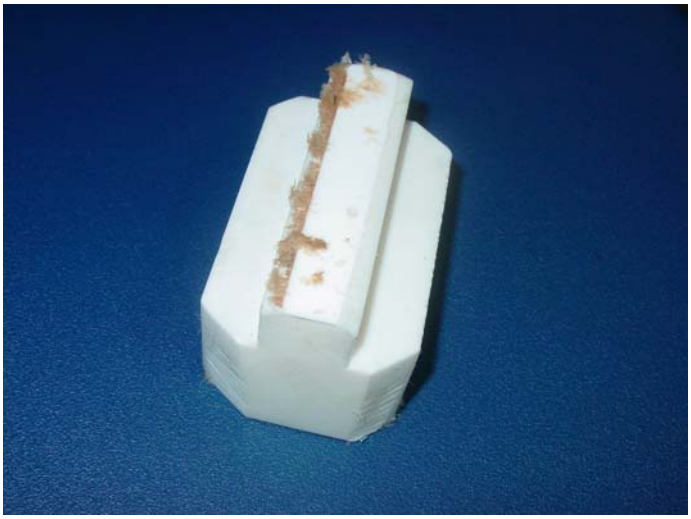

Figure 6: PTFE (applied at 10 PLI, 270 F)

Clearly, load and temperature can be optimized to produce the desired level of deposition with minimum waste of the PTFE.

The coefficient of friction measurements, summarized in **Table 2**, revealed a definitive change in the surface properties. The initial kinetic coefficient of friction (at operating speed) was approximately 20-22g with a static friction value of 8-10g. The range in values appears because two different types of felt (PPS & PET) were used. However, for each individual test, the same side of an individual felt was employed for both the pre- and post-run measurement. Also, shown is the change in weight of the blocks. It should be noted that for the samples in which shredding occurred, the weight change reflects an amount greater than that of the material deposited on the surface.

Sample	Experiment	Weight Change (g)	Coefficient of Friction
PTFE # 1	5 PLI/10 min/170 F	0.08	15-16
PTFE # 1	10 PLI/10min/170 F	0.09	14
PVDF # 1	5 PLI/1.5 min/170 F	0.19*	n/a
UHMW PE # 1	5 PLI/5.2 min/170 F	0.72 *	n/a
PTFE # 2	5 PLI/10 min/265 F	0.68	17
PTFE # 3	10 PLI/10min/265 F	1.56*	18

*sample flaked off

Table 2: Results Summary

The coefficient of friction values consistently drop after the PTFE is applied to the cylinder surface. It is interesting to note that at the highest load and temperature, the coefficient of friction is actually higher than at the other conditions. Thus, higher temperatures and loads are not necessarily conducive to better deposition as might have been expected. One explanation for this phenomena is that the shredding of the polymer could have "contaminated" the surface with large flakes of materials.

The weight change data also shows considerable differences at the various conditions. At low temperatures, the weight changes are much smaller than at the high temperature experiments. It is important to remember that some of the weight change at the high temperature is due to shredding of the polymer in addition to actual deposition. Again, it is a matter of optimization to find the most suitable load and temperature conditions. It may be that for operating at high temperatures, loads can be decreased significantly while obtaining the same level of deposition. The weight change data is significant since it reflects the wear rate of the PTFE, a critical factor when considering the economics of a Teflon doctor blade.

Contaminated Felt Testing

After testing the various polymer blocks, contaminated felts were installed on the apparatus to investigate the effectiveness of the surface treatments. These dirty felts were collected from paper mills operating with high recycle content. In order to maintain the temperature of the felts, the third induction heater was turned on directly above the felt as it came off the cylinder. The belts were maintained at 80-90 lbs of tension. The dryer cylinder had not been cleaned after applying the PTFE block so that two sections on the roll had been treated with an area in between that was left untreated. A clean section of the felt was also contaminated with Carbotac (Noveon) and Vinac (Air Products), two of the compounds used for WADS testing at IPST. These materials are common adhesives used by the paper industry and are composed of substances that frequently appear on actual contaminated dryer cylinders. They were coated onto the felts to observe whether any transfer from the felt to the cylinder occurred.

After running the felt on the machine for approximately 30 minutes, visible transfer of contaminant (adhesive plus flakes/fibers from the contaminated felt) was observed on the untreated section of the roll. The exact nature of the contaminant was verified with a chemical analysis (see **Appendix D**) of the residue scrapings from this section. The compound collected from the cylinder surface matched that of Carbotac. The PTFE treated portion of the cylinder showed no contamination and no adhesion of fibers or adhesive. Moreover, these sections still showed the shiny coating of PTFE that was visible after application of the block onto the cylinder (see **Figure 7**).

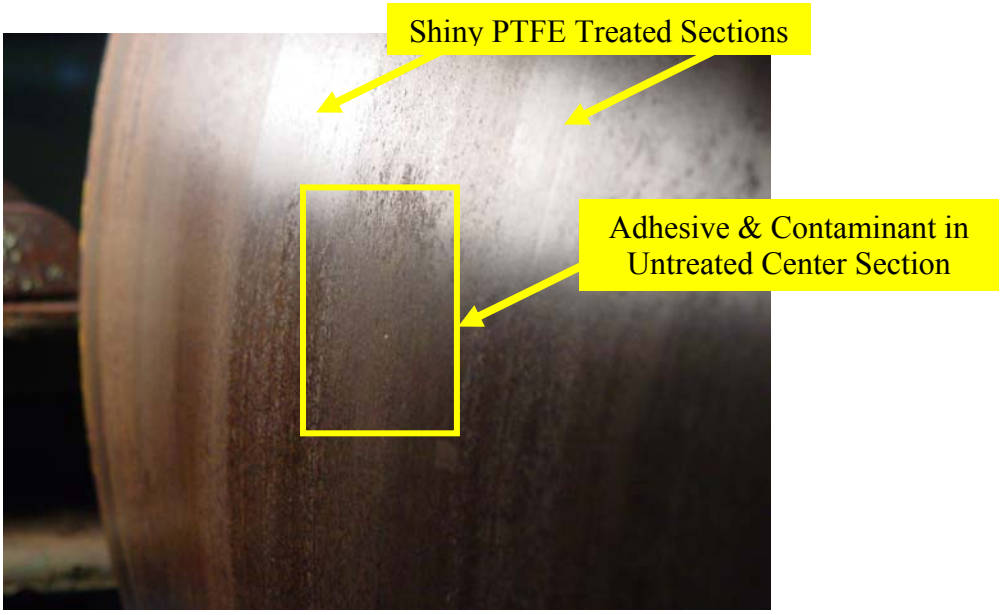

Figure 7: Cylinder Surface

The coated section of the felt contained numerous picked fibers and chunks of materials from the contaminated felt, particularly on the Carbotac side as evidenced in **Figure 8**.

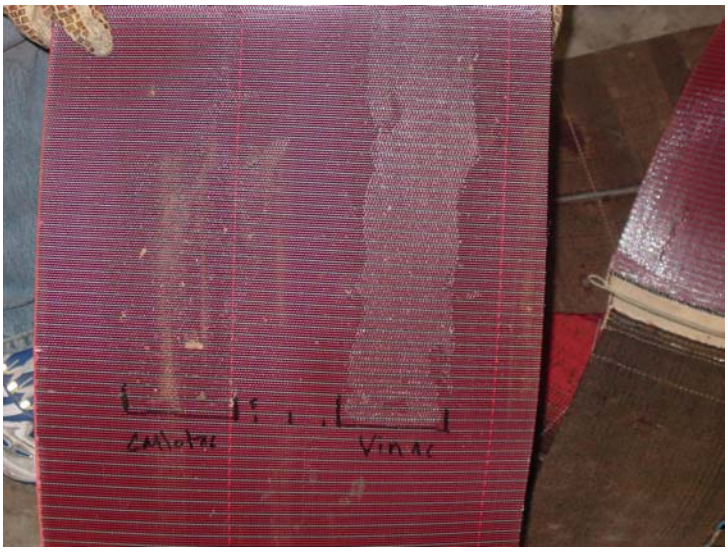

Figure 8: Adhesive Coated Felt Section

Conclusion

The pilot scale experiments have proved to be successful and have demonstrated some meaningful results. Clearly not all polymers/fluoropolymers have the appropriate properties for use in this application. The PVDF, in particular, showed very promising results in the lab. However, as this trial has demonstrated, the lab results do not necessarily translate well in the production setting. The PVDF and UHMW PE can be ruled out due to the poor results from this trial.

The coefficient of friction data has revealed definite changes/improvements in surface properties when the cylinder is treated with PTFE. The wear data is critical for economic analysis but the operating conditions must be optimized first. Most importantly, the experiments with the dirty felt has verified that the treated sections do appear to resist transfer of some contaminants/adhesives in comparison with untreated sections. These results are particularly promising. The next stage of this trial should involve evaluating different loads, temperatures and contact times in order to find the optimum conditions/wear rates. Load and temperature undoubtedly have an effect on wear. So the questions that remain are how long the block needs to be applied to the surface and how long the treated surfaces last before having to be retreated. Also, will a block of material do, or will this have to be a true doctor blade? Further mill trials at Walterboro will certainly help to address some of these issues.

APPENDICES

APPENDIX A: Descriptions of the Polymers

Polytetrafluoroethylene (PTFE)

Better known by the trade name Teflon®, PTFE is an opaque white fluoropolymer that has the lowest coefficient of friction of any solid. Because of the strength of the Carbon-Fluorine bond, PTFE is extremely inert and non-reactive.

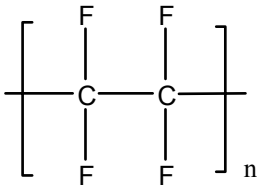

PTFE

Polyvinylidene Fluoride (PVDF)

Also known as Kynar®, PVDF is an opaque white solid resin. The chemical structure differs from PTFE with alternating CH_2 and CF_2 groups. The material has a lower maximum- use temperature than PTFE but superior abrasion resistance and mechanical strength.

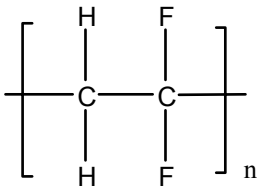

PVDF

Ultra-High-Molecular Weight Polyethylene

UHMW PE is polyolefin with minimal branching making it rigid and chemically inert. Often called the “poor man’s Teflon”, PE offers a very low coefficient of friction for a fraction of the cost of Teflon.

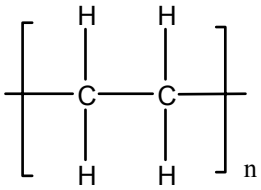

UHMW PE

Table 2: Physical Properties

Polymer	**Max Use Temp (ºF)**	**Water Absorption (%)**	**Tensile Strength (psi)**	**Hardness (Shore D)**
PTFE	500	<0.01	3350	50-65
PVDF	230	0.05	5200-7400	80
UHMW PE	248	< 0.01		

APPENDIX B: Speed Calibration

Using a tachometer, the surface speed of the cylinder was determined for the various settings on the controller. An average of 3 values was used for each setting. These values are enumerated in the table below:

Controller Setting	Average Surface Speed (ft/min)
0	73.0
20	532.0
40	1223
60	1816
80	2066
100	2111

APPENDIX C: Raw Data

Table 1: Sample Pre & Post Weights

Sample	Pre-Weight (g)	Experiment	Post Weight (g)
PTFE # 1	644.80	5 PLI/10 min/170 F	644.72
PTFE # 1	644.72	10 PLI/10min/170 F	644.63
PVDF # 1	538.77	5 PLI/1.5 min/170 F	537.58*
UHMW PE # 1	306.50	5 PLI/5.2 min/170 F	305.78 *
PTFE # 2	644.36	5 PLI/10 min/265 F	643.68
PTFE # 3	637.70	10 PLI/10min/265 F	636.14*

*sample flaked off